Ollscoil na hÉireann, Corcaigh

National University of Ireland, Cork

Development of a sensor-based rapid microbial testing platform for the Irish meat industry

Thesis presented by

Sophia Elisseeva, BSc.

https://orcid.org/0000-0001-9451-5184

for the degree of

Doctor of Philosophy

University College Cork

School/Department of Biochemistry and Cell Biology

Head of School/Department: Prof. Justin McCarthy

Supervisors: Prof. Dmitri Papkovsky and Prof. Joseph Kerry

2023

This is to certify that the work I am submitting is my own and has not been submitted for another degree, either at University College Cork or elsewhere. All external references and sources are clearly acknowledged and identified within the contents. I have read and understood the regulations of University College Cork concerning plagiarism.

Digital signature of the candidate: 

Table of Contents

List of Abbreviations

ANOVA: analysis of variance

ATP: adenosine 5’ triphosphate

BERA: bioelectronic recognition assay

BSA: bovine serum albumin

CFU: colony forming units

CO_2: carbon dioxide

DNA: deoxyribonucleic acid

dH_2O: distilled water

EC50: half maximal effective concentration

EFSA: European food safety authority

ETC: electric transport chain

ELISA: enzyme linked immunosorbent assay

FCM: flow cytometry

FDA: food and drug administration

GC: gas chromatography

GRAS: generally recognised as safe

IMC: isothermal microcalorimetry

INT: p-iodonitrotetrazolium chloride

LAE: lauryl arginate ethyl ester

LAMP: loop-mediated isothermal amplification

LT: lifetime measurements

MALDI-TOF: matrix assisted laser desorption ionisation time-of-flight

MAP: modified atmosphere packaging

MIC: minimum inhibitory concentration

MHB: Mueller-Hinton broth

MPN: most probable number

MRD: maximum recovery diluent

MS: mass spectrometry

M/Z: mass to charge ratio

NB: nutrient broth

O_2: molecular oxygen

$^3O_2$: ground state oxygen

$^1O_2$: singlet oxygen

OCR: oxygen consumption rate

OD600: optical density

PCA: plate count agar

PCAs: principal components analysis

PCR: polymerase chain reaction

Pt (II): platinum II

PtBP: platinum (II)-tetrabenzoporphyrin

PtCP: platinum (II) coproporphyrin

PtOEP: platinum (II) octaethylporphyrin

PtOEPK: platinum (II)-octaethylporphyrin-ketone

PtTBPs: platinum-tetrabenzoporphyrins

PtTFPP: platinum (II)-meso-(pentafluorophenyl) porphyrin

PtTPTBPF: platinum (II)-meso-tetra(4-fluorphenyl) tetrabenzoporphyrin

QC: quality control

RLD: rapid lifetime determination

RLU: relative light units

RNA: ribonucleic acid

Ru-dpp: ruthenium tris(4,7-diphenyl-1,10-phenanthroline)

SCRS: single cell Raman spectra

SD: standard deviation

Si-NPS: silica nanoparticles

SME: standard measurement error

S/N: signal to noise ratio

TR-F: time resolved fluorescence

TT: threshold time

TVC: total aerobic viable counts

VBNC: viable but nonculturable cells

Acknowledgements

I would like to thank my supervisors Prof. Dmitri Papkovsky and Prof. Joseph Kerry for their guidance and support throughout this project. I wish to express my gratitude to Dr. Elisa Santovito and Dr. Thomaz Bastiaanssen, whose expertise in statistics and bioinformatics was much appreciated. To my colleagues Dominic, Lauryn, Rafael, Rajannya, Chiara, Stephanie, Emer, and Liang, thank you for the great atmosphere in the lab and the supportive discussions. Finally, I would like to thank my parents for their love and support.

Abstract

Microbial spoilage and foodborne diseases cause significant productivity and economic losses for the food industry. There is a need for novel approaches to extend shelf life of products, improve quality and microbial safety, reduce spoilage and waste, and new assessment methods. Traditional methods are time consuming, labour intensive, centralised, have lengthy time to result, and some cannot analyse crude food homogenates. In this project, funded by the Irish Department of Agriculture, Food and the Marine and performed in partnership with a large Irish food company (Dawn Meats), several new optical oxygen sensor based systems were devised to increase efficiency and accuracy of testing.

Chapter 1 (Literature review) describes the state of the art in the area, the range of existing approaches and analytical systems, and their capabilities. Experimental methods used in this study are summarised in Chapter 2 (Materials and Methods).

The first experimental section (Chapter 3) describes the development of new multi-parametric toxicity testing platform based on the soluble oxygen probe, MitoXpress-Xtra, and 96 well plate format, which was used to investigate the antimicrobial effects of the compound Lauroyl Arginate Ethyl Ester (LAE) on pure cultures and whole meat microbiota. Through the measurement and analysis of the oxygen probe time profiles (phosphorescent lifetime) under different assay settings, we were able to assess and quantify the toxicity of LAE on different bacterial species, generating dose-response curves, and calculating EC50. The assay allowed for the simultaneous assessment of multiple variables and conditions such as bacterial species, temperature, growth media, sample type, and antimicrobial concentrations.

The second experimental part (Chapter 4) describes the new portable and autonomous system(s) based on disposable vials integrated with solid state sensors, tailored for the analysis of meat samples, carcass swabs, and environmental swabs. Along with the disposable sensor vials, the system is composed of two additional parts; a handheld, autonomous sensor reader and a portable incubator/heater. Up to 20 samples were prepared using the standard methods (ISO 4833-1:2013; ISO 18593:2018) in sensor vials, incubated at 30°C and measured hourly in a non-invasive, contactless manner. Such a simple system with manual measurements also revealed dissolved oxygen time profiles which were used to determine the threshold time of the sensor signal, which in turn, was used to calculate TVC values (CFU/ cm^2 or CFU/g) using developed calibration equations. The method was validated using: i) meat samples and carcass swabs obtained from Dawn Meats, ii) brush swabs of artificially contaminated surfaces with *E. coli*, iii) swabs of surfaces contaminated

with meat microbiota and iv) environmental swabs. No statistical difference was found between the sensor based method and reference method, providing the opportunity for the former to potentially replace the latter.

Finally, in Chapter 5 the new respirometric sensor based system was applied to a shelf-life study with four different types of MAP mincemeat samples: beef, turkey, lamb and pork, together with the analysis of these samples by 16S rRNA sequencing. Respirometric profiles revealed unusual linear profiles for pork and lamb mince, the origins of which remain to be investigated. In addition to respirometric microbiological assessment, the whole microbiome of each mincemeat type was analysed using 16S rRNA sequencing, which revealed an overall decrease in alpha diversity with some taxa exhibiting statistically significant changes over shelf-life and after exposure to respirometry. Beta diversity was seen to be dictated by mincemeat type.

Overall, the new optical oxygen respirometry systems are highly efficient and attractive for the food industry, with both developed systems improving existing methods in time to result, accuracy, user-friendliness, and on-site use. Furthermore, the portable sensor based system can be combined with cutting edge techniques such as next generation sequencing to provide more detailed information on the microbiota of food samples.

Chapter 1: Literature Review

1.1. Introduction

Approximately 25% of global food loss is due to microbial spoilage, which incurs significant economic and environmental burdens for producers (Bondi et al., 2014). Fresh meat products are highly susceptible to microbial contamination due to minimal pre-treatment and richness of essential nutrients (Jayasena & Jo, 2013). Spoilage can be defined as the process of food deterioration leading to differences in appearance (compared to fresh), presence of odours, and changes in texture and colour (Stellato et al., 2016). The influence of microbial spoilage can be attributed to both biotic and abiotic factors. Initial microbial colonisation can come from soil, live animals, personnel, water, air, and equipment used, which make up the biotic factors. The selection and subsequent dominance of certain bacteria is influenced by abiotic factors such as gaseous atmosphere, pH, temperature and NaCl levels (Stellato et al., 2016). The main bacterial culprits associated with meat spoilage are *Enterobacteriaceae*, *Pseudomonas*, *Brochothrix thermosphacta*, and *Lactobacillus* spp. (Jayasena & Jo, 2013; Stellato et al., 2016). Alongside microbial spoilage, bacteria such as *Escherichia coli*, *Staphylococcus aureus*, and *Salmonella* spp. can cause foodborne disease and are frequently found in meat products, which have become a widespread concern for productivity losses and public health (Jayasena & Jo, 2013).

To monitor both spoilage and pathogenic bacteria in the meat industry, two types of sample methods exist: i) food samples and ii) swab samples. Food samples are a destructive method in which a piece of the food product is taken for analysis and subjected to homogenisation using a recovery diluent and stomacher producing a crude homogenate. It is considered to be the more reliable technique as it allows for an almost complete recovery of viable bacteria from the product (Capita et al., 2004). The non-destructive alternative are swab samples, in which a swab (cotton or sponge) is used to sample a surface or carcass. These samples are also processed using a recovery diluent and agitation to create a bacterial suspension. Although the recovery rate is not as high as with food samples (Capita et al., 2004), swabbing allows for the tracing and controlling of contamination and cross-contamination in both environmental and microbiological surveillance (Jones et al., 2020). Both types of samples are analysed using a variety of methods which this review will cover.

1.2. Traditional Microbiological Methods

Considered the 'gold standard' in industry and standardised internationally (ISO 4833-1:2013; ISO 18593:2018), the colony count method relies on determining the total number of viable bacteria within a food product or swabbed surface by inoculating the surface of solid growth medium (agar plates) using a series of dilutions of the homogenised sample. Based on the desired target microorganism, plates are incubated at a fixed temperature (7°C to 55°C) and gaseous atmosphere (aerobic or anaerobic) for up to 72hrs. As each cell on solid media multiples into a colony (colony forming units, CFU) detectable by the naked eye, colonies are counted and the total number of viable bacteria from the original product is calculated (Figure 1.1). The detection limit of this method is approximately 4 CFU/mL for liquid foods and 40 CFU/g for solid foods (Jasson et al., 2010).

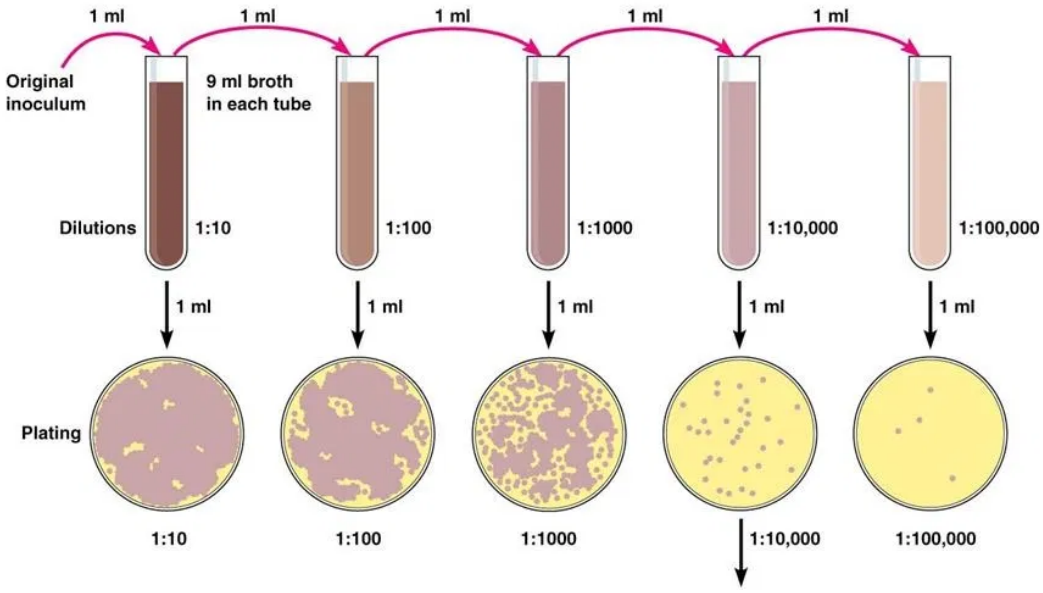

Figure 1.1: Calculating initial microbial load using the colony count method. Adapted from Pearson (2006).

However, if the total number of bacteria within a product are expected to be low (< 50/g), an estimation can be done using the Most Probable Number (MPN) method. Dilutions are prepared as in the colony count method with 3 serial dilutions transferred into 9 or 15 tubes of appropriate medium for the 3 or 5 tube method, respectively. After incubation, the number of positive tubes for each dilution is counted and MPN is determined using a

standardised table and dilution factor (Jasson et al., 2010). The MPN method is used solely as an estimation due to the level of uncertainty in comparison to the colony count method. Both methods are considered labour intensive and time-consuming as they require laboratory expertise, large amounts of consumables, and lengthy incubation periods.

There are several main modifications to the colony count method: i) compact plates and ii) selective media**.** Compact plates are a variation of the colony count method which rely on commercially available films or plates. They typically contain dehydrated nutrients and differentiating components that aid in enumeration (Jasson et al., 2010). Examples include 3M™ Petrifilm™, Compact Dry, and SimPlate®. Although having advantages like ease of use and saving space, compact plates still require some degree of expertise, sample preparation, and lengthy time to result.

Selective media is utilised to isolate a particular bacterium of interest while supressing unwanted microbiota through the use of selective agents that target Gram-positive or Gram-negative bacteria. Bile salts, ox gall, and dyes such as methylene blue and crystal violet, can inhibit Gram-positive bacteria while allowing the growth of Gram-negative bacteria. On the other hand, the growth of Gram-negative bacteria is inhibited by lithium chloride, sodium azide and antiseptic acriflavine while the growth of Gram-positive bacteria is promoted (Bonnet et al., 2020). Examples of selective media can be seen in Table 1.1. Additional selectivity can be increased via the addition of chromogenic and fluorescent substrates linked to enzyme substrates to create colour or fluorescent changes. Microorganisms that possess metabolic systems that interact with these enzyme substrates can thus be detected and enumerated (Jasson et al., 2010).

Table 1.1: Examples of selective media with chromogenic substrates highlighted.

Selective media	Species selective for	Ingredients	Selective components
Maconkey Broth	Coliforms, *E. coli*	Peptone, lactose, bile salts, sodium chloride, neutral red (pH indicator).	Lactose fermentation with inhibition of Gram positive spp with bile salts.
Rapid Coliform Chromoselect Broth	Coliforms, *E. coli*	Peptone special, sodium chloride, sorbitol, dipotassium hydrogen phosphate, sodium lauryl sulphate, X-Gal, MUG, IPTG.	Sodium lauryl sulphate (surfactant) inhibits accompanying microbiota especially Gram positive spp.
Minerals Modified Glutamate Media	*E. coli*	Lactose, sodium formate, L-cystine, L(-) aspartic acid, L(+) arginine, thiamine, nictonic acid, pantothenic acid, magnesium sulphate $7H_2O$, ferric ammonium citrate, calcium chloride, sodium glutamate, ammonium chloride.	Glutamate cleaved by β glucuronidase-positive *E. coli.*
M-lauryl Sulphate Broth	Coliforms, *E. coli*	Peptone, yeast extract, lactose, phenol red (pH indicator), sodium lauryl sulphate.	Lactose fermentation with inhibition of Gram positive spp due to sodium lauryl sulphate

Although being time-consuming and labour intensive, culture based colony count techniques are still used by many. Colony counts and selective media were used to determine the total aerobic counts, *Enterobacteriaceae*, and *E. coli* from swab samples of pig carcasses. They found that high counts of *Enterobacteriaceae* were a good indicator of hygiene and that there was significant variability of contamination between different areas of the carcass (Biasino et al.,2018).

Another study used 3M Petrifilm™ Select *E. coli* and SimPlate® Coliforms & *E. coli*, for the detection and enumeration of *E. coli* using swab samples from naturally contaminated pork and lamb carcasses that were collected before and after chilling. Chilled carcasses gave less agreement between methods than warm carcasses. In addition, the authors found that the compact plates could be easily overloaded with sample (Hauge et al., 2017).

1.3. Molecular Methods

Moving away from traditional microbiological methods allows for the introduction of selective molecular methods which focus on protein, antigen, or DNA/RNA of target pathogens. They require a higher level of laboratory expertise but in return, offer a higher degree of specificity when compared to traditional methods.

1.3.1. Immunoassays

Immunoassays are based on the highly specific recognition of various antigens by corresponding antibodies. They tend to be used in food diagnostics and have commercially available kits based on Enzyme Linked Immunosorbent Assays (ELISA), which couples an immunoassay with an enzyme label (Jasson et al., 2010; Nagaraj et al., 2016). However, the multi-step process of an ELISA (coating, blocking, incubation, washing and colour generation) is labour intensive and time consuming. In addition, pH, salt ions, and temperature can easily interfere with ELISAs (Xiao et al., 2021). Protein precipitation is commonly used for the extraction of desired proteins for immunoassays from complex homogenate, however this process is laborious and time-consuming, usually requiring specific temperatures (Mandli et al., 2018; Seddaoui & Amine, 2021). Furthermore, the assay cannot distinguish between viable and non-viable cells.

A paper based ELISA assay was developed for the detection of *Escherichia coli* 0157: H7 using pre-treated Whatman No.1 filter papers. The assay took less than 3 hours, required only 5 μL of sample and had a detection limit of 10^4 CFU/mL (Pang et al., 2018). For visualisation of results, tetramethylbenzidine-hydrogen peroxide (TMB-H_2O_2) was added to the assay and the colour change was quantified using a scanner or smartphone and Image J software. However, the relatively high detection limit and the stability of the activated filter papers may limit the application of this assay.

Another immunoassay was developed in which cotton swabs were used as both sample collector and detection device. Bacterium specific antibodies were immobilised on cotton swabs, which were then submerged in coloured nanobead conjugated antibody solutions to create a sandwich assay with a detection limit of 10 CFU/mL. Semi-quantitative results were determined based on colorimetric changes on the swabs, corresponding to specific bacteria, but could be further quantified using smartphones and Image J software (Alamer et al., 2018). As only artificially contaminated surfaces were tested, the cotton swabs may be limited by potentially complex contamination present in industrial settings. Furthermore, the stability of the cotton swabs was not tested and could provide limitations for production and storage.

1.3.2. Polymerase Chain Reaction (PCR)

Another common technique in the detection of bacteria in food is the polymerase chain reaction (PCR). PCR relies on the ability of DNA polymerase to copy a specific region on a template strand of DNA. The specific region is defined by choice of primers, short oligonucleotides that have matching sequences to the end region of interest. Amplification occurs over a series of cycles in which DNA is heated and cooled to produce double-stranded DNA of interest (Jasson et al., 2010). With the introduction of fluorescent dyes specific for double-stranded DNA (Jasson et al., 2010) further development of PCR was possible. Real-time PCR (qPCR) allows for the continuous amplification of target DNA and detection of the fluorescent signal (Jasson et al., 2010). In addition, it allows for the estimation of initial concentration of target organism present within the sample. Multiplex PCR allows for the simultaneous detection of multiple primers (for multiple targets) in a single reaction well (Jasson et al., 2010; Hameed et al., 2018).

For all PCR techniques, sophisticated DNA isolation and purification from samples is necessary. The food matrix is highly heterogenous, with inorganic particles, biochemical compounds and indigenous microbiota that can directly interfere and inhibit PCR assays (Rodríguez et al., 2016; Wang & Salazar, 2016). Therefore it is essential to develop highly specific primers for new PCR methods. In addition, PCR is highly susceptible to contamination (Pahlow et al., 2015).

A real-time PCR *Salmonella* screening method was developed and validated for environmental swab samples. Results were produced in 18 to 24h in comparison to traditional methods which require at least 2 days. Primers and probes were designed based on the gene *invA*, group D, and *Salmonella enterica* serovar Enteritidis. The study demonstrated a high specificity of the primers and probes by screening against a panel of 329 *Salmonella* isolates. Sample pre-enrichment was still necessary for the described assay (Kasturi & Drgon, 2017).

For the detection of enterotoxin-producing *Staphylococcus* spp. in meat products, a real-time PCR assay was developed. Once again the design of specific primers was critical in the development of the assay and were thus based on the conserved regions of enterotoxin genes. The detection limit of the assay was 2 - 40 CFU/g in 12h which included an 8h pre-enrichment step (Rodríguez et al. 2016).

1.3.3. Loop-mediated isothermal amplification (LAMP)

Further developments of the PCR method include loop-mediated isothermal amplification (LAMP). LAMP is based on a DNA polymerase and a set of four specifically designed primers that recognise a total of 6 distinct regions within the target sequence of DNA. The inner primer with both sense and antisense strands initiates LAMP while the outer primer allows for strand displacement, releasing single stranded DNA. This strand of DNA then acts as a template primed by the second inner and outer primers which produce stem-looped DNA. In subsequent cycles, one inner primer hybridises to the loop and initiates displacement DNA synthesis. The reaction, which takes place at 65°C for 1 hour, produces 10^9 copies of DNA, which include stem-loop structures and cauliflower-like structures with multiple loops (Notomi et al., 2000).

A multiplex real-time LAMP assay was established to simultaneously detect and differentiate *Salmonella* spp. and *Vibrio parahaemolyticus* DNA within a single reaction. The amplified products were then subjected to melting curve analysis, which clearly showed a distinction between products. In addition, the assay showed 100% inclusivity and exclusivity, with a detection limit similar to that of multiplex PCR (Liu et al., 2017).

A combination of multiplex LAMP and lateral flow dipstick was developed for the rapid detection of *Salmonella* spp., *Carnobacter* spp., and *Staphylococcus aureus* from powdered infant formula. The accumulation of sandwich composites formed a red band on the device, allowing for visual inspection. The detection limits of the assay for *Salmonella* spp., *Carnobacter* spp., and *S. aureus* in formula without enrichment were 4.2, 2.6, and 3.4 CFU/g, respectively. The entire method can be completed within one hour (Jiang et al., 2020).

Although LAMP does not require expensive laboratory equipment, it still necessitates sophisticated DNA extraction procedures, which are performed by highly skilled personnel. Furthermore, complex heterogenous food samples could limit DNA extraction procedures and cause potential contamination.

1.3.4. Sequencing methods

The focus of the aforementioned molecular methods has been the targeting of one or several specific bacterial species. With next generation sequencing, whole microbial communities can be examined in greater detail for their functional diversities. There are two main categories of next generation sequencing: i) amplicon sequencing in which specific marker gene families are amplified and sequenced and ii) metagenomics, where random shotgun sequencing is used for the whole genomic content of communities (Jagadeesan et al., 2019). Both sequencing types require the purification and isolation of DNA from a variety of samples. With amplicon sequencing, the extracted DNA undergoes targeted PCR amplification, commonly the 16S rRNA marker gene for bacteria (Jagadeesan et al., 2019). Indices are then attached to these amplicons by an additional round of PCR. The subsequent libraries are normalised, pooled and sequenced. This allows for the identification of the microbial community at a genus level and can follow the succession of microbial populations over time (Jagadeesan et al., 2019). In metagenomics, the extracted DNA undergoes fragmentation followed by shotgun sequencing. Reads are then classified to various genomic

locations. This, in turn, allows for the analysis of individual strains and the predication of their function within the microbial community (Jagadeesan et al., 2019). Both sequencing types produce large datasets which are then processed using bioinformatics pipelines.

Next generation sequencing has the potential to be instrumental in food diagnostics and food safety. Shotgun metagenomic sequencing was used to analyse differences in chicken breast microbiomes as well as profiling antimicrobial resistance genes (ARG). The study found that packaging type and processing environment had a greater effect on microbiome composition than antibiotic usage and seasonality. Furthermore, the composition of the poultry microbiomes could be indicative of potential metagenomic markers for food safety and quality, which in turn could be translated to the evaluation of processing environments and practices (Li et al. 2020).

A combination of amplicon and target-enriched shotgun sequencing was used to profile the microbiome and resistome of ground beef products in the US. The results indicated no difference between products that claimed 'raised without antibiotics' and those raised by conventional means. Similarly to the aforementioned study, the authors found that product management had a greater influence on ground beef microbiome than the resistome. Furthermore, the novel target-enriched shotgun sequencing implemented in this study allowed for the analysis of samples with low microbial abundance. (Doster et al. 2020)

Although next generation sequencing has a great many advantages, there are still some limitations. As previously mentioned the sample preparation and subsequent analysis required is complicated, labour-intensive, and expensive. The analysis of the data produced requires highly skilled individuals and is time-consuming. Furthermore, low microbial abundance and high amounts of host (off-target) DNA can limit the effectiveness of next generation sequencing as a technique.

1.4. Instrumental Methods

The use of instrumental techniques has been widely applied to the analysis of food safety. Although they may vary greatly, their underlying components remain the same. Each method has a dedicated detection platform to which samples are added and analysed.

1.4.1. ATP Bioluminescence

This method is based on the involvement of ATP in an enzyme-substrate reaction between luciferin and luciferase, which produces bioluminescence as a by-product. The light emitted is proportional to the concentration of ATP and can be measured in Relative Light Units (RLU) using luminometers (Jasson et al., 2010; Ríos-Castillo et al., 2021). The bioluminescence reaction can occur at very low levels of ATP and requires the lysis of cells. All living cells contain ATP which is essential for the maintenance of enzyme systems, biosynthesis of cellular components, and regulation of stored metabolic energy (Bottari et al., 2015). However, this technique can only provide a rapid estimation of bio-load present and cannot differentiate between microorganisms and organic debris. Furthermore, many food samples such as meat can contain high levels of somatic ATP, which can cause interference and high background levels of bioluminescence. In order to focus solely on microbial ATP, pre-treatment of samples is required (Bottari et al., 2015; Monica et al., 2021). In addition, to convert RLU to CFU/mL or CFU/g, a standard curve must be established using known concentrations of bacteria (Bottari et al., 2015).

Ready-to-use ATP bioluminescence kits are available with portable luminometers, with the most common use being to monitor surface hygiene levels (Bottari et al., 2015; Ríos-Castillo et al., 2021). The accumulation of organic debris typically provides an ideal environment for microbial growth, thus being an indicator of poor hygiene. One study used ready-to-use, pre-moistened surface swabs (Clean-Trace™ Surface ATP Test Swab UXL100) from 3M to evaluate bacterial populations on supermarket food contact surfaces. When compared to traditional plate count methods, surfaces that were deemed satisfactory were in fact unsatisfactory based on ATP bioluminescence. The difference could be accounted for by the presence of biofilms (which would be underestimated by traditional methods) and by the presence of viable but nonculturable cells (VBNC) (which contain similar ATP levels to viable cells) (Ríos-Castillo et al., 2021). The samples used were relatively clean and therefore did not require additional treatment apart from lysis to access intracellular ATP.

The effects of various interfering compounds along fish processing on ATP bioluminescence measurements using two commercially available kits were investigated. Sodium chloride and acidic liquid smoke had the highest rates of bioluminescence quenching and RLU values of the same sample varied between kits. Although based on the same

principle, the results from commercially available kits are not directly comparable and must be converted using a standard curve, as previously mentioned. High protein and high fat fish samples also showed large variation in ATP bioluminescence as the cells proved to be difficult to lyse. The different stages along fish processing and possibly other food processing plants would therefore require different acceptable levels of RLUs to ensure proper hygiene and subsequent food safety (Møretrø et al., 2019). With an increase in the complexity of samples, there is a decrease in ATP bioluminescence and additional sample pre-treatment is required, which is not provided by most commercially available kits.

ATP bioluminescence was applied for the detection of yeast and bacteria in wine. However since the technique is non-specific, additional treatment of samples was required. Wine samples were filtered using two sets of membrane filters to discriminate between yeast and bacteria. Filters were then incubated in selective media for 24hrs with ATPase (hydrolyses free ATP) and analysed via luminometer. The technique was able to discern between varying levels of contamination with yeast and bacteria (Monica et al., 2021). Once again, pre-treatment of samples was necessary to remove inhibiting compounds as well as to add specificity to the technique.

1.4.2. Flow cytometry

Flow cytometry (FCM) is the quantitative measurement of optical characteristics from individual cells in front of a focused light beam, which can be either a high-pressure mercury vapour lamp or an assortment of lasers (Jasson et al., 2010). There are three measured parameters as particles pass through the light beam: forward scatter, side scatter and fluorescence. The forward and side scatter are influenced by cell refractability, which in turn is related to surface properties such as size and internal structures. Due to natural fluorescence emitted by some cellular components, additional labelling is needed in order to distinguish between micro-organisms and debris. Thus, fluorescent dyes can be used to investigate the metabolic state and viability of micro-organisms (Jasson et al., 2010).

A staining system combining fluorescent labelled antibodies and propidium iodide (cell permeable red fluorescent dye) to detect viable *S. aureus* cells in milk and milk powder using FCM was developed. With a 5hr pre-enrichment period, the method could detect low numbers of *S. aureus* in 6 hrs with a detection limit of 7.50 cells/mL in milk and 8.30 cells/g in milk powder (Liu, Wang, et al., 2021).

Another FCM method was developed for the detection and differentiation of probiotic strains of *B. subtilis* and other *Bacillus* species. Two fluorescent dyes were used, SYTO24 (cell-permeant green fluorescent nucleic acid stain) and Laser Dyes Styryl 751(cell-permeant fluorescent stain) which in combination with FCM were able to differentiate three subpopulations: spores, vegetative cells, and VBNC/ dead cells (Genovese et al., 2021).

FCM was used to quantify the ability of electrolysed water to induce *E. coli* O157:H7 and *Listeria monocytogenes* into the VBNC state. With the use of SYTO® 9 stain (which can penetrate all cells and produce a green fluorescence) and propidium iodide, the authors were able to determine that at low chlorine concentrations of electrolysed water, cells were induced into a VBNC state as a significant portion of cells retained cell integrity by emitting green fluorescence (Afari et al., 2018).

The sample itself is a limiting factor for FCM analysis as high particulate samples such as crude food homogenate could interfere with readings by producing high levels of background noise. Furthermore, correct staining of samples requires relatively skilled personnel and a laboratory setting.

1.4.3. Raman spectroscopy

Raman spectroscopy is a technique which makes use of the effect that laser light can be scattered inelastically to a small extent when interacting with a sample, which allows for energy transfer between incident photons and the sample molecules (Pahlow et al., 2015; Hameed et al., 2018). The amount of energy transferred directly corresponds to specific molecule vibrations within a sample, which can then be visualised in unique Raman spectra. However, Raman spectra can be masked by broad and intense background fluorescence and requires sample preparation that preserves intact bacterial cells (Pahlow et al., 2015).

With Raman spectroscopy, single cell Raman spectra (SCRS) can be generated based on the same principle, as mentioned above, of energy change in chemical bond vibration and rotation when a single bacterial cell is irradiated by a laser. Different vibration modes of various chemical cell components such as proteins and lipids, are reflected in SCRS and provides unique information for a given single bacterial cell without the need of sample pre-

treatment or pre-incubation (Yan et al., 2021). Although highly specific, SCRS are difficult to classify by the naked eye as different bacterial cells have minute differences in spectra.

To overcome this challenge, databases of Raman spectra are produced and analysed using chemometrics. Depending on the application, a classification model is produced via machine learning which is then validated using independent spectra not included in the original database. The database can then be used for the identification of unknown samples (Pahlow et al., 2015). When compared to genotypic methods such as next generation sequencing, Raman spectroscopy offers a relatively rapid and inexpensive method for the classification of bacterial species (Yamamoto et al., 2021).

A database of SCRS from 7 common food-borne pathogen genera (23 strains) was created and the use of chemometrics was applied for the analysis. Machine learning helped distinguish SCRS and achieved bacterial classification of 87.1% - 95.8% at the serotype level (Yan et al., 2021). This dataset can potentially be applied for the identification of food-borne pathogens in food samples, however this has yet to be tested.

The use of Raman spectroscopy in the classification of 6 food-spoilage bacteria as well as their tolerance to food additives was investigated. Using support vector machine learning, Raman spectra were distinguished based on bacterial species and three types of stress conditions with different classes within each type based on minimum inhibitory concentrations (MIC). The model was able classify species with an 88.2% accuracy and with a 91.2% accuracy for stress tolerances (Yamamoto et al., 2021).

For Raman spectroscopy, samples need to be processed accordingly as to avoid spectra interference and have intact bacterial cells. Therefore, crude homogenates require additional concentration and isolation procedures. In order to correctly classify Raman spectra, a corresponding dataset and correct model is required. The right choice of bacterial representatives as well as their preparation is crucial in establishing a correct dataset (Meisel et al., 2014)

1.4.4. Mass spectrometry

Mass spectrometry is a technique based on ionisation of chemical compounds, creating charged molecules. The ratio of mass to charge (m/z) is then measured (Singhal et al., 2015). Traditionally, mass spectroscopy has only been applied to chemical classifications, but in recent years there has been a shift to applications in food safety, namely matrix-assisted laser desorption ionisation time-of-flight (MALDI-TOF) mass spectrometry (Domínguez et al., 2020). MALDI-TOF MS is based on the simultaneous desorption and soft ionisation of sample-matrix mixture, in which unfragmented peptides are detected. The matrix, which co-crystallises with the sample, absorbs energy from short laser pulses and aids in the release of intact peptides from the microbial sample (Jadhav et al., 2014). This creates a spectral fingerprint in which whole cell proteomes (typically within a m/z range of 2-200kDa) are analysed (Jadhav et al., 2018). Similar to Raman spectroscopy, MALDI-TOF MS relies on pre-existing spectral libraries in order to correctly analyse a spectral fingerprint. However, current libraries are clinically oriented and there are limited ones available for food safety applications (Domínguez et al., 2020).

In light of these limitations, a method was proposed that that combines MALDI-TOF MS and bioinformatics to create custom spectral libraries for the analysis of raw milk isolates. When compared to 16S rRNA amplicon sequencing, similar clustering patterns and significant discriminatory power was observed (Vithanage et al., 2017).

A combination of MALDI-TOF MS (proteomics) and gas chromatography mass spectroscopy (GC-MS) (metabolomics) were able to identify three red meat pathogens directly from enrichment broth, which would allow for the further development of this method as a diagnostic tool. (Jadhav et al., 2018).

Both MALDI-TOF MS and 16S rRNA amplicon sequencing were used to investigate and characterise the microbial populations of wild boar meat (Peruzy et al., 2019).

The limitations regarding mass spectroscopy is the need for expensive equipment and extensive sample preparation. Furthermore, spectral fingerprints must be compared against a pre-existing database and therefore new species cannot be identified.

1.4.5. Calorimetry

Calorimetry is based on the principle of heat exchange into the environment by any type of physical, chemical or biological process. Bacterial growth can be monitored via microcalorimetry as biological processes such as metabolism release assimilated Gibbs energy into the environment which in turn can be detected (Fricke et al, 2020). Furthermore, there is no limitation on sample matrix as long as heat can be transferred (von Ah et al., 2018). The sample is placed into a closed ampoule within a controlled isothermal chamber at a fixed temperature where the heat exchange between sample and surrounding environment is measured (Khalef et al., 2016).

Three factors associated with isothermal microcalorimetry (IMC) were examined to further investigate the possibility of reducing detection time of aerobic microbial contaminations: i) initial number of bacteria; ii) performance of the microcalorimeter; and iii) the provision of oxygen in solid or liquid state mediums. It was found that increased number of bacteria via membrane filtration reduced the detection time as well as setting correct threshold limits. Additionally, solid state media had greater availability of oxygen for growing bacteria than liquid state due to the slow diffusion of oxygen from headspace into media (Fricke et al., 2020).

Isothermal microcalorimetry was used to determine the minimum inhibitory concentrations (MICs) of antibiotics in raw mixed cultures derived from Swiss hard cheeses grown in milk. Changes in metabolism due to the efficacy of antibiotics produced distinct heat flow curves which allowed for the determination of MICs. IMC allowed for the direct measurement of samples without additional preparation, however, an extensive calibration of 2 days was required (von Ah et al., 2018).

1.5. Biosensor systems

Biosensors are composed of two main parts: the biological recognition component which interacts with the sample (antibodies, cell receptors, enzymes, microbial cells, nucleic-acid, organelles, and tissues) and the transducer component that detects and transmits signals via various physicochemical pathways (electrochemical, optical, thermometric, or piezoelectric). The interaction between these two parts results in an initial signal that is transformed into a

detectable one which can be easily quantified (Hameed et al., 2018). Various combinations have been implemented depending on the target of interest.

A paper based portable biosensor was used for the detection of *Staphylococcus aureus* with magnetic nanoparticles (Suaifan et al., 2017). The biosensor was based on carboxyl terminated magnetic nanobeads linked to *S. aureus* specific protease peptide substrate. The linked magnetic nanobeads were then immobilised on a gold strip on paper via the formation of a gold-sulphur complex with the cysteine residue, covering the strip in black. A magnet was added at the back of the sensor to accelerate the collection of dissociated magnetic nanobeads once exposed to protease activity, which revealed the gold strip underneath and was visible to the naked eye. The biosensor was able to detect *S. aureus* in a variety of food and environmental samples with detection limits of 100 CFU/mL and 40 CFU/mL, respectively. However, the samples were centrifuged and filtered and thus the effects of crude homogenate on the biosensor were not investigated.

Another paper based DNA biosensor was developed for the detection of *Campylobacter* spp in chicken meat (Vizzini et al., 2020). The biosensor was an enhanced version of a dot blot in which extracted genomic DNA was immobilised on a nylon membrane and detected using a 16S rRNA *Campylobacter* based probe linked with biotinylated silica-nanoparticles (Si-NPs). Hybridisation was evidenced by chemiluminogenic substrate luminol in the presence of the activator H_2O_2. The use of Si-NPs allowed for a 30 fold signal enhancement compared to a single biotin linked probe. Although the assay requires 24 hrs to complete, the limit of detection of the biosensor is 3pg/µl or 600 CFU. However, DNA extraction and subsequent immobilisation on the membrane requires skilled personnel and a laboratory setting.

Biosensors based on living cells have also been developed in which live cells act as receptors. An example of such biosensors is the Bioelectronic Recognition Assay (BERA), wherein receptor molecules (antibodies, enzymes, etc.) are inserted on the cell membrane in large quantities using electroporation. The assay measures the change in membrane potential once the target molecule binds to the inserted receptors, which creates an ionic current. Recently, BERA was used for the recognition of *Listeria monocytogenes* by inserting anti *L. monocytogenes* antibodies into the cell membrane and measuring the response using a handheld multichannel potentiometer connected via Bluetooth to an android device, allowing

for instantaneous data analysis (Hadjilouka et al., 2020a). The limit of detection for the assay was 10^2 CFU/mL, however only samples in sterile saline solution were tested. The assay was further developed to include food samples (Hadjilouka et al., 2020b) which hindered the detection of *L. monocytogenes* and required a 24 hr sample pre-enrichment step.

1.6. Optical Oxygen Respirometry

1.6.1. Principles of oxygen sensing

Optical oxygen respirometry is a group of detection methods that rely on dedicated sensor materials (solid state coatings or soluble probes) and measurement setups. These sensor materials are based on the ability of molecular oxygen (O_2) to quench the phosphorescence of electronically excited triplet state dye molecules via a collisional mechanism (Lakowicz, 2006) (Figure 1.2). When the dye molecules collide with O_2 molecules, ground state molecular ($^3O_2$) accepts energy from the excited triplet state of the chromophore which leads to the formation of singlet oxygen ($^1O_2$) and subsequent deactivation of the chromophore. This quenching mechanism decreases both the emission intensity and lifetime of the phosphorescent dye molecules in a concentration dependent manner. However, the process is photophysical meaning that it is reversible and does not affect characteristics of the phosphorescent dye (Wang & Wolfbeis, 2014).

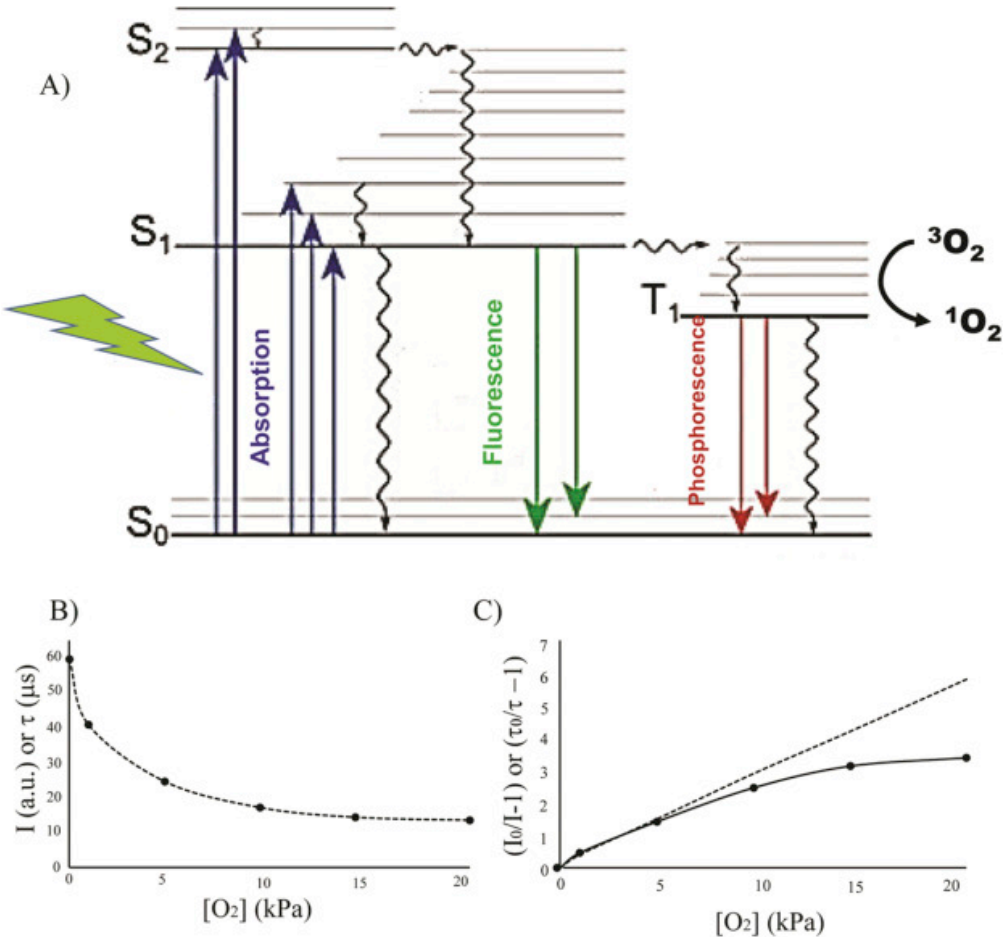

Figure 1.2: (A) Diagram showing the main photophysical processes occurring within oxygen sensitive luminescent dyes when excited by electromagnetic radiation and the subsequent quenching by molecular oxygen**. (B)** Oxygen concentration dependence on luminescent signal from dye either in intensity (I) or lifetime (τ) values. **(C)** Stern-Volmer plots for intensity or lifetime showing both ideal (dotted line) and more common (curved solid line) cases. Taken from Banerjee et al., 2016.

The O_2 concentration or partial pressure can be quantified based on intensity (I) or lifetime (τ) measurements, whose relationship is described by the Stern-Volmer equation (Lakowicz, 2006):

$$\frac{I_0}{I} = \frac{\tau_0}{\tau} = 1 + k_q \tau_0 [O_2] = 1 + K_{SV}[O_2]$$

Where I_0 and I are dye luminescent intensities, in the absence and presence of O_2, respectively. τ_0 and τ are the corresponding lifetime values; k_q is the bimolecular quenching rate constant and K_{SV} is the Stern-Volmer quenching constant.

Based on the aforementioned equation, Stern-Volmer plots offer a visual representation between O_2 concentration and sensor luminescence parameters (Figure 1.2). The linear plot is based on the assumption that the dye dispersion within the sensor material

is homogenous. However, in practice, dye dispersion is heterogenous and O_2 access varies. For such cases, the dependence is better described using 'two-site' model (Demas et al., 1995):

$$\frac{I_0}{I} = \frac{\tau_0}{\tau} = \frac{f_1}{1 + K_{SV}^1\,[O_2]} + \frac{f_2}{1 + K_{SV}^2\,[O_2]}$$

Where I and I_0 are dye luminescent intensities, in the presence and absence of oxygen, respectively and τ and τ_0 are the corresponding lifetime values. f_1 and f_2 represent the fractions of total emission coming from each component with $f_1 + f_2 = 1$. K^1_{SV} and K^2_{SV} are the Stern-Volmer constants corresponding to each component. Designed primarily for intensity quenching, the two site model can also be used for lifetime based O_2 sensing (Borisov et al., 2014; Banerjee et al., 2015; Banerjee et al., 2016).

While still useable for some respirometric applications, intensity measurements are more error-prone and difficult to use. They can be influenced by factors such as fluctuation of light-source intensity, position of sensor, degradation of dye molecules within the sensor, changes in path light, detector drift and instrument to instrument variability, and sample matrix (Banerjee et al., 2016). This, in turn, results in sensor and batch variation, large measurement errors, and unstable calibrations.

Luminescent lifetime, on the other hand, is an intrinsic parameter of the sensor material, which is independent of instrument variability and dye concentration (albeit self-quenching can occur at high concentrations, affecting lifetime), allowing for more stable calibration. Lifetime can be measured in either time or phase domains. In time domain measurements, phosphorescence decay of the sample is measured directly under a short pulse excitation. Rapid Lifetime Determination (RLD) can be used to increase sensitivity and signal to noise ratio (S/N) by introducing a time delay between excitation of the sample and measurement of its emission. This delay, which is immediately after the initial excitation, allows for autofluorescent components to dissipate, after which recording of sample emission takes place during 'gate time' (Figure 1.3). Thus, RLD provides effective elimination of sample autofluorescence and scattering, increased improvement in sensitivity and selectivity of probe detection, and reduced interferences (Papkovsky et al., 2012).

With phase domain methods, the phase shift of the luminescent intensity signal is measured using a periodically modulated light source which allows for a sinusoidal emission

after a delay. The difference between the excited and emission waves is defined as the phase shift or angle (Φ) (Figure 1.4) (Andrzejewski et al., 2002). Moreover, with O_2 sensitive dyes, the shift is also O_2 sensitive.

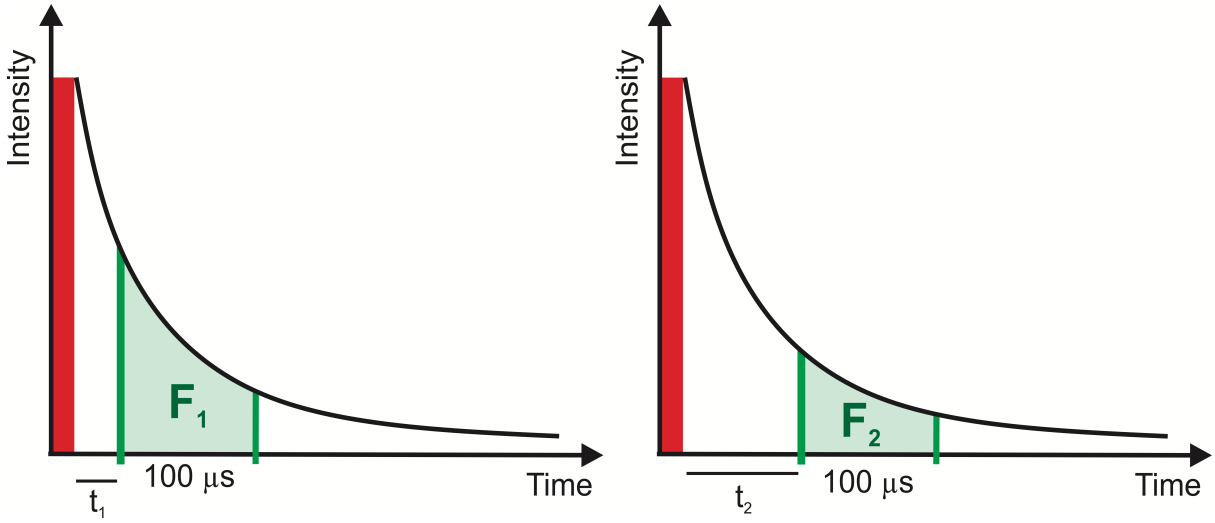

Figure 1.3: Scheme of Rapid Lifetime Determination (RLD). A time delay between emission light and measurement allows for background autofluorescence signals to decay. This improves signal to noise (S/N) ratios and sensitivity of the readout.

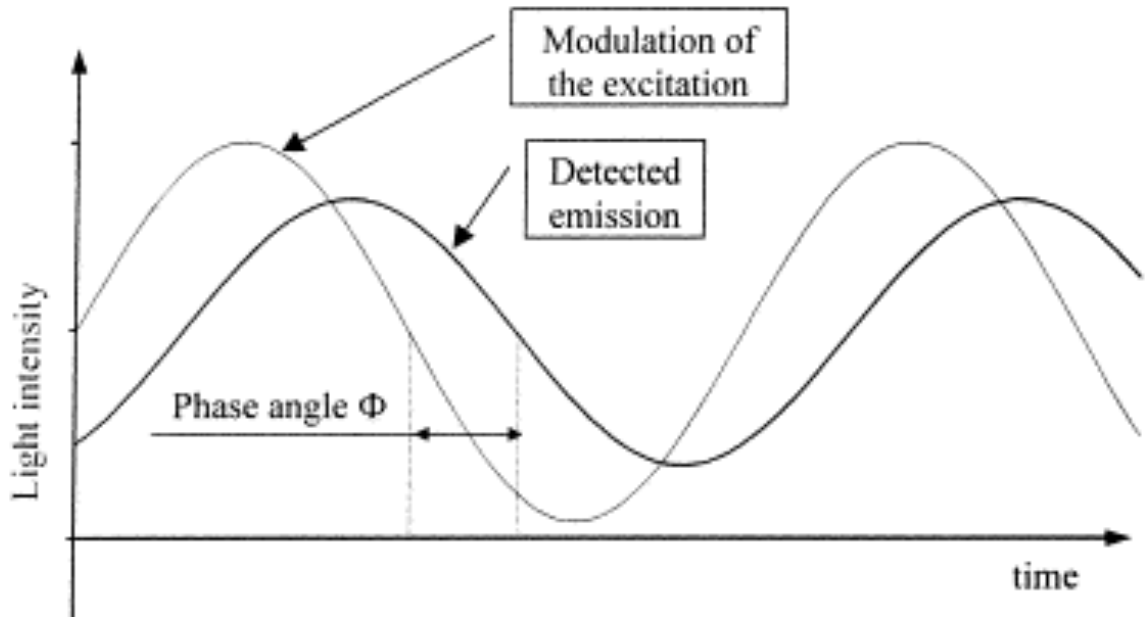

Figure 1.4: Principle of phase-resolved luminescence lifetime measurement (Andrejewski et al., 2002).

1.6.2. Sensor materials

A variety of O_2-sensitive dyes are available, which are dependent on the application in question. Polypyridyl complexes of ruthenium, with ruthenium tris(4,7-diphenyl-1,10-phenanthroline) (Ru-dpp), have been extensively studied due to their one step synthesis and high photostability. Exhibiting moderate luminescence brightness, Ru-dpp is limited with high temperature sensitivity, relatively short lifetimes (1-4μs), and shortwave excitation and emission (Lakowicz, 2006; Borisov, 2018).

Platinum (II) porphyrin complexes are very popular due to their simple synthesis and commercial availability. In addition, a number of modifications of the porphyrin ring structure increases their versatility (Borisov, 2018). Pt (II) complexes are more sensitive to oxygen quenching than ruthenium-based dyes to due to longer lifetimes. They have lifetimes of 50-100 μs and are moderately quenched by ambient oxygen, making them suitable for physiological analysis (0% - 21% O_2) (Papkovsky, 1995). Pt (II) octaethylporphyrin (PtOEP) offer good brightness (defined as the molar excitation coefficient x luminescence quantum yield) (Wang & Wolfbeis, 2014) upon excitation in the UV range but with moderate photostability, leading to photobleaching (Borisov, 2018). To overcome this limitation, the aforementioned complexes have been substituted with Pt (II)-meso-(pentafluorophenyl) porphyrin (PtTFPP) which have increased photostability but a lower brightness (Borisov, 2018). Other examples include Pt (II)-coproporphyrins, which have high phosphorescence when excited in the UV range and relatively long decay times at room temperature (Wang & Wolfbeis, 2014). In addition, they are water-soluble and non-toxic, making them ideal for sensing dissolved O_2 in aqueous samples.

Near infrared emitting phosphorescent dyes such as Pt-tetrabenzoporphyrins (PtTBPs) are preferred over those emitting in the visible light range due to minimal interference from sample autofluorescence, background from support media, and reduced effects of excitation on light-sensitive products (Banerjee et al., 2016). Furthermore, PtTBPs have high molar absorption coefficients, high emission quantum yields and are relatively photostable (Quaranta et al., 2012). However, due to their phenol groups they are hydrophobic and require immobilisation in polymers.

1.6.3. Main types of sensor materials

1.6.3.1. Solid state sensors

In solid state O_2 sensors, luminescent dye is incorporated into a polymer matrix, which provides optimal quenchability by O_2, shields from unwanted quenching interferences and facilitates sensor handling. In addition, since the sensor components are immobilised and do not directly interact with the sample, solid state sensors are reusable and cannot be contaminated. Polymer matrices are chosen based on the following criteria: i) oxygen permeability; ii) compatibility with the dye (i.e. no aggregation); and iii) physical properties (insolubility in water) and chemical stability over time (Borisov, 2018).

Luminescent dyes dictate the type of polymer matrix, with relatively short lifetime dyes such as $[Ru(dpp)_3]^{2+}$ requiring polymers with high oxygen permeability. Dyes with longer lifetimes such as Pt (II)-porphyrins require polymers with medium to low oxygen permeability. Common polymers include sol-gel (organic porous polymer), polystyrene, and polysulfone. They have moderate to high gas permeability, high chemical and mechanical stability, and ability to form transparent coatings (Wang & Wolfbeis, 2014, Banerjee et al., 2016). Once the dye has been dissolved in a suitable organic solvent and mixed with a polymer of choice to form a sensor cocktail, it can be further applied onto a solid support to form a solid state sensor coating. The application of a sensor material onto a solid support allows for extra mechanical support, provides a suitable area for biological modification, and eliminates difficulties associated with adhesion of the sensing layer to the environment in question.

1.6.3.2. Water soluble probes

Water-soluble probes are comprised of several categories. The small molecule probes are based on hydrophilic oxygen-sensitive dyes that have multiple charged or polar groups which provide solubility in aqueous solutions. Unfortunately, such probes have several limitations such as: i) non-specific binding to proteins, cells and surfaces; ii) sensitivity to sample composition (protein content, pH, ionic strength); and iii) heterogeneous O_2 sensing properties (Papkovsky et al., 2012). These impediments can be partially addressed by supramolecular probes, which combine several distinct functionalities with the oxygen-sensitive dye to form one chemical entity (Papkovsky et al., 2012). This usually involves conjugation to a hydrophilic protein or dendrimer (O'Donovan et al., 2005; Lebedev et al.,

2009; Borisov, 2018) An example of a supramolecular probe is the Pt (II) coproporphyrin dye covalently linked to bovine serum albumin (BSA), commercially available as MitoXpress™. Conjugation with BSA allows for effective shielding and optimal sensitivity to O_2 (O'Donovan et al., 2005). However, since these probes are exposed to the sample, they are susceptible to interference from sample components.

1.6.3.3. Nanoparticle based probes

Nanoparticle based probes combine the functional properties of solid-state sensors and soluble probes (Ast et al., 2012). These structures tend to be 30-200 nm in size and consist of a polymeric matrix in which the indicator dye is incorporated by either: physical inclusion in a gel, co-precipitation and formation of core-shell structures or chemical linkage to the polymer backbone or surface groups (Papkovsky et al., 2012). Nanosensors have several advantages including low toxicity, measurement of intracellular oxygen gradients, high specific brightness and photostability, low interference from proteins, as well as minimal dye leaching (Ast et al., 2012; Papkovsky et al., 2012). Nonetheless, there are some challenges associated with nanoparticle based probes which include variable size, distribution and physical properties, instability during prolonged storage, and difficulties in controlling the composition and structure during fabrication (Papkovsky et al., 2012). NanO2 is an example of a nanoparticle based probe which is composed of the cationic polymer Eudragit RL-100 and the hydrophobic phosphorescent dye PtPFPP. It exhibited self-loading capabilities, very high brightness and photostability as well as a low degree of cell specificity (Fercher et al., 2011).

1.6.4. Main formats of oxygen respirometry

There are various formats for the detection and measurement of oxygen respirometry due to the versatility of probe chemistries which allows for a broad range of applications and analytical tasks. The traditional set-up for oxygen respirometry is the simple air-tight cell, which consists of a quartz cuvette with a stopper (Papkovsky et al., 2012). This allows for the accommodation of the biological sample with the probe and measurement occurs on a spectrometer. The probe phosphorescent signal and subsequent changes over time are determined and related to oxygen concentration. For accurate quantification the anaerobic cuvette should have the following: i) no headspace or bubbles as air has much higher capacity for O_2 than aqueous media; ii) maintained at a constant temperature and iii) stirred to

uniformly to distribute respiring matter (Papkvosky et al., 2012). Although multiple cuvettes can be set up using a fluorescent reader with a multi-cell holder, it is still limited by sample throughput and requires modifications to the anaerobic cuvette.

The LightCycler® system, originally developed for quantitative PCR, makes use of narrow-bore capillary cuvettes which are measured by a dedicated fluorescent detector (Papkovsky et al., 2012). The glass cuvettes are impermeable to ambient oxygen and their geometry (narrow neck and long sample bottom) aid in the elimination of oxygen diffusion to the bottom of the capillary, where optical measurements take place (Zitova et al., 2010). The limitations of this system are sample throughput as well as high probe concentrations (O'Mahony et al., 2005).

Conventional microtiter plates (96 or 384 well plates being the most common) are particularly advantageous for miniaturisation of assays and high sample throughput. In addition, they make use of available laboratory equipment such as multi-channel pipettes and TR-F plate readers (Papkovsky et al., 2012). Plates can be unsealed or sealed with a layer of mineral oil, which creates a barrier for oxygen diffusion into the sample. However, both the mineral oil and polystyrene plates are permeable to ambient oxygen and therefore only relative OCR measurements can be obtained. Another variation of the microtiter plate is the low volume sealable microplate developed by Luxcel Biosciences. A small excess of sample is added to each well, which is retained by capillary forces, and the application of the lid starts the oxygen uptake assay (O'Mahony et al., 2005). The lid drives the excess sample to overspill areas, removing excess oxygen and creating a seal from ambient air. Similar limitations exist as to the microtiter plates since oxygen can still diffuse through the capillary liquid gap and plastic plate body. Moreover, sample throughput is significantly decreased as each plate can only handle six samples.

Another measurement format are microfluidic biochips, also known as lab-on-a-chip platforms, which are characterised by the integration and miniaturisation of various biochemical operations.

1.6.5. Applications of oxygen respirometry

Optical oxygen respirometry has a wide range of applications due to its ability for contactless and non-invasive measurements. This is an added benefit in biological applications as sterility is an ongoing issue. The system setup with the implementation of both liquid probes and solid-state sensors can be adjusted based on the biological application of choice.

An initial application of the solid-state sensor was the cell viability assay developed for the monitoring of the fission yeast *Schizosaccharomyces pombe* (O'Riordan et al., 2000). The assay comprised disposable phosphorescent sensors made from Platinum (II)-octaethylporphine-ketone (PtOEPK) in polystyrene spotted on microporous filter membranes and inserted at the bottom of microwells. This allowed for contactless measurement of oxygen respiration.

One of the current trends is the application of solid-state sensors in microdevices. A microbioreactor with integrated sensors for monitoring dissolved oxygen, pH, glucose levels and optical density of *Saccharomyces cerevisiae* cultivations was developed (Lladó Maldonado et al., 2018). The dissolved oxygen sensor spot was based on the Pt (II)-*meso*-tetra(4-fluorophenyl)tetrabenzoporphyrin (PtTPTBPF) dye and measured using the handheld phase shift fluorimeter, FirestingO_2 (Pyrosciences, Germany). The microbioreactor provided valuable information on cell cultivation kinetics.

A microfluidic system was designed for the monitoring of oxygen consumption of mammalian cells using PtTFPP in polystyrene as the oxygen sensor (Bunge et al., 2019). Aside from the microfluidic chip with phosphorescent oxygen sensor film, the system included heater and temperature sensor, external optical readout, and 3-D printed holders and housing. Another microfluidic thermoplastic chip was designed for the monitoring of cellular respiration and acidification utilising PtTPTBPF as the oxygen sensor (Müller et al., 2021).

A biochip system was developed as an integrated platform for the assessment of antimicrobial susceptibility (Liu, Lehnert, et al., 2021). A bacterial oxygen consumption rate (OCR) assay was developed using a dedicated microchamber based isothermal platform,

which incorporated a solid-state PtTPTBPF sensor spot, to monitor growth of bacteria when exposed to three clinically relevant antimicrobials. OCR curves were dependant on antimicrobial concentration and time to oxygen depletion was prolonged for increased antimicrobial concentrations.

Contactless measurement of hypoxia in coastal waters was done using commercially available sensors and FirestingO_2 (Pyrosciences), which outperformed traditional methods (Sukigara et al., 2021).

Liquid probes have had a multitude of applications ranging from analysis of cellular components to small aquatic organisms. One of the initial applications using the PtCP-BSA oxygen probe was the high throughput viability screening of mammalian cells (Hynes et al., 2003). The PtCP-NCS probe was first conjugated with BSA then used in screening cellular respiration utilising the previously described 96 well plate format with mineral oil. A linear dependency was observed based on the phosphorescent slope and initial cellular concentration. In addition, the oxygen probe did not exhibit cellular toxicity. This assay was an improvement on pre-existing assays as it greatly reduced time to result, required relatively low concentrations of both cells and oxygen probe, and allows for drug library screening (Hynes et al., 2003). An important parameter of drug screening is the drug-induced toxicity to mitochondria (Hynes et al., 2006), which readily consumes oxygen. Furthermore, the assessment of oxygen consumption is a direct reflection of the function of the electric transport chain (ETC) which in turn is responsible for oxidative phosphorylation and cellular metabolism (Will et al., 2006). An assay was developed using the aforementioned conjugated oxygen probe to monitor mitochondrial oxygen consumption rates when exposed to classical inhibitors and uncouplers of oxygen phosphorylation (Hynes et al., 2006; Will et al., 2006). Similarly, the assay allowed for rapid screening of numerous drugs in a high throughput manner. An integrated respirometric biochip was developed for the assessment of oxygen consumption of preimplantation mouse embryos using the phosphorescent oxygen probe (O'Donovan et al., 2006).

The liquid probe assay was further developed for the study of small aquatic organisms and animal-based toxicity screening (O'Mahony et al., 2005). Three different formats of the respirometric assay using the PtCP based oxygen probe were implemented (sealable 96 well plates, 384 well plates, and LightCycler glass capillary tubes) and two animal models were

used (*Artemia salina* and mouse embryos). All three formats allowed for the monitoring of oxygen consumption across the two models, however, the LightCycler capillary tubes outperformed the plates. However, as previously mentioned, the LightCycler capillary tubes are themselves limited in sample throughput and require higher probe concentrations. The effects of toxicants on *Artemia* were also investigated and 50% effective concentration (EC50) values were determined from dose-response curves. Building on the toxicity screening assay, the effects of chemical and environmental samples using a panel of test organisms ranging from prokaryotes to vertebrate was developed using the standard 96 well plate format (Zitova et al., 2008). The assay enabled the detection of minute, sublethal toxicological effects while providing extensive toxicological data.

Aerobic bacteria consume oxygen relatively quickly due to fast generation times and thus make ideal candidates for respirometric analysis. The growth of three different bacterial species (*E. coli*, *P. fluorescens*, and *M. luteus*) and microbial growth in complex food homogenates was investigated using the aforementioned liquid probe (O'Mahony & Papkovsky, 2006). Clear respiration profiles were achieved, which allowed for further analysis of initial bacterial concentrations, doubling times, and effects of toxicants. TVCs of food samples were further investigated using meat homogenates with the now standard fluorescent probe and microplate setup (O'Mahony et al., 2009). The test provided rapid and accurate results and correlated well with the traditional ISO method. The system was also used to enumerate bacteria in fish samples (Hempel et al., 2011) and to assess bacterial growth patterns in a panel of selective media (Jasionek et al., 2012). Furthermore, the system was commercialised and validated against traditional methods using meat samples (Fernandes et al., 2013).

More recent applications of the liquid probe have been in the analysis of cell metabolism. The Agilent Seahorse XF24 extracellular flux analyser, which uses two sensor types to monitor cellular oxygen consumption and extracellular acidification rates, was applied to three different cancer cell lines when exposed to the natural cytotoxic product mensacarcin (Plitzko & Loesgen, 2018). The combined analysis of respiration, glycolytic flux, Krebs cycle activity, ATP-levels and total biomass allowed for an informative initial assessment of the current metabolic state of the cell (Papkovsky & Zhdanov, 2021).

1.7. Conclusions

The above sections outline the current methods available for the detection microbes and pathogens in the food industry. Current methods tend to rely on sophisticated laboratory equipment, have lengthy time to result, and require skilled personnel in a centralised or external lab away from food processing facilities. Although some handheld/portable devices are available (such as ATP bioluminescence kit, and Petrifilm plates), they cannot handle crude food homogenates and can be easily overloaded with sample. There is a need for rapid and de-centralised microbial methods for the food industry as well as the research community.

Chapter 2: Experimental Methods

2.1. Materials

Ethyl Lauryl Arginate (LAE; IUPAC name: Ethyl N5-(diaminomethylene)-N2-dodecanoyl-l-ornithinate) and Plate count agar (PCA) were purchased from Sigma-Aldrich Merck (Dublin, Ireland). Nutrient Broth (NB), Luria-Bertani (LB) Broth, Mueller-Hinton Broth (MHB), and Maximum Recovery Diluent (MRD) were from Fisher Scientific Oxoid (Dublin, Ireland). 30 mL Sterilin™ clear polystyrene vials were purchased from Fisher Scientific. Sterile 10 mL swab tubes and polystyrene 96 well microplates were purchased from Sarstedt (Waterford, Ireland).

Phosphorescent O_2-sensing probe MitoXpress® Xtra (Pt(II)- coproporphyrin conjugated with Bovine Albumin Serum (BSA)) was purchased from Agilent (Cork, Ireland). The sensor coating cocktail, comprised of polymeric micropracticles impregnated with a Pt(II)-tetrabenzoporphyrin (PtBP) dye and suspended at a 40 mg/mL concentration in 95% ethanol containing 5% hydrogel (polymeric binder) was kindly provided by Agilent. To create the sensor vials, the cocktail (stored at 4°C in the dark) was sonicated for 2 min (Fisherbrand Ultrasonic Bath FB15047, Fisher Scientific, United Kingdom) and quickly vortexed. 5 µL of the sensor cocktail was dispensed either onto the bottom of the sterile vial (30 mL) or onto the bottom side wall (10 mL) in a sterile environment, using a Distriman™ repetitive pipette (Gilson). All tubes were left to air dry in a laminar flow hood for 1 hr then sealed with caps to maintain sterility. Typically, batches of 50-100 sensor vials were produced and stored in the dark at room temperature for up to 3 months until further use.

Stock cultures of *Escherichia coli* NCIMB 11943 (*E. coli*), *Pseudomonas fluorescens* DSM 50091 (*P. fluorescens*), *Staphylococcus aureus* ATCC 1448 (*S. aureus*), and *Bacillus cereus* NCIMB 9373 (*B. cereus*) were obtained from the School of Microbiology, University College Cork and Teagasc Food Research Centre (Ashtown, Dublin) and stored at -80°C in 80% glycerol in LB broth. Working cultures were prepared by inoculating 50 µL of semi-defrosted stock in 5 mL of LB broth and incubating on a rotary shaker at 250rpm at either 37°C (*E. coli* and *S. aureus*) or 30°C (*P. fluorescens* and *B. cereus*) until an OD600 OF ~ 0.8 was reached (typically overnight).

Meat samples were obtained either from a local meat processing factory, from a local butcher or store-bought. Carcass swab samples were collected by the meat processing factory according to the ISO 17604:2015 procedure using Carcass Sponge Sampling Kits (Technical Service Consulting Ltd) to swab a 10 × 10 cm area of the carcass.

2.2. Determination of total aerobic viable counts (TVCs) by agar plating

1:10 serial dilutions of overnight bacterial cultures were prepared using NB and 100 µL aliquots of these suspensions were spread-plated onto PCA in duplicate. Plates were incubated at either 37 °C or 30 °C overnight and then grown colonies were enumerated using an automatic counter pen (VWR International, Dublin, Ireland). Concentrations of the initial bacterial stocks were calculated from plate counts (typically 10^9 CFU/mL) and then diluted to the desired working concentrations (10^8-10^2 CFU/mL) using LB broth or MRD.

The microbial load (CFU/g) of meat samples was calculated in accordance with the standard method (ISO 4833-1:2013). A 10g meat sample was taken from the surface and placed in a sterile mesh lined stomacher bag (Filter Bag, 400 Series, Grade; Spark Lab Supplies, Dublin, Ireland) to which 90 mL of MRD was added. The contents were then stomached using a Colworth Stomacher 400 (Colworth, UK) for 2.5 min. The resulting meat homogenate was serially diluted using 900 µL of MRD and plated on PCA plates in duplicate. Plates were then incubated for 48- 72 hrs at 30 °C and counted.

For swab samples, the microbial load (CFU/cm^2) was calculated in accordance with the standard method (ISO 18593:2018). For carcass swab samples, 100 mL of MRD was added directly to the sampling bag and stomached using a Stomacher 400 for 2.5 min. For in-house swab samples (artificially contaminated with *E. coli* or natural meat microbiota and environmental swabs), 10 mL of MRD was added to sample vials and vortexed for 30 seconds to create a bacterial suspension. For all swab types, the resulting suspension was serially diluted using 900 µL of MRD and plated on PCA plates in duplicate. Plates were then incubated and enumerated as mentioned above.

2.3. Respirometric plate reader assays

MitoXpress®-Xtra probe stock was reconstituted in 1 mL of dH_2O and further diluted in 15 mL of NB. The solution (media and probe) was dispensed in 100 µL aliquots to each test well of a 96-well plate. In-plate serial (1:3) dilutions of LAE stock (2 mg/mL) were prepared to produce concentrations ranging from 166.7 µg/mL to 2.1 µg/mL. 15 µL of bacterial stock was added to assay wells to give a final concentration of 10^4, 10^5 or 10^6 CFU/mL in the well. For each condition, 3 replicates were included on the plate, plus positive (bacteria with no antimicrobial) and negative (media only) controls (Figure 2.1). Using the same range of LAE concentrations, the assay was also performed using 100 µL of meat homogenate (section 2.2) per well in triplicate.

40 µL of mineral oil was then added to each well to seal the samples from ambient air, the plate placed in a Victor4 (PerkinElmer) reader pre-heated to 30 °C or 37 °C and monitored in time resolved fluorescence (TR-F) mode for 10 hrs measuring probe signal for each well every 5 min in kinetic mode. TR-F settings were: excitation filter – 340 nm, emission filter - 642 nm, delay times of 30 µs and 70 µs (two windows), gate time - 100 µs (for each delay window). For each reading and sample well, the phosphorescence lifetime values (LT) were calculated in Excel using the formula: $LT= (t_2-t_1)/\ln(F_1/F_2)$ where t_1 and t_2 are the delay times (30 and 70 µs) and F_1 and F_2 are the corresponding intensity signals (O'Mahony et al., 2005). The resulting LT profiles were plotted and analysed to determine the time required (time to result) to reach the threshold LT signal, which was set at 35 µs. For consistent results preparation time for the plate was kept under 15 min.

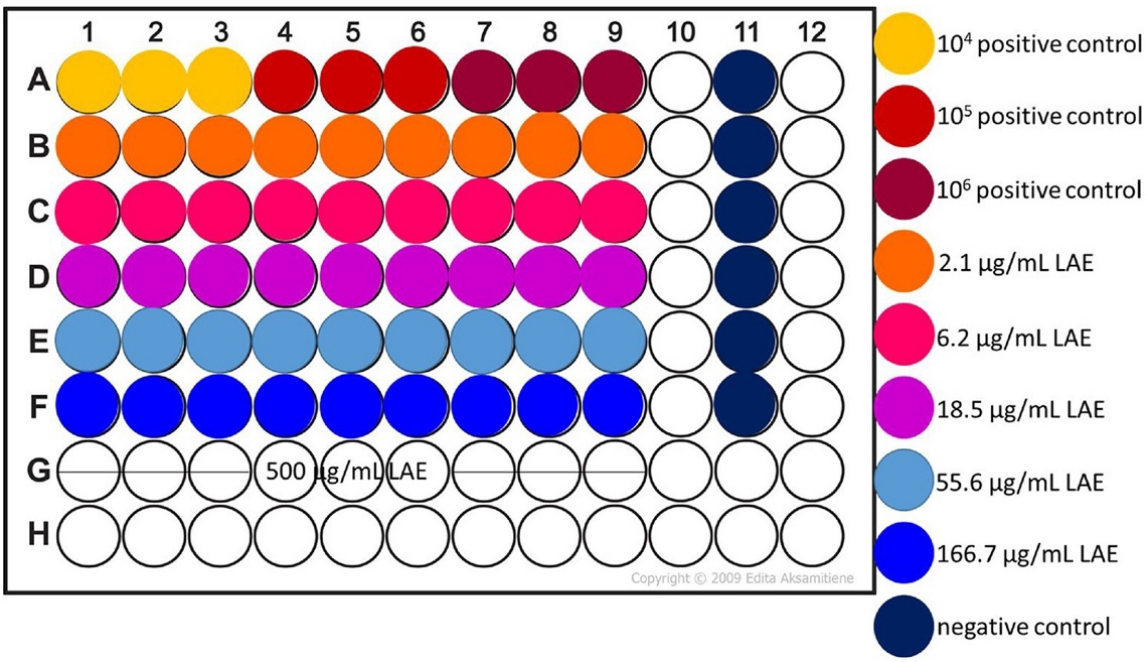

Figure 2.1: Typical plate layout used in respirometric assays with concentrations of LAE ranging from 166.7 µg/mL to 2.1 µg/mL, bacterial cultures at 10^4, 10^5 and 10^6 CFU/mL in wells, the required replicates, positive and negative controls.

2.4. Reference antimicrobial test

A reference method for the Minimum Inhibitory Concentration (MIC) determination (adapted from Eloff (1998) and Wiegand et al. (2008)) was applied to two representative bacteria, *E. coli* (Gram-negative) and *S. aureus* (Gram-positive). 100 µL aliquots of MHB were added to each assay well and LAE was serially diluted (1:3) on the plate to give the same concentration range as mentioned in section 2.3. 100 µL of bacterial suspension was added to the wells to give a final concentration of 10^5 CFU/mL, with each condition set up in triplicate. The plate was sealed with mineral oil (40 µL) and an initial reading of optical density was measured at a wavelength of 600 nm using a plate reader. Following an overnight incubation (18 hrs) at 37 °C, the optical density was measured again. MIC was determined using the interpretation suggested by Wiegan et al. (2008), in which the lowest concentration of the antimicrobial that inhibits visible growth is said to be its MIC.

2.5. Respirometric assays in sensor vials

2.5.1. Vial measurement and QC

Sensor vials were measured using the autonomous hand-held sensor reader FirestingGO$_2$ (Pyroscience, GmbH), which recorded both the phosphorescence intensity (mV units) and phase shift (degrees angle units, dphi) signals from the sensor. The FirestingGO$_2$ was set at default LED frequency 4 kHz, Intensity 100% and amplification 400×. Batches of up to 20 sensor vials were incubated at 30 °C for 10 hrs and the sensor signal, dphi, was measured manually every hour through the sensor either located at the side or at the bottom of the vial (Figure 2.2). Care was taken as to ensure no mixing of the vial contents occurred when measurements were taken.

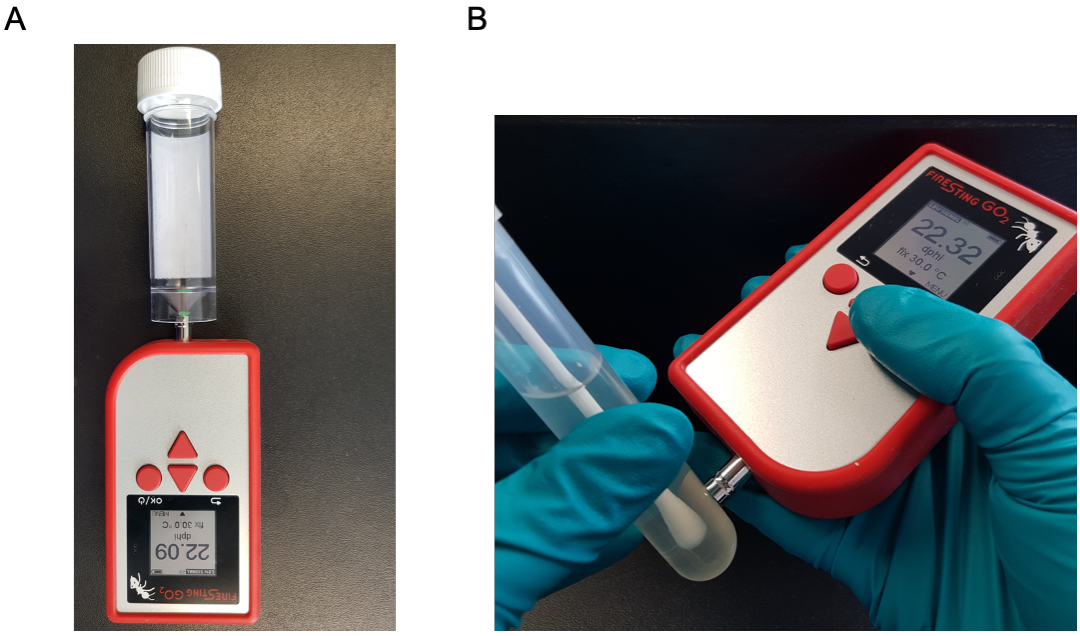

Figure 2.2: Measurement of sensor vials for two types of vials: **(A)** 30 mL Sterilin™ vials and **(B)** 10 mL swab vials.

2.5.2. Oxygen calibration

For sensor spot oxygen calibration, vials were filled with NB and placed in a water bath equilibrated to 30 °C. The vials were then purged sequentially using standard O_2/N_2 gas mixtures produced by a precision gas mixer/tonometer (LNI, Switzerland) and gradually changing the ratio from 0 kPa to 21 kPa (21% O_2). Measurements of the sensor signal (*dphi*) were taken using the FirestingGO$_2$ after temperature and O_2 equilibration occurred (seen as stable phase readings). The phase signal readings were then plotted as a function of O_2 concentration in Excel, from which an analytical equation was derived (see section 4.2.2).

2.6. Preparation and analysis of meat and carcass swab samples

To first establish the relationship between initial microbial load (Log CFU/g or Log CFU/cm^2) and primary sensor signal, *dphi,* the sensor system was calibrated with *E. coli*. An overnight *E. coli* culture (approximately 10^9 CFU/mL) was serially diluted in MRD (2 mL or 10 mL) and added to sensor vials in the following sample to NB ratios (for a total volume of 20 mL): 1:1 or 1:9, respectively. All vials were incubated for 10 hrs at 30°C and measurements were taken hourly using the FirestingGO_2. Initial readings were taken before incubation.

To account for the complex sample matrix associated with food homogenates, the 30 mL sensor vials were further calibrated using spiked meat homogenate. Fresh meat samples, obtained from the meat processing factory, with microbial loads of less than 10 CFU/g (verified using the ISO4833-1: 2013 method) were frozen at -20°C for 48 hrs, thawed, and subsequently exposed to UV light (in a laminar flow hood) for 15 min per side to kill any remaining microbiota. These samples were then homogenised as described in section 2.2, from which 39.6 mL aliquots were taken and spiked with 400 µL of varying *E. coli* concentrations (10^2 to 10^8 CFU/mL in MRD). Inoculated homogenates were thoroughly vortexed for 20 seconds. 10 mL of each inoculated homogenate was then added to sensor vials in either 1:1 or 1:9 ratios to NB. Vials were incubated and signal readout was determined as previously mentioned. TVC method (section 2.2) was done in parallel.

The 30 mL sensor vials were validated using the meat samples (n = 58) and carcass swab samples (n = 24) obtained from the meat processing factory. Homogenates were made as described in section 2.2 and added to sensor vials in a 1:1 ratio with NB. Vials were then incubated as mentioned previously and signal readout was recorded using the FirestingGO_2 (Figure 2.2).

2.7. Preparation and analysis of swab samples

The 10 mL swab vials were initially calibrated using pure *E. coli* culture (10^9 CFU/mL) serially diluted in 900 µL MRD (10^8- 10^3 CFU/mL) to establish the relationship between sensor signal and microbial load (CFU/cm^2). To each vial, 1 mL of *E. coli* dilution was added to 9 mL NB and all vials were incubated and analysed as in section 2.5.3.

The system was then validated by analysing the following surfaces: i) artificially contaminated with *E. coli*, ii) environmental swabs and iii) contaminated with meat

microbiota. In the first case, an overnight culture of *E. coli* was serially diluted 1:10 in 20 mL of MRD for a range of concentrations from 10^8 to 10^4 CFU/mL. These *E. coli* dilutions were transferred into individual 30 mL plastic spray bottles (bought from a local chemist, sterilised with 70% ethanol), from which two pumps of the spray (~ 200 µL) were applied on each surface of 10 x 10 cm plastic trays with lids (Sarstedt) and allowed to air dry in a laminar flow hood for 20 min. Artificial contamination of surfaces was done in replicate as to use swabs for both the sensor system and reference method (ISO 18593: 2018). Swabs from the 10 mL vials (with sensor coating and without) were pre-wetted with approximately 1 ml MRD and used to swab each surface as per standard procedure. For the sensor system, 10 mL of NB was added directly to the vial and vortexed for approximately 30 seconds. Readings were taken using the FirestingGO_2 as described in section 2.4 (Figure 2.2).

For the second case, samples were obtained by swabbing (according to ISO 18593: 2018) laboratory surfaces such as sinks, benchtops, etc. with pre-wetted (MRD) swab from 10 mL vials. Swabbing of surfaces was done in replicate as to analyse the samples using the sensor system and the reference method. Environmental swabs were analysed exactly as the artificial contamination swabs were (see above).

For the third case, meat samples (n = 9) purchased from a local butcher were individually placed into the plastic trays, such that their bottom side was covering the tray surface, while the top surface was in contact with air (aerobic environment). The samples were stored in the cold room at 4 ± 1°C for 24 hrs, 48 hrs, or 72 hrs. After this, each meat sample was flipped into the top part of the tray to create an imprint of the microbiota from the top surface. Pre-wetted (MRD) swabs from 10 mL sensor vials were used to swab the tray surfaces with meat sample imprints, using a different swab for the top and bottom of the tray.10 mL of NB was added directly to sensor vials and vortexed for approximately 30 seconds. 200 µL of the suspension was removed from the vial for analysis via agar plating method (section 2.2).

2.8. Shelf life studies with packaged meats

Mincemeat samples (n = 32) of beef, pork, turkey, and lamb were purchased from a local supermarket and ensured to be of Irish origin. 4 packs per meat type were purchased at once and counted as a batch. The age of mincemeat samples (Days) was calculated based on printed Best Before dates printed on packs, and the anticipated shelf life of 10-days for these products. A general sampling method was used in which samples were taken for analysis on the following days: day of purchase, 3 days after purchase, Best Before date, and 3 days after Best Before. Samples were stored in the fridge (4± 1°C). On each sampling day, one pack was chosen, opened, and a 10 g sample was taken from the top and from the bottom, creating two sampling points. Meat homogenates were prepared as mentioned in section 2.2 and were analysed using the TVC method (section 2.2) and sensor vial method (section 2.6).

2.9. DNA isolation and 16S rRNA amplicon sequencing

1.8 mL of each mincemeat homogenate was taken and used for genomic DNA extraction with the DNeasy PowerFood Microbial Kit (Qiagen) according to manufacturer's instructions. Two time points were used for extraction: i) before respirometry and ii) after respirometry (when signal threshold of 30dphi (°) was reached). DNA was eluted in 50 µL elution buffer. DNA concentrations as well as the A260/A280 ratio were measured using the NanoDrop One spectrophotometer (Thermo Fisher Scientific). Finally, DNA samples were stored at - 20°C until sent to Macrogen, a DNA sequencing company, and analysed using 16S rRNA amplicon sequencing.

2.10. Bioinformatics analysis of 16S rRNA amplicon sequencing

Three hundred base pair paired-end reads were pre-filtered based on a quality score threshold of >30 and trimmed, filtered for quality and chimaeras using the DADA2 library in R (version 4.1.2). Only samples with >10.000 reads after QC were used in analysis. Taxonomy was assigned with DADA2 against the SILVA SSURef database release v138. Parameters as recommended in the DADA2 manual were adhered to unless mentioned otherwise. ASVs were aggregated at genus level. As ratios are invariant to subsetting and this study employs compositional data analysis techniques, features that were unknown on the genus level were not considered in downstream analysis, as were genera that were only detected as non-zero in 10% or few of total samples.

2.11. Data processing and statistical analysis

All respirometric experiments were repeated at least 2–3 times, to ensure consistency of the data. The dose-response graphs and EC50 values were calculated by plotting the reciprocal of time to result values vs the log of LAE concentration and processing the data in Quest Graph™ EC50 Calculator (AAT Bioquest, Inc). Results are presented as the mean ± standard deviation.

All sensor vials were measured 3 times per reading to ensure consistency of signal readout. The *dphi* values recorded for the vials with FirestingGO_2 reader were extracted from the instrument using Pure Oxygen Logger software (PyroScience) and underwent statistical analysis using SigmaPlot 11 (Systat Software Inc., USA). Results are presented as mean ± standard deviation among replicates. One-way ANOVA test (P = 0.05) and Pearson correlation analysis were done to compare results obtained with the sensor method and reference ISO methods. To analyse the phase and intensity signals from the 30 mL sensor vials, ANOVA test was performed with either Tukey comparison test or Games–Howell method and 95% confidence interval. The consistency of swab vials was analysed using the Mann Whitney Wilcoxon Test, comparing phase and intensity signals obtained in dry vials and in vials containing NB. In respiration tests, time profiles of the phase signal for each assay vial were plotted, then sigmoidal fitting using the Dynamic Fitting Tool in SigmaPlot was applied and signal threshold time, TT (h), was determined for each sample. By applying the calibration equation obtained with either *E. coli* spiked meat or pure *E. coli* culture, these TT values were converted into CFU/g or CFU/mL values, respectively. For swab samples, an additional 0.1x conversion factor was applied to CFU/mL values to convert them into CFU/cm^2 values, which reflect the bacterial load on a 100 cm^2 surface. In addition, non-linear regression analysis of the phase signal data with the four-parameter sigmoidal model was performed (Santovito et al., 2019). Advanced statistical analysis was kindly assisted by Dr. Elisa Santovito (Institute of Sciences of Food Production, National Research Council of Italy).

Further data-handling of bioinformatics data was done in R (version 4.2.2) with the Rstudio GUI (version 1.4.17172022.7.2.576). Stacked barplots were generated by normalizing counts to 1, generating proportions. Genera that were never detected at a 5% relative abundance

or higher were aggregated and defined as rare taxa for the purposes of the stacked barplots. These ‘rare taxa’ were not removed from statistical analysis. The iNEXT library was used to compute alpha diversity for the first three hill numbers (Chao1, Shannon entropy and Simpson Index) (Hseih, Ma & Chao, 2016). Differences in alpha diversity were assessed using linear models. Principal component analysis was performed on centred log-ratio transformed (clr) values as a visual companion to the beta diversity analysis. Zeroes were imputed using the “const” method (Lubbe, Filzmoser, & Templ, 2021). Beta diversity was computed in terms of Aitchison distance (Euclidean distance of clr-transformed counts) and differences in beta diversity were assessed using the PERMANOVA implementation from the vegan library using 10,000 permutations (Aitchison et al., 2000). Differential abundance of taxa and functional modules was assessed by fitting linear models on the clr-transformed count tables. To correct for multiple testing (FDR) in tests involving microbiome features, the Benjamini-Hochberg post hoc procedure was performed with a q-value of 0.1 as a cut-off. Plotting was handled using ggplot2. Custom scripts are available at https://github.com/thomazbastiaanssen/Tjazi (Bastiaanssen, Quinn, & Loughman, 2022). Bioinformatics analysis was performed under the guidance of Dr. Thomaz Bastiaanssen (APC Microbiome Ireland, University College Cork).

Chapter 3: The use of oxygen micro-respirometry to quantify the effects of antimicrobials on common food spoilage bacteria and food samples

3.1. Introduction

There is continuous demand from producers to extend the shelf life of food products, improve their quality and microbial safety, reduce spoilage and waste (Becerril et al., 2013). To combat these challenges, various strategies are being implemented, including packaging materials with antimicrobial treatments (Becerril et al., 2013), new packaging processes (Kerry, 2012), antimicrobial additives to foods (Manrique et al., 2017), smart packaging systems (Kerry, 2012) and (bio)sensor technologies (Banerjee et al., 2016).

With the application of traditional antimicrobials being limited due to their effects on product and colour (in the case of organic salts and acids) or possible toxic and carcinogenic effects (in the case of sulphates, nitrites, and parabens) (Jayasena & Jo, 2013; Carocho et al., 2014), there is a need for new antimicrobials with minimal to no effects on food quality and consumer health. Consumers are more aware of the possible negative effects of additives and actively look for 'clean products'.In addition, the consumer perception of the aforementioned products is also key. A promising antimicrobial compound is the cationic surfactant Lauroyl Arignate Ethyl Ester (LAE) (Ruckman et al., 2004; Manrique et al., 2017). LAE interacts with the charged proteins present in microbial membranes and enzymatic systems, which leads to protein denaturation, increased cell permeability (Pezo et al., 2012), inhibition of growth and ultimately cell death, but without cell lysis (Rodriguez et al, 2004). Although synthetically produced, LAE is metabolised by humans into the natural components of lauric acid and arginine and has thus been classified as Generally Recognised as Safe (GRAS) by the EFSA and FDA (FDA, 2005; EFSA, 2007). In addition, LAE is odourless and tasteless (Pezo et al., 2012), making it an ideal antimicrobial for many food products.

Currently there are several assays to determine the efficacy of antimicrobials. In the disc diffusion method, a disc with a known concentration of antimicrobial is placed on a pre-inoculated agar plate and incubated to determine a zone of inhibition (Hudzicki, 2009). Similarly, the agar diffusion test involves the making of holes of a known diameter in agar plates, filling them with different concentrations of the antimicrobial in question and incubating them to also determine a zone of inhibition (Shin et al., 2001). Alternatively,

chromogenic substrates such as Purple broth and p-iodonitrotetrazolium chloride (INT) dye can be used to visually assess toxicity. Purple broth, which changes colour in the presence of acids, relies on the metabolic activity of bacteria to break down carbohydrates which produce organic acids resulting in a decrease in pH of the growth media (Eloff, 1998). After an overnight incubation, INT dye is added and changes colour from colourless to pink in the presence of growing bacteria (Eloff, 1998). Optical Density (OD6000) can also be used to monitor bacterial growth in the medium in the presence of an antimicrobial (Eloff, 1998).

The aforementioned assays have relatively long time to result (18-20 hrs), crude estimation of toxicity, and lack of automation. In addition, the assays are ill-suited for complex food samples such as crude homogenates, which tend to have plenty of debris, colour, and low clarity. There is a need for a user-friendly, quick alternative to the conventional microbial methods.

3.2. Results & Discussion

3.2.1. Design of the O_2 sensing method for toxicological assessment of antimicrobials

A versatile detection platform, optical oxygen micro-respirometry has already proven its high utility in the analysis of mammalian (Hynes et al., 2005; Will et al., 2006), bacterial cells (O'Mahony et al., 2005) and environmental samples (Zitova et al., 2009). However, its potential with respect to the assessment of antimicrobials remains under-explored. To address this, we have designed a dedicated testing platform, which can provide advanced, high-throughput multiparametric assessment of the action of antimicrobials on bacterial cells. Figure 3.1 illustrates the general concept of this method, with its flexibility and applicability to various bacteria, compounds, testing conditions, and sample types. Furthermore, the biosensing platform can be configured based on user requirements to produce several different, but complementary, readouts. These readouts can be further utilised, either individually or combined, to report on a compound's toxicity in a quantitative and accurate manner.

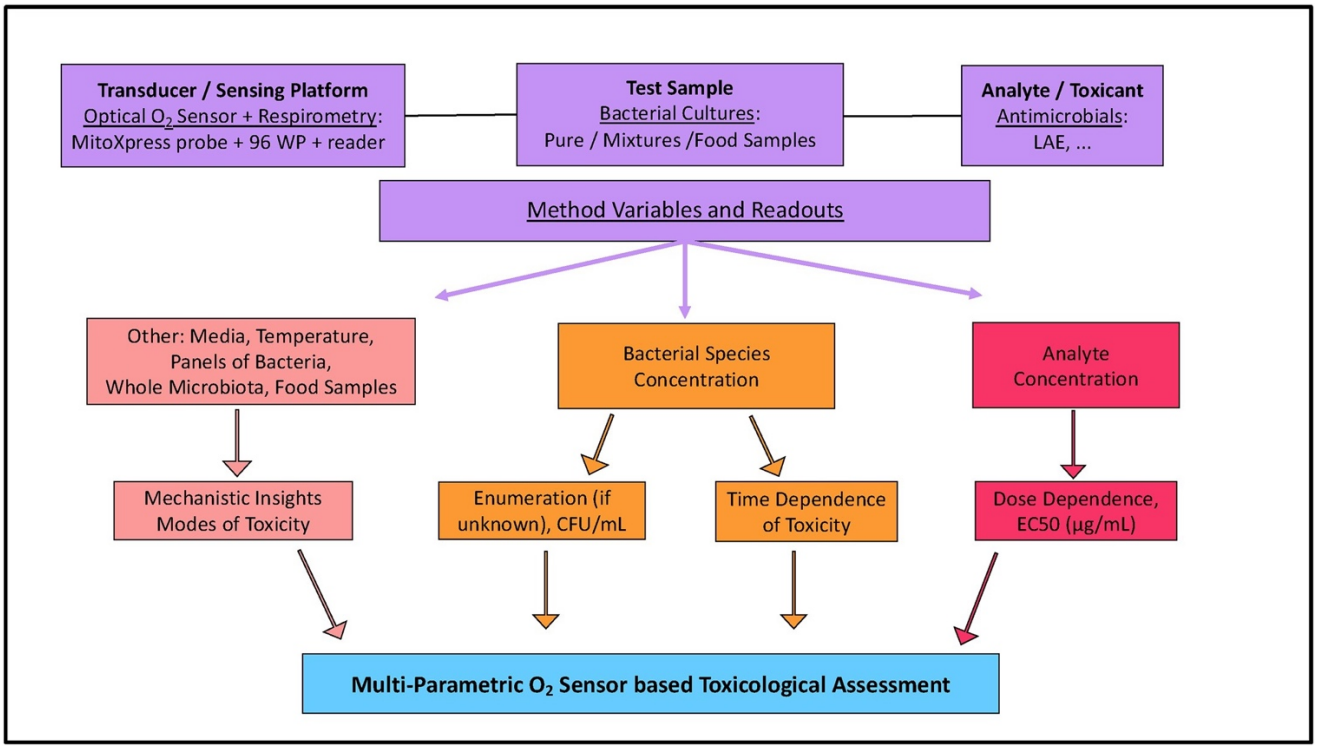

Figure 3.1: General design of the O_2 sensing method for multi-parametric toxicological assessment of antimicrobials, showing the main components of the assays, controllable variables, analytical readouts, and their inter-connection.

3.2.2. Determination of antimicrobial activity of LAE on pure cultures using respirometry

Respirometric analysis of microbial cultures tends to produce sigmoidal time profiles of the sensor/probe optical signal (either in phosphorescence intensity or lifetime). The transition from low to high optical signal is reflective of the steep change from air-saturated sample to deoxygenated sample, which occurs when bacteria reach a certain cell density during their exponential growth (O'Mahony et al., 2005). The onset time of this transition correlates with the sample's initial load of viable cells and can therefore be used for the enumeration of bacteria in unknown samples or quantifying the effects of different factors on test cells.

To test the antimicrobial activity of LAE, samples of two Gram-negative (*E. coli* and *P. fluorescens*) and two Gram-positive (*S. aureus* and *B. cereus*) bacterial species were prepared according to the plate layout in Figure 2.1, at known initial concentrations (10^4, 10^5, or 10^6 CFU/mL) on a 96-well plate in appropriate media containing the O_2 probe and known concentrations of LAE (1:3 serial dilutions for a range of 166.7 µg/mL to 2.1 µg/mL). The

plate was then incubated at 37°C or 30°C for approximately 10 hours in a plate reader while each sample well was measured every 5 minutes. These assay settings allowed us to assess the dose and time dependence of LAE toxicity via EC50 calculation, and the effects of LAE on metabolism and growth of different bacterial cells cultured under various conditions.

Respiration profiles of the different cultures are shown in Figures 3.2 to 3.5. For the Gram-negative species, *E. coli* showed the steepest change from oxygenated to deoxygenated state (Figure 3.2) while *P. fluorescens* showed a more gradual change and (Figure 3.3). As for the Gram-positive species, both *S. aureus* and *B. cereus* exhibited similar changes in the slopes of their profiles (Figures 3.4 & 3.5).

From each respiration profile for a given bacterial concentration, the Threshold Time (TT), i.e. time to reach threshold LT value (set at 35 μs), was determined. The TT values were then converted to their reciprocal value and plotted against log [LAE] (Figure 3.6). For the profiles which produced no signal changes characteristic to cell growth and respiration, zero reciprocal TT values were assigned (i.e. $TT = \infty$). The plots were fitted using sigmoidal fitting to determine EC50 values for each culture and are compared in Figure 3.7.

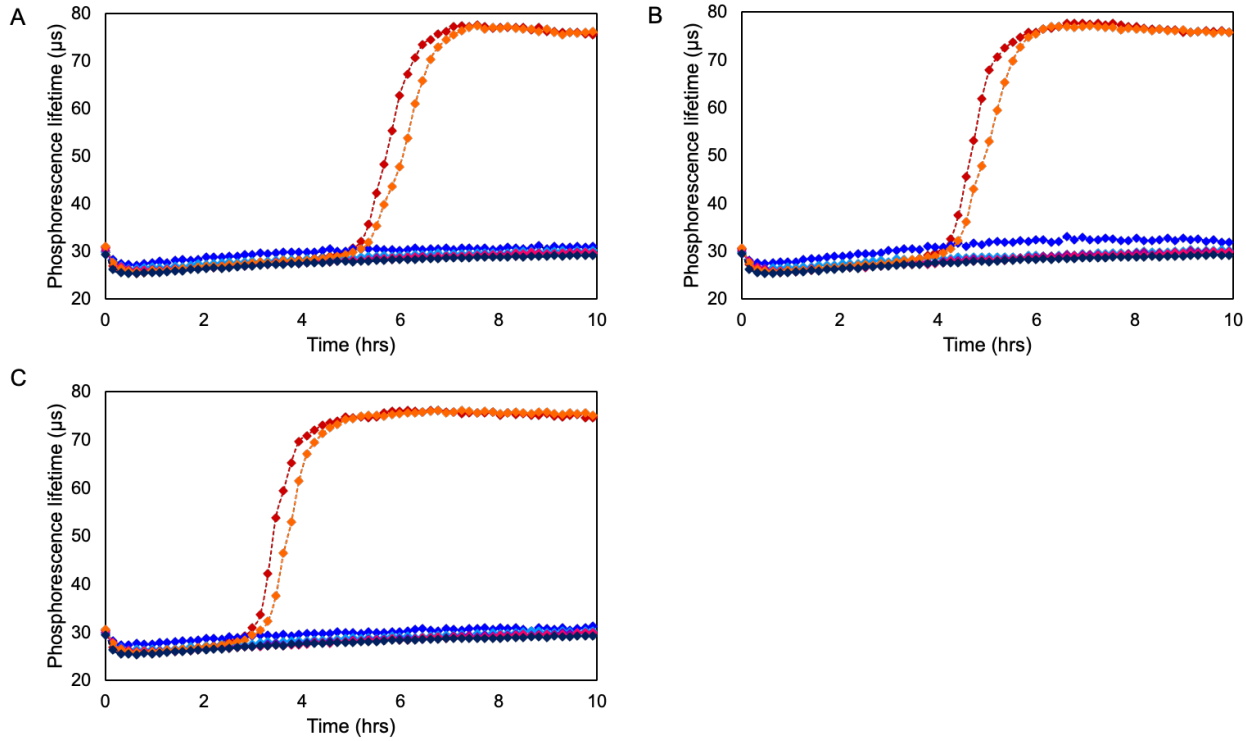

Figure 3.2: Profiles of phosphorescence lifetime of MitoXpress-Xtra probe for Gram-negative *Escherichia coli* exposed to LAE (166.7 µg/mL to 2.1 µg/mL) over 10 hrs. The figure shows combined data of three independent experiments with each value determined in triplicate. Legend: positive control ( ), 166.7 µg/mL ( ), 55.6 µg/mL ( ), 18.5 µg/mL ( ), 6.2 µg/mL ( ), 2.1 µg/mL ( ), and negative control ( ). **(A):** bacterial concentration of 10^4 CFU/mL. **(B):** bacterial concentration of 10^5 CFU/mL and **(C):** bacterial concentration of 10^6 CFU/mL.

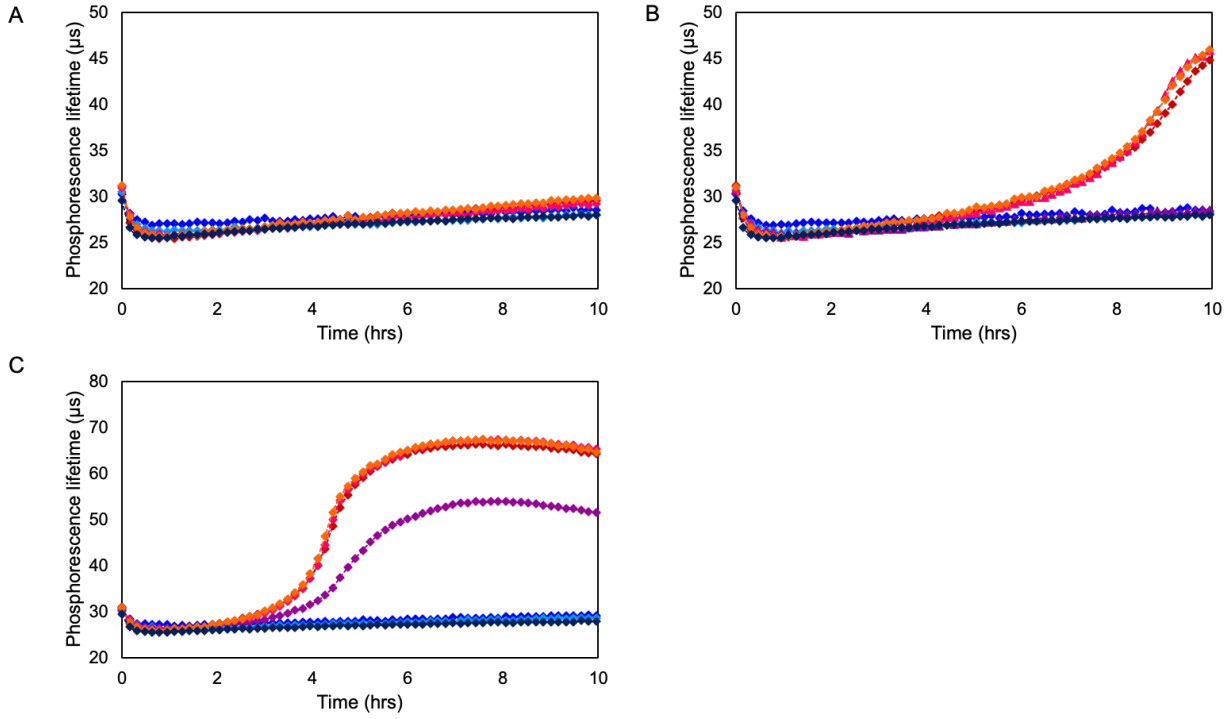

Figure 3.3: Profiles of phosphorescence lifetime of MitoXpress-Xtra probe for Gram-negative *Pseudomonas fluorescens* exposed to LAE (166.7 µg/mL to 2.1 µg/mL) over 10 hrs. The figure shows combined data of three independent experiments with each value determined in triplicate. **(A):** bacterial concentration of 10^4 CFU/mL. **(B):** bacterial concentration of 10^5 CFU/mL and **(C):** bacterial concentration of 10^6 CFU/mL.

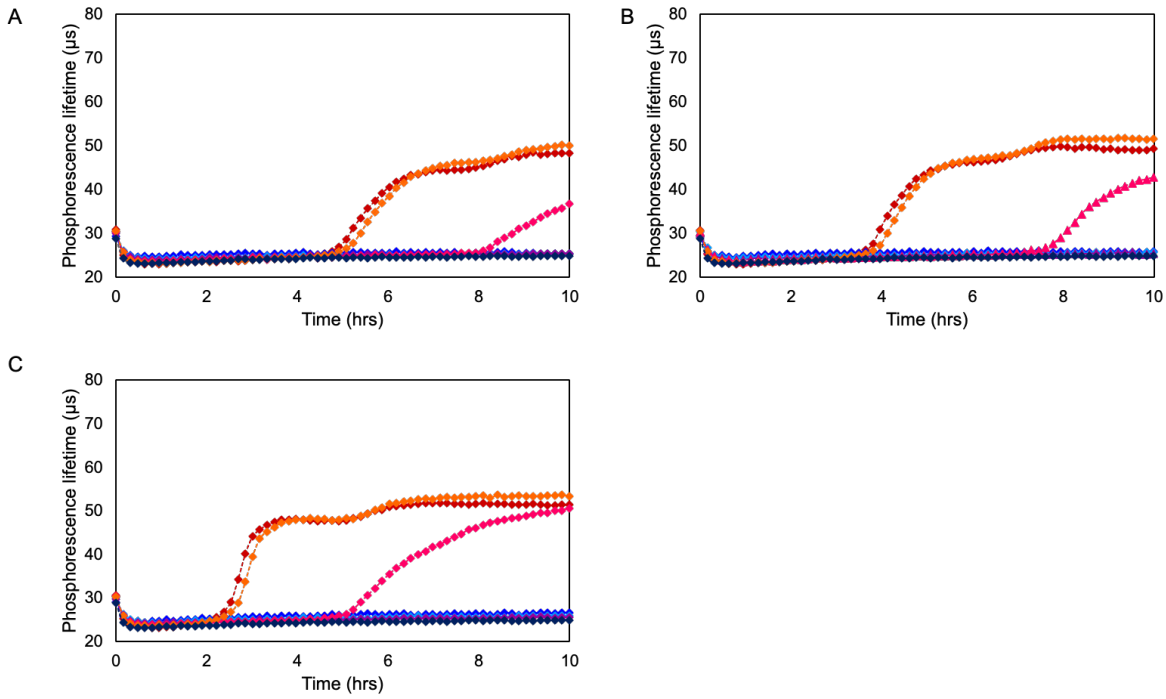

Figure 3.4: Profiles of phosphorescence lifetime of MitoXpress-Xtra probe for Gram-positive *Staphylococcus aureus* exposed to LAE (166.7 µg/mL to 2.1 µg/mL) over 10 hrs. The figure shows combined data of three independent experiments with each value determined in triplicate. **(A):** bacterial concentration of 10^4 CFU/mL. **(B):** bacterial concentration of 10^5 CFU/mL and **(C):** bacterial concentration of 10^6 CFU/mL.

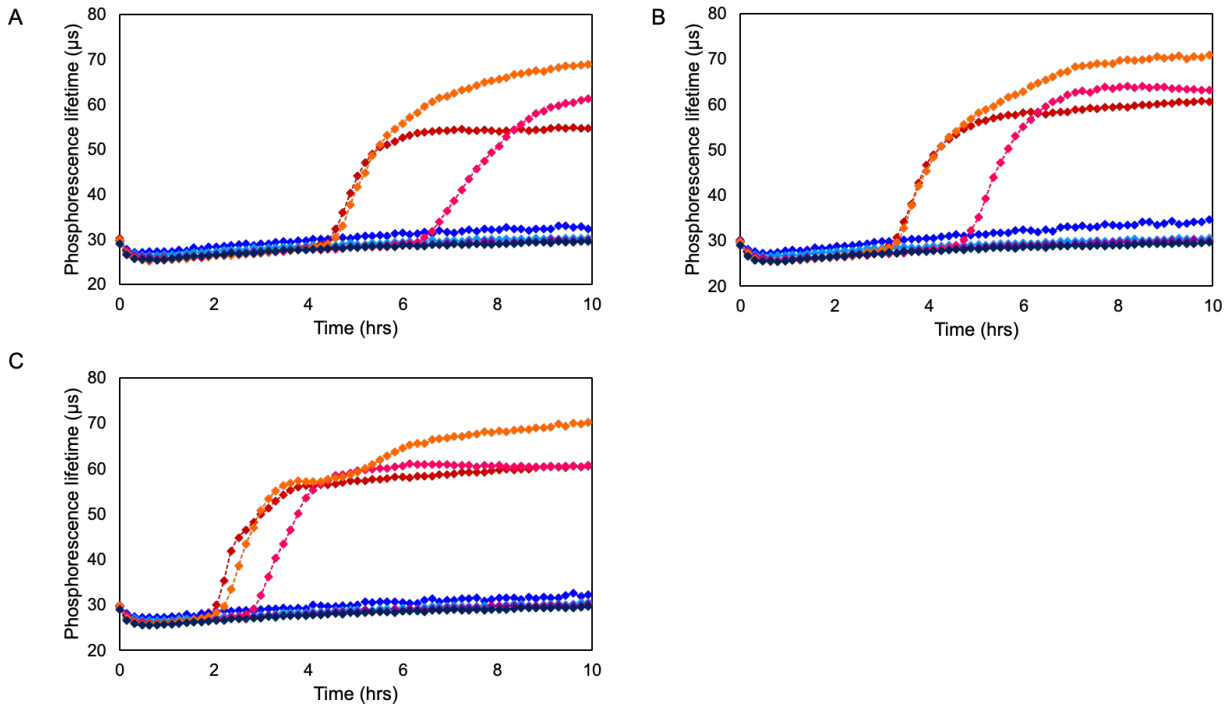

Figure 3.5: Profiles of phosphorescence lifetime of MitoXpress-Xtra probe for Gram-positive *Bacillus cereus* exposed to LAE (166.7 µg/mL to 2.1 µg/mL) over 10 hrs. The figure shows combined data of three independent experiments with each value determined in triplicate **.(A):** bacterial concentration of 10^4 CFU/mL. **(B):** bacterial concentration of 10^5 CFU/mL and **(C):** bacterial concentration of 10^6 CFU/mL.

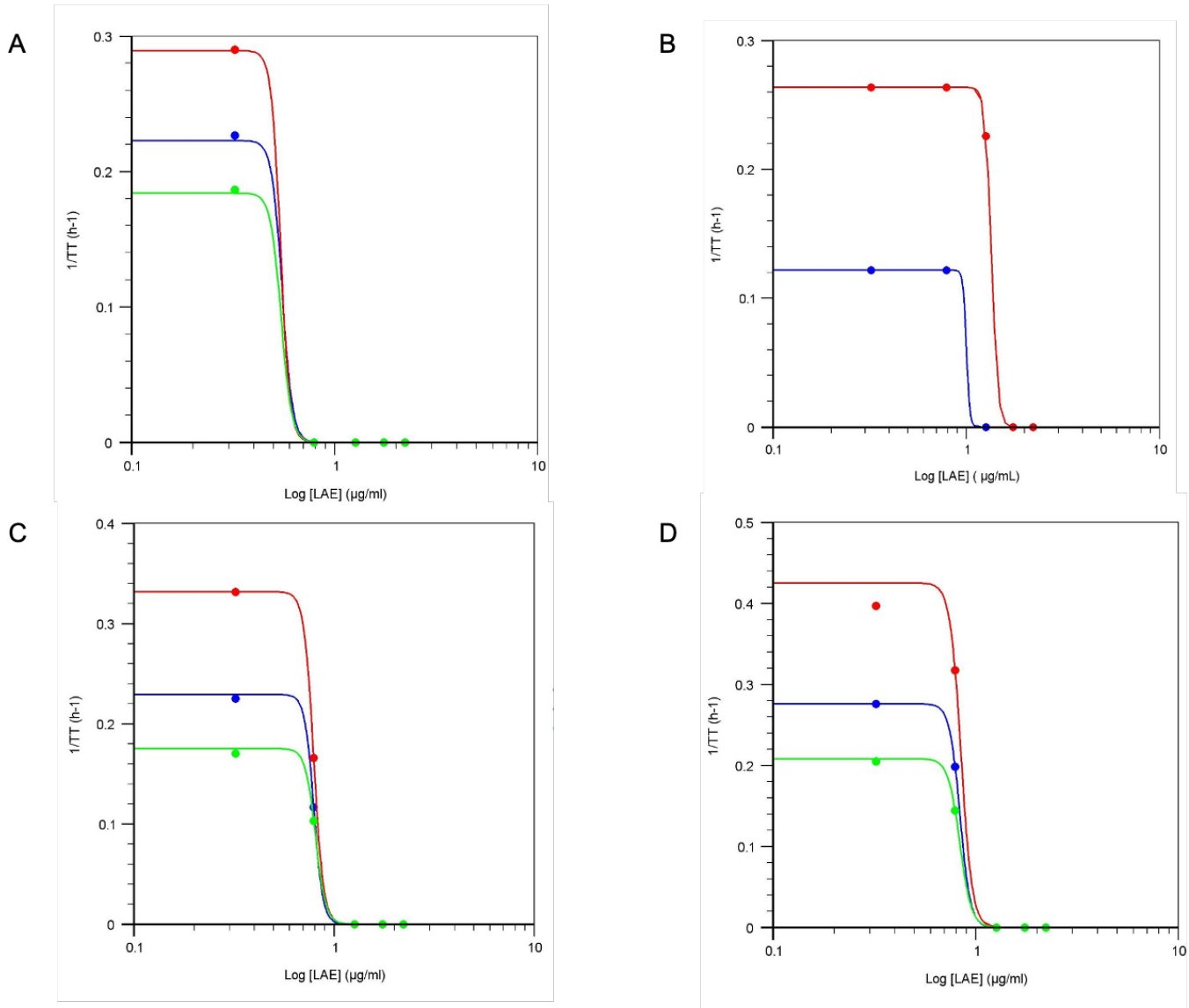

Figure 3.6: Dose-response curves for pure bacterial cultures exposed to LAE (166.7 µg/mL to 2.1 µg/mL). Curves represent the average of three independent assays. **(A):** *Escherichia coli*, **(B):** *Pseudomonas fluorescens*, **(C):** *Staphylococcus aureus*, and **(D):** *Bacillus cereus* at initial seeding concentrations (CFU/mL) of 10^4 (green), 10^5 (blue), and 10^6 (red).

For the Gram-negative bacteria, *P. fluorescens* showed a lower sensitivity to LAE and higher EC50 values than *E. coli* (Figures 3.2, 3.3 & 3.7). The higher resistance of *P. fluorescens* to LAE is most likely It was possible to vary the exposure time for the antimicrobial by changing the initial concentration of bacteria, which correlates with signal onset time that can range from < 1 hr to ~ 8 hrs (Figure 3.2 to 3.5). Furthermore, this parameter can be used to optimise the time to result for the respirometric toxicity assay. Figure 3.6A shows that *E. coli* gives practically identical EC50 values for all three concentrations (10^4, 10^5, and 10^6 CFU/mL), which indicates that LAE exhibits rapid and non-specific toxic effects on these bacterial cells. The antimicrobial effects of LAE were also seen to be temperature dependent for *E. coli* as there was a 2-fold increase in EC50 values from

3.43 ± 0.16 μg/mL to 6.81 ± 0.64 μg/mL when temperature was increased from 30°C to 37°C (Figure 3.7). This increase can be related to the additional stress imposed by sub-optimal growing conditions. In contrast, *P. fluorescens* showed a 2-fold increase in EC50 from 11.51 ± 1.04 μg/mL to 20.61 ± 2.33 μg/mL (Figure 3.7) when initial concentration increased from 10^5 to 10^6 CFU/mL. Moreover, assay time decreased from 8 hrs to 3.5 hrs (Figure 3.3). Therefore, the toxic effects of LAE on *P. fluorescens* cells are slower than on *E. coli*.

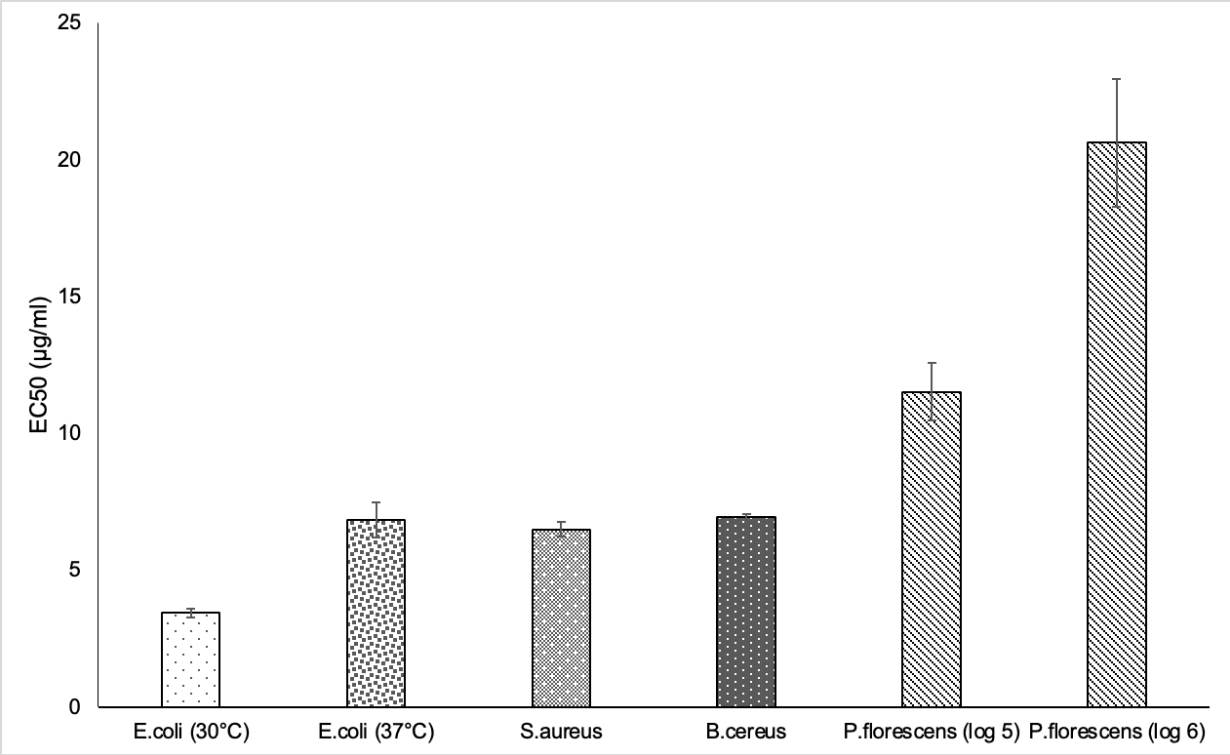

Figure 3.7: Graphical comparison of EC50 (μg/mL) values for the pure cultures of *Escherichia coli* (*E. coli*), *Staphylococcus aureus* (*S. aureus*), *Bacillus cereus* (*B. cereus*), *and Pseudomonas fluorescens* (*P. fluorescens*). The effects of testing conditions (temperature, initial seeding concentration) are also shown. Error bars denote standard deviation of 3 independent replicates per pure culture.

For *S. aureus* and *B. cereus*, the Gram-positive bacteria, the effects of LAE seemed to be similar (Figures 3.6 & 3.7) with EC50 values of 6.47 ± 0.27 μg/mL and 6.93 ± 0.10 μg/mL, respectively. Interestingly, Gram-positive bacteria are known to be more sensitive to antimicrobials than their Gram-negative counterparts as the latter have an additional outer lipid membrane, which restricts the diffusion of exogenous molecules (Russel, 1995; Higueras et al., 2013). However, this difference was not observed as both *S. aureus* and *B. cereus* produced similar EC50 values to *E. coli* (37°C) (Figure 3.7). In addition, spore-forming Gram-positive bacteria typically incur greater resistance to antimicrobials (Russel,

1995). However the *B. cereus* strain used herein was in a vegetative state and did not show this effect with LAE.

For comparison, LAE toxicity was analysed on representative Gram-negative *E. coli* and Gram-positive *S. aureus* using the established densitometry method, which involved OD600 measurement and MIC determination (Weigand et al., 2008). For both bacteria, MIC of 18.5 µg/mL was obtained, which is consistent with literature values for *E. coli*, but not for *S. aureus* (Rodriguez et al., 2004; Higueras et al., 2013). The MICs obtained were also significantly higher than the EC50 values produced in the respirometric assays, although MIC assays are inherently more sensitive than EC50 assays. Thus, respirometric assays provide more sensitive detection of antimicrobial action, as they can detect subtle and sublethal changes in cell metabolism. A comparison of the different toxicity assays is given in Table 3.1.

Table 3.1: Summary of EC50 and MIC values including standard deviation obtained using respirometric and OD600 assays.

Microorganism	**Bacterial Strain**	**EC50 (µg/mL) (MitoXpress)**	**Exposure Time Dependent**	**MIC (µg/mL) (OD600)**
Gram-negative	*E. coli* (30°C) (log 4 – 6)	3.43 ± 0.16	No	
	E. coli (37°C) (log 4 – 6)	6.81 ± 0.64		18.5
	P. fluorescens (log 5)	11.51 ± 1.04	Yes	
	P. fluorescens (log 6)	20.61 ± 2.33		
Gram-positive	*S. aureus* (log 4 – 6)	6.47 ± 0.27	No	18.5
	B. cereus (log 4 – 6)	6.93 ± 0.10	No	
Natural meat spoilage microbiota		39.99	No	

3.2.3. Effects of LAE on whole meat microbiota

The limitation of the toxicity tests previously described is that they can only operate with 'clean' samples such as pure bacterial cultures and media. On the other hand, respirometric assays with quenched-phosphorescence detection and lifetime readout are more robust as they are internally referenced. This means that the assays are not so dependent on the intensity signal and probe concentration, which are affected by sample optical properties (Jasionek et al., 2012). As a result, respirometric assays can reliably analyse complex biological samples, including crude homogenates of food products, opaque, coloured, and particulate samples (Jasionek et al., 2012). This feature allowed for the application of O_2 microrespirometry to assess the effects of LAE on the whole microbiota of fresh red meat homogenates.

Due to the fact that fresh meat samples tend to have low microbial loads, an artificially spoiled beef steak sample was used, which was obtained from a local butcher and stored at 4°C in air atmosphere for five days. Using the TVC method, the microbial load of the meat sample was determined to be 7.4 $\log_{10}$ CFU/g, which is well within the range for spoilage (Ray & Bhunia, 2013). A crude meat homogenate was produced using standard procedure (ISO4833-1:2013) on which the antimicrobial effectiveness of LAE was tested.

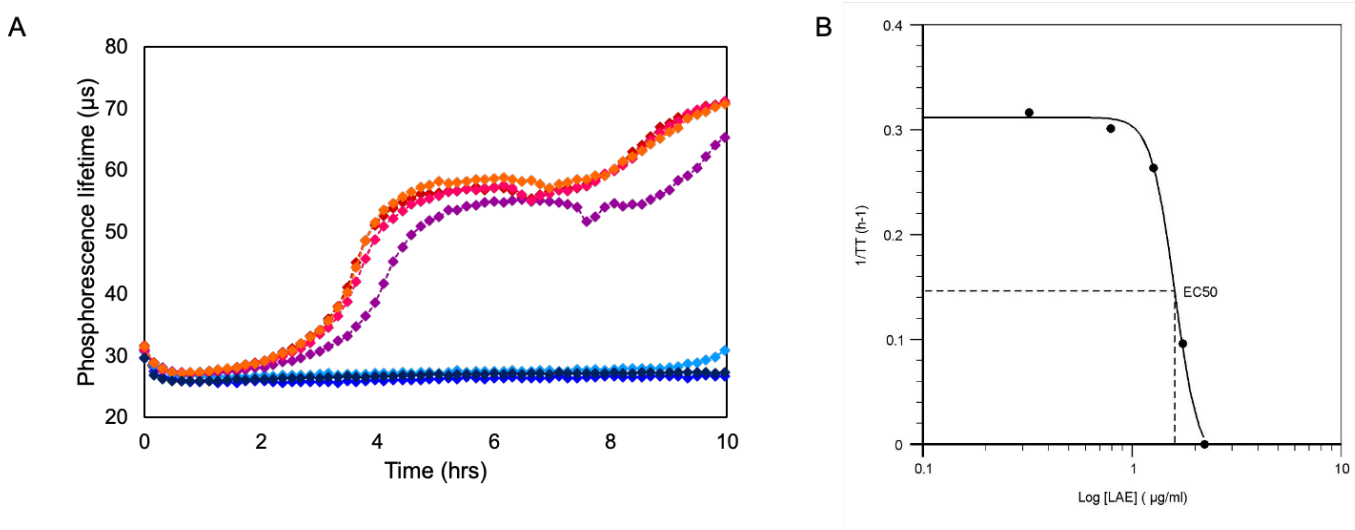

Figure 3.8: The effects of LAE on spoiled meat microbiota. **(A):** Phosphorescent lifetime profiles of undiluted spoiled beef homogenate. Profiles are the average of three replicates within the assay. The assay was conducted in triplicate. Legend: positive control ( ), 166.7 µg/mL ( ), 55.6 µg/mL ( ), 18.5 µg/mL ( ), 6.2 µg/mL ( ), 2.1 µg/mL ( ), and negative control ( ). **(B):** Dose-response curve of spoiled beef homogenate treated with LAE.

The respiration profiles of spoiled meat homogenate are shown in Figure 3.8A, in which the effects of LAE concentrations revealed a similar pattern of toxicity to that of pure cultures (Figures 3.2 to 3.5), but with slight variations. A significantly higher resistance to LAE was observed when EC50 (39.99µg/mL) was calculated using the same method as for pure cultures (Figure 3.8B). The difference can be attributed to two factors: i) the partial adsorption of LAE molecules on the fine particles of the meat homogenate and ii) a higher diversity of bacteria present in the sample. The former would mean that less LAE is available in solution to affect the microbial population present. The diversity of bacteria can be visually seen by the bi-phasic respiration profiles in Figure 3.8A, which suggests the presence of two populations of bacteria. The first population is more abundant or fast growing, producing the first step in the LT profile. However, being either more sensitive to low O_2 levels or LAE, it ceases to grow and consume oxygen. The second population has a slower growth rate or is more resistant to LAE (Ray & Bhunia, 2013) and can respire at lower oxygen levels than the first population, thus producing the second LT step.

Furthermore, the presence of certain bacterial species within the meat microbiota could further attribute to the resistance to LAE. Stellato et al., (2016) showed using 16S rRNA sequencing that *Pseudomonas* spp. are predominant in meat microbiota. As seen in

Figure 3.7, *P. fluorescens* pure culture showed the highest levels of LAE resistance. This in combination with other bacterial species not analysed (*Streptococcus* spp., *Brochonthrix* spp., etc.) could attribute to the observed high level of LAE resistance in the spoiled meat homogenate.

Based on the results of the respirometric antimicrobial assay, a practical application can be derived. As low as 80 μg/mL of LAE can be applied to fresh beef products, which is well below the human consumption levels stated by the EFSA (160 ppm or 160 μg/mL) and FDA (200 ppm or 200 μg/mL) (FDA, 2005; EFSA 2007). This will allow for maximum antimicrobial activity to be achieved with the minimum application of LAE. Furthermore, this will fit the trend for both producers and consumers by extending shelf-life while maintaining quality produce with minimal additives.

3.3. Conclusions

The micro-respirometry testing platform, based on the standard fluorescent reader and commercially available phosphorescent O_2-sensing probe MitoXpress-Xtra was applied to the assessment of antimicrobial activity of LAE on pure bacterial cultures and whole meat microbiota. By measuring and analysing the time profiles of O_2 probe signal (phosphorescence lifetime) in incubating test samples, we were able to visualise the toxic effects of LAE on the different bacterial species, generate time and dose response curves, calculate EC50 and generation times of test microorganisms. The assay outperformed the reference densitometry method in both sensitivity and duration with consistent and reproducible results in 3 to 10 hours. The new multi-parametric toxicity testing platform allows for rapid, automated and parallel analysis of multiple samples under a range of antimicrobial concentrations and conditions.

Chapter 4: A biosensor-based system for rapid on-site quantification of total viable counts in meat samples and environmental swabs

4.1. Introduction

Over the past 50 years, meat consumption has quadrupled worldwide and consumer demand is continuously growing (Ritchie & Roser, 2019). Fresh meats, particularly beef, are an essential part of the food market, however microbial contamination is of major concern for the industry. Contamination can occur from equipment surfaces, insufficient hygiene, food processing personnel, and from food products themselves (Jones et al., 2020). Although food processing plants have strict procedures to minimise microbial contamination, reservoirs of possible spoilage and pathogenic bacteria can occur within live animals, various equipment, and parts of the food processing chains. Therefore, routine sampling of both meat products and surfaces is essential.

With many analytical techniques recently developed, the determination of total aerobic viable counts (TVCs) by plate counting (ISO 4833-1: 2013; ISO 18593:2018) remains the gold standard within the industry. The technique is a non-selective culture based method that gives an estimation of total aerobic bacteria counts from a given sample, with a higher TVC being indicative of contamination and a reduction in quality of a product (Kim & Yim, 2017). This method is time consuming and labour intensive, involving multiple dilutions and counting, with results taking up to 72 hours and an accuracy of ±0.5 Log CFU/g or CFU/cm^2. Furthermore, conventional TVC testing involves several steps clearly separated in time and space (Figure 4.1), which makes upscaling and automation difficult. Centralised or external laboratories are commonly used for sample analysis to which collected samples are transported on ice over long distances. This not only increases the already lengthy time to result by further separating the steps in time and space, but also induces additional stresses on the samples. As a result, the industry is looking for advanced methods that are quick (same day or even same shift result), reliable, user-friendly, automated, and affordable for routine microbiological surveillance.

In this study, we developed a simple and transportable system for food safety testing, which uses disposable vials with built-in phosphorescent oxygen sensors. This allows for the real-time monitoring of microbial growth via oxygen respiration in a contactless

manner. It is configured as a simple sample and measure platform, which can be easily operated by non-skilled personnel and deployed at various sites.

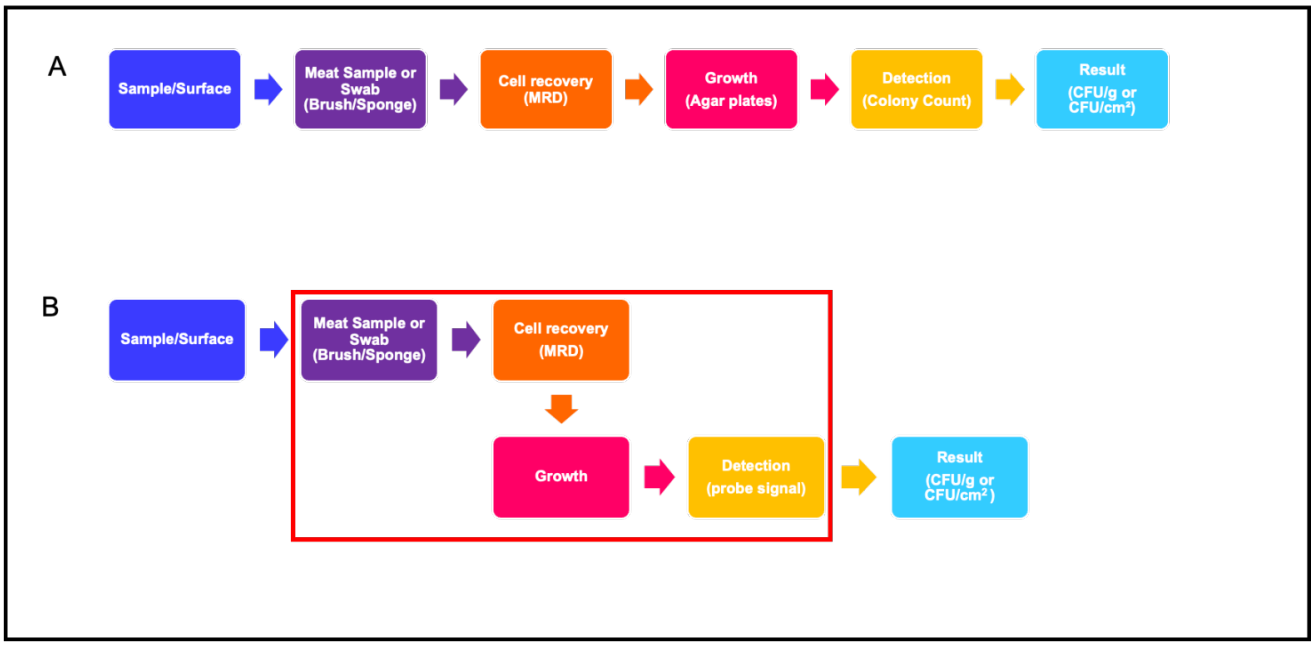

Figure 4.1: Workflow for microbial TVC testing. **A:** traditional method **B:** sensor based method. The proposed system retains the original sample preparation procedure but allows for the integration of four key functions (red rectangle) into one disposable element, the sensor vial.

4.2. Results & Discussion

4.2.1. Platform design

Previous respirometric platforms were realised as stationary lab-based systems implementing sophisticated, bulky, and expensive detectors such as benchtop plate readers or carousel vial readers (Hynes et al., 2006; O'Mahony & Papkovsky, 2006; Hempel et al., 2011; Fernandes et al., 2013). With typical start-up costs in the range of $25-35k, these platforms exclude potential small users, particularly in the food industry. In addition, recent advancements in O_2 sensing instrumentation and sensor materials are not fully utilised by the aforementioned platforms. Based on this knowledge and the available commercial components, a new sensor-based system for the detection of microbial contamination in meat samples and environmental swabs has been designed.

The system is simple, flexible, and modular with the main components including: i) disposable testing vials each containing an O_2 sensor coating with modifications depending on the application (meat sample vs swab sample); ii) an autonomous handheld reader with data logger, FirestingGO_2, which can read sensor signals from the vials in a non-invasive

manner; iii) a block heater, in which vials are maintained at the optimal assay temperature (normally 30°C). Variations of the block heater such as a standard gas incubator with a pebble tray, an egg incubator, or a water bath can be used for the incubation of the samples. Images of the system components and experimental settings for meat and swab samples are shown in Figure 4.2.

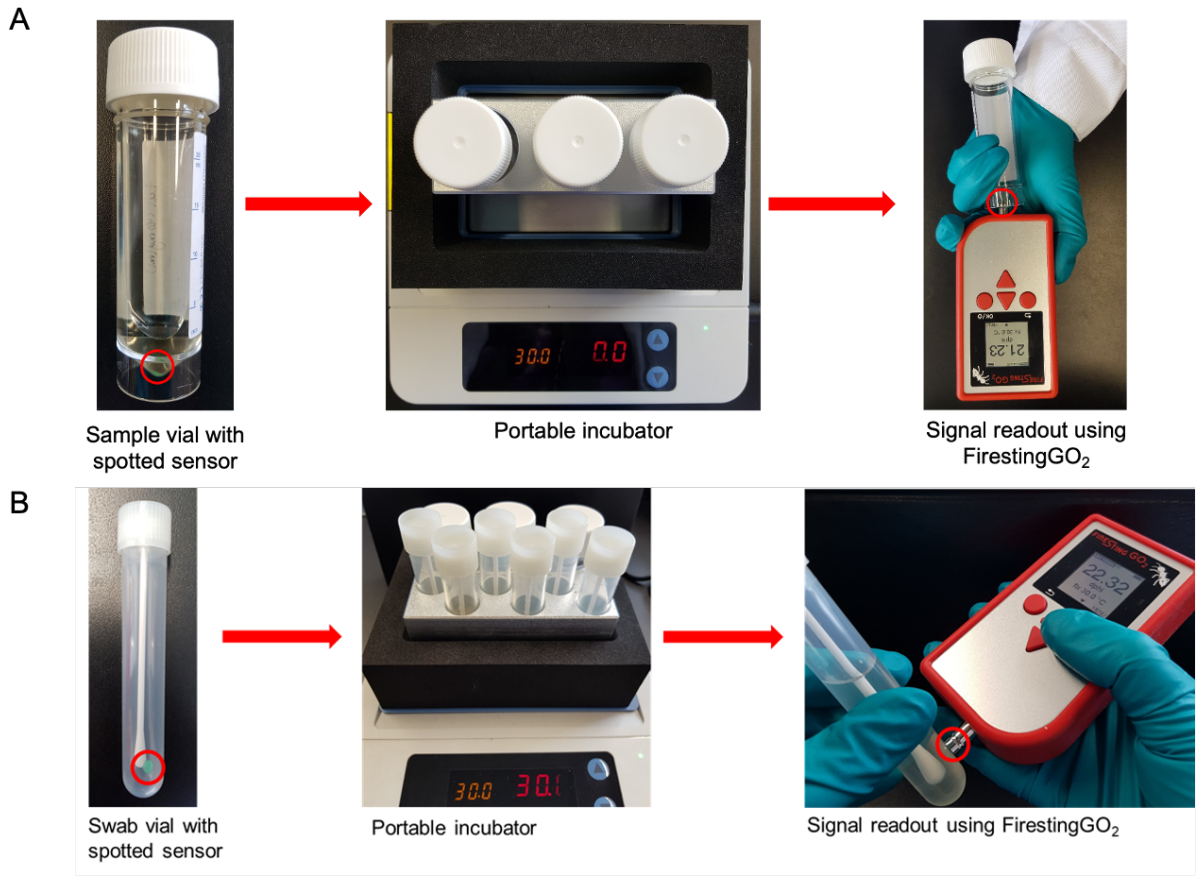

Figure 4.2: The main components of the sensor based portable testing platform. Sterile vials with spotted sensors (red circle) are filled with samples and incubated on benchtop block heater at 30°C and analysed hourly via signal readout using the portable data logger FirestingGO_2.**A:** Disposable 30 mL sensor vials for the analysis of meat samples and carcass swabs. **B:** Disposable 10 mL swab testing sensor vial with an integrated swabbing tool.

The key component of the whole system is the sensor vial, which has been designed by incorporating both sample types. For meat samples, standard 30 mL Sterilin™ vials were chosen (sterile, clear, capped, stand alone, and graded) with the sensor spot applied at the bottom. The placement of the sensor allows for ease of pipetting during preparation and ease of measurement during the assay. The use of relatively large graded vials allows for the elimination of pipetting (solutions can be poured by hand to desired grading without dilutions), improvement of sensitivity (one viable cell in 10 mL sample vs 1 mL sample for

GL930 or 0.1 mL for GL960) (O'Mahony et al., 2009; Fernandes et al., 2013), and a reduction in costs. In addition, the use of capped vials prevents spillage and microbial contamination. For swab samples, sensor spots were incorporated into pre-existing swab vials, allowing for the retention of original sample preparation function while enabling subsequent respirometric analysis of the swabbed material within the vial. For both sample types, respirometric analysis is performed by simply incubating the vials in a block heater and measuring their sensor signals periodically and in a contactless manner with an external autonomous reader, FirestingGO_2. Therefore, a range of key functions (Figure 4.1, red rectangle) are integrated into one simple disposable element. Simultaneously, sample preparation procedure for meat and swab samples remains unchanged and compliant with industry standards.

4.2.2. Optimisation and quality assessment of sensor vials

For swab vials, initial sensor coatings underwent optimisation due to the presence of thick plastic at the bottom of each tube which affected optical measurement by reducing intensity signals. The sensor cocktail was dispensed in different locations on the swab vial while maintain the tubes at different angles. The side of the vial (Figure 4.3A) was the preferable sensor location as it gave high intensity signals and relatively easy access for FirestingGO_2 measurements. However, the angle at which the vials were dried was problematic as the retention of the sensor shape is crucial for signal intensity. At first, a 45° angle was used for drying, but this became unsuitable as the sensor dried in a streak rather than a localised spot (Figure 4.3A). The optimal set up for swab vial preparation was maintaining the vials completely horizontally (Figure 4.3B), allowing for proper sensor spot drying.

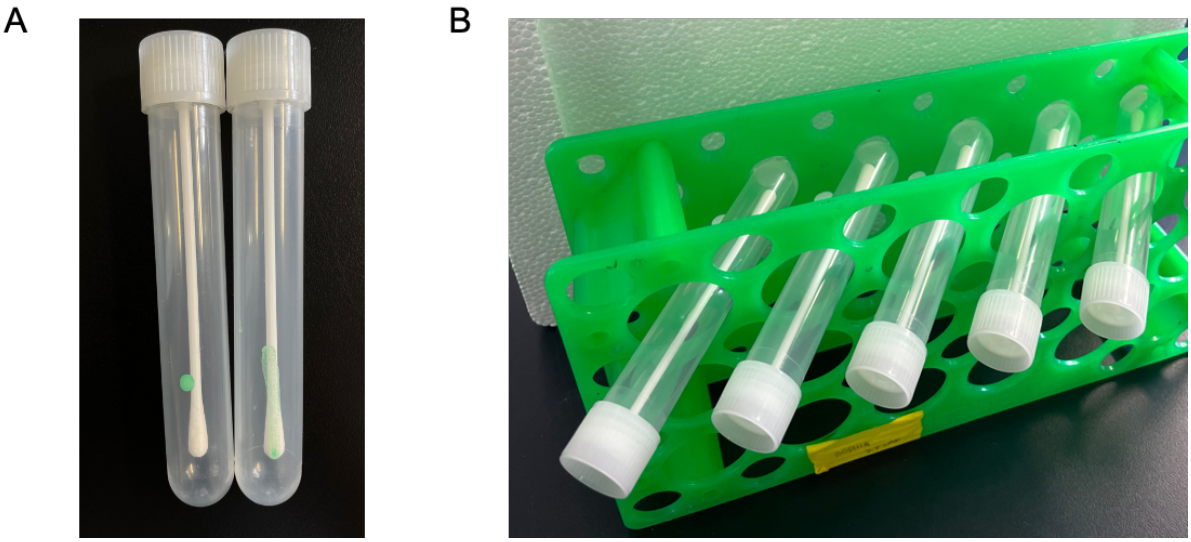

Figure 4.3: Optimisation of swab vial production**. A:** Sensor spot drying at 180° (left) and 45° (right) **B:** Optimal set-up for swab sensor vial drying.

Quality assessment of both sensor vial types was done by measuring both intensity (mV) and phase signal (*dphi*, °) with the FirestingGO_2. Sensors were measured first in ambient air followed by the addition of NB media at room temperature. For both sensor vial types, measurements obtained in NB were significantly different ($P \leq 0.001$, Mann Whitney Wilcoxon Test for swab vials, ANOVA test for sensor vials) for both intensity and phase signals than those obtained for dry (AIR) vials, with phase signal median value higher in NB than in AIR (Figure 4.4). For 10 mL swab vials, the lowest *dphi* signal measured was 20.39 ° in AIR and the highest measured was in NB, 23.95 °. For 30 mL sensor vials, the lowest *dphi* signal was also measured in AIR with a value of 19.99 (°) and the highest was measured in NB at 24.04 (°). Intensity signals, which are influenced by spot shape, geometry, and measurement distance, showed large variation between individual vials and between batches. For 10 mL swab vials, intensity signals obtained from NB vials were significantly lower ($P \leq 0.001$, Mann Whitney Wilcoxon Test) than AIR vials (Figure 4.5), with median values of 44.05 and 54.50 mV, respectively (Table 4.1). Intensity values ranged from 29.53 to 88.63 mV in AIR and from 21.63 to 96.60 mV in NB. A similar pattern was observed for 30 mL sensor vials, with intensity signals from NB vials being significantly lower (ANOVA test) than from AIR vials (Figure 4.4B), with median values of 80.6 mV and 131.35 mV, respectively (Table 4.1). In addition, intensity values also showed large variation with signals ranging from 109.15 mV to 174.65 mV in AIR and from 49 mV to 127.33 mV in NB.

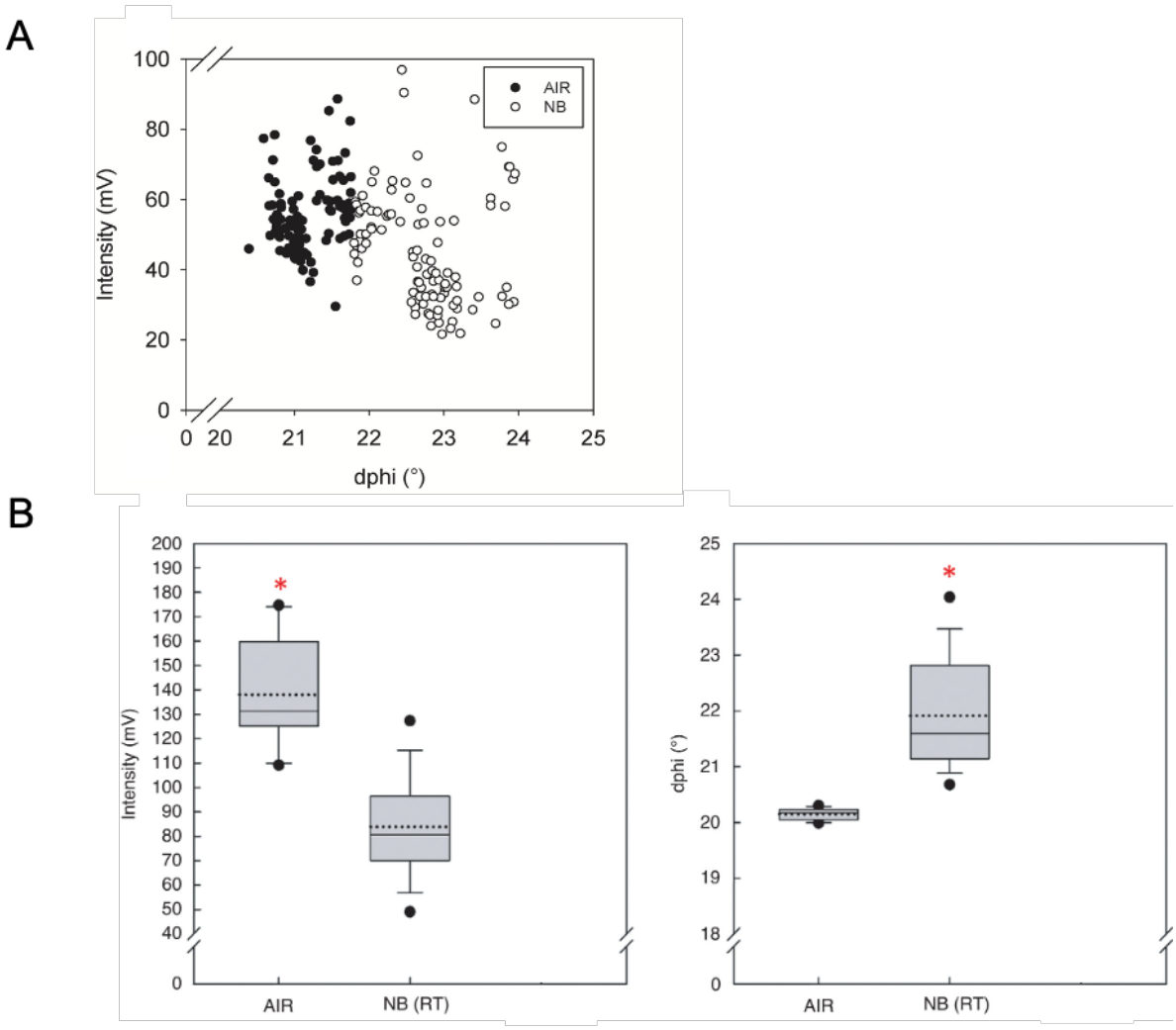

Figure 4.4: Quality control of sensor vials by measuring intensity (mV) and phase signals (*dphi* (°)) in dry vials (AIR) and in Nutrient Broth (NB). **(A):** Variation of intensity and phase signals for 10 mL swab vials. **(B):** Intensity and phase signals for 30 mL sensor vials. All measurements were done in triplicate and the experiment was conducted three separate times. The middle line in the box represents the median, while the dotted line—the mean value. The interquartile range box represents the middle 50% of the data. The whiskers extending from either side of the boxes represent the ranges for the bottom 25% and the top 25% of the data values, excluding outliers. Outliers are identified by (●). Means that are statistically different according to ANOVA are marked with a red asterisk.

Table 4.1: Statistical analysis of mean, standard deviation, maximum and minimum values, and median of intensity (mV) and *dphi* signal (°) in dry sensor vials (AIR) and in the presence of Nutrient Broth (NB).

Vial type	Group	Mean	Std Dev	Max	Min	Median
10 mL	*dphi* (°) in AIR	21.17	0.36	21.77	20.39	21.07
	dphi (°) in NB	22.73	0.60	23.95	21.80	22.74
	Intensity (mV) in AIR	55.97	10.54	88.63	29.53	54.50
	Intensity (mV) in NB	45.85	15.88	96.90	21.63	44.05
30 mL	*dphi* (°) in AIR	20.14	0.1	20.30	19.99	20.17
	dphi (°) in NB	21.91	0.96	24.04	20.67	21.59
	Intensity (mV) in AIR	138.04	21.43	174.65	109.15	131.35
	Intensity (mV) in NB	83.85	19.82	127.33	49.00	80.6

As seen in Table 4.1, the standard deviations for phase signals (0.36 & 0.60 for 10 mL vials; 0.1 & 0.96 for 30 mL vials) are much lower than those for intensity readings (10.54 &15.88 for 10 mL vials; 21.43 & 19.82 for 30 mL vials), indicating an overall homogeneity in the prepared sensor vials. Although intensity readings are useable in respirometric applications, they tend to be error-prone and thus more difficult to interpret (Papkovsky et al., 2009). On the other hand, phase (or lifetime) signals are internally referenced and therefore remain stable despite large variations in intensity signals. A slight once-off increase in phase signal readings when changing from AIR to NB was likely due to the swelling of sensor material in water (Borisov, 2018), a known phenomenon affecting the Stern-Volmer constant. In summary, phase signals are more suitable for microbial respirometry and subsequent meat and swab testing.

In addition to intensity and phase signal, the *dphi* signal, can be converted into oxygen concentration. To evaluate oxygen consumption, an O_2 calibration was generated for a swab sensor vial by purging it with standard O_2/N_2 gas mixtures and recording *dphi* readings with the FirestingGO_2. The relationship between O_2 concentration ($[O_2]$, %) and *dphi* was ascertained from the O_2 calibration curve (Figure 4.5), resulting in an analytical equation:

$$[O_2] = 0.02(dphi^2) - 2.34(dphi) + 62.67 \quad (1)$$

A representative respiration profile of pure culture *E. coli* was selected and monitored with continuous reading using the relevant option on the FirestingGO_2. The aforementioned O_2 calibration equation (Equation 1) was applied to the respiration profile curve, which converted the *dphi* values into O_2 concentrations. Figure 4.5 shows that the O_2 profile is inverted with respect to the *dphi* profile. There was a steep change observed from air-saturated (21%) levels to zero levels at approximately the 5 hr threshold time point (TT). This TT value corresponds to the signal threshold value of 25° or 18% $[O_2]$, respectively. The additional conversion, although useful for visual representation, could bring additional errors and complications in data processing. For routine sample testing, this conversion is unnecessary and thus readout of raw phase signal is simpler and more accurate.

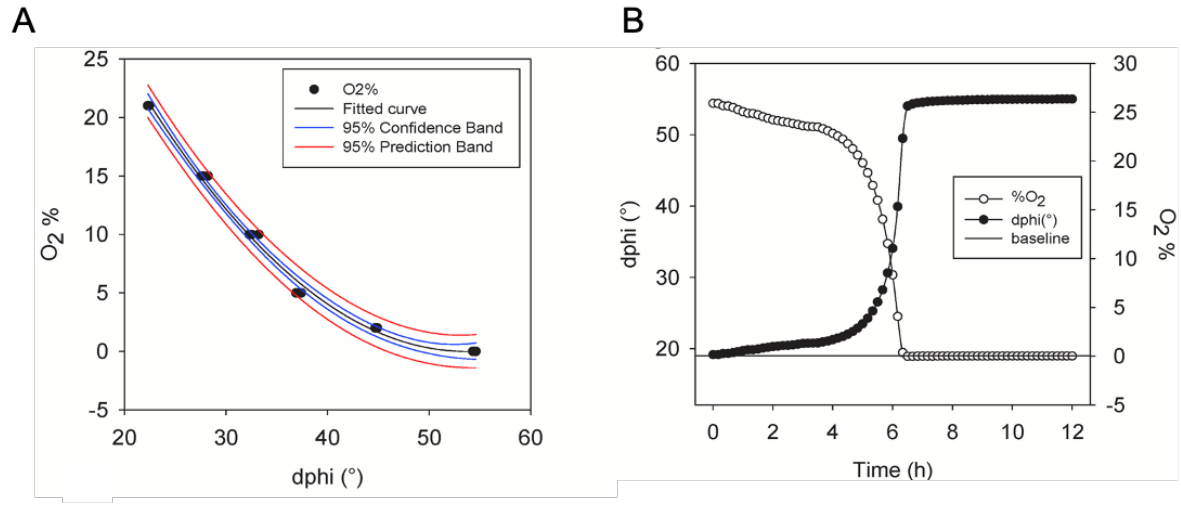

Figure 4.5: Oxygen calibration using 10 mL swab vials. **(A):** oxygen calibration curve using different O_2 standards. **(B):** oxygen respiration of *E. coli* incubated at 30 °C in sensor swab vials and measured continuously with FirestingGO2 reader. Each point represents the average of three measurements per sensor. Calibrations were done in triplicate. Comparison of phase signal and oxygen concentration profile, the latter was calculated using the calibration equation achieved in A. Baseline signals and Time to Threshold (TT) are shown.

4.2.3. System calibration

Calibration of the systems was necessary as previous calibrations of the O_2 sensor based respirometric assays were conducted under different experimental settings (O'Mahony et al., 2005; O'Mahony & Papkovsky, 2006; Jasionek et al., 2013), including the type of sensor/probe, temperature, assay substrate (microplate or tube) as well as sample (food homogenate) used. Therefore existing calibrations are not valid for the new platform and a new calibration which establishes the relationship between initial microbial load of samples (Log CFU/g or Log CFU/cm^2) and measured TT values (in hours) had to be newly generated.

The calibration of the system was performed using both 30 mL and 10 mL sensor vials and *E. coli* as a model organism for aerobic mesophilic microbiota (Blount, 2015). For carcass and surface swabs, *E. coli* was serially diluted (1 in 10) in MRD which mimicked the sample matrix. For meat samples, the sample matrix is more complex and thus spiked meat homogenates with *E. coli* were used for the calibration. Two separate dilution ratios in NB were also examined for meat samples; 1:9 and 1:1. All vials were analysed immediately by respirometry, which produced sigmoidal respiration profiles seen in Figures 4.6 and 4.7. Analysis of TT (hrs) values at 25 ° threshold for the spiked meat homogenates showed a delay in detection of 0.8 ± 0.2 hrs when using the 1:9 dilution compared to the 1:1 dilution (Figure 4.6). Furthermore, the distance between the dilution curves for the 1:9 dilution was

1.39 ± 0.19 hrs and 1.40 ± 0.14 hrs for the 1:1 dilution. With the 1:1 dilution producing a faster response and lower TT values than the 1:9 dilution, the 1:1 dilution was selected for further use.

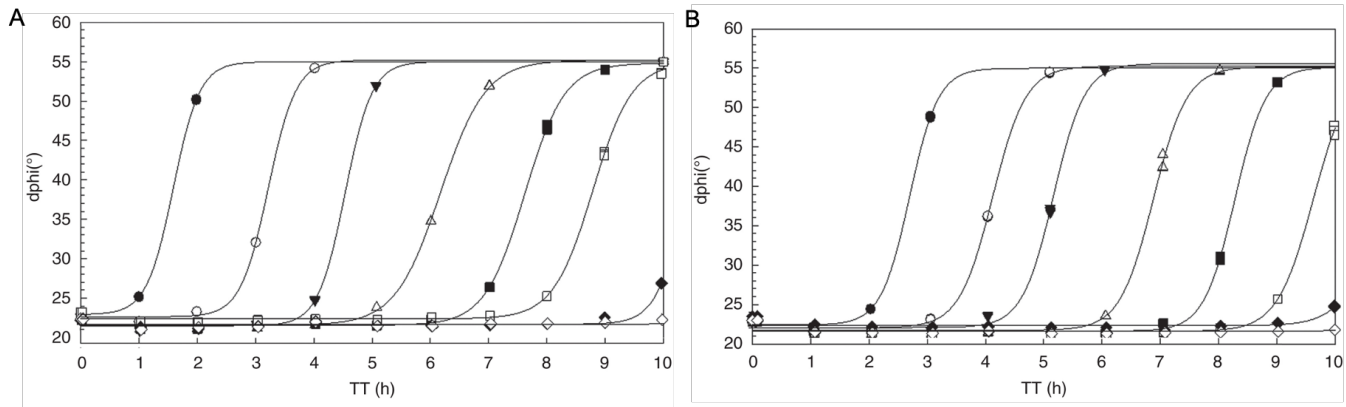

Figure 4.6: Respiration profiles for meat samples spiked with different concentrations of *E. coli*. **(A):** Measurement points and fitted curves for the different *E. coli* concentrations (1–8 Log(CFU per g)) in meat homogenates, with a 1:1 ratio of NB **(B):** Similar curves for 1:9 volume ratio of spiked meat homogenates and NB. Data for three replicates per sample at each time points are shown. Measurements were conducted on three separate occasions. Labels for the respiration profiles: ● – 8 Log(CFU per g); ○ – 7 Log(CFU per g); ▼ – 6 Log(CFU per g); ▵ – 5 Log(CFU per g); ■ – 4 Log(CFU per g); □ – 3 Log(CFU per g); ♦ – 2 Log(CFU per g); ◊ – 1 Log(CFU per g).

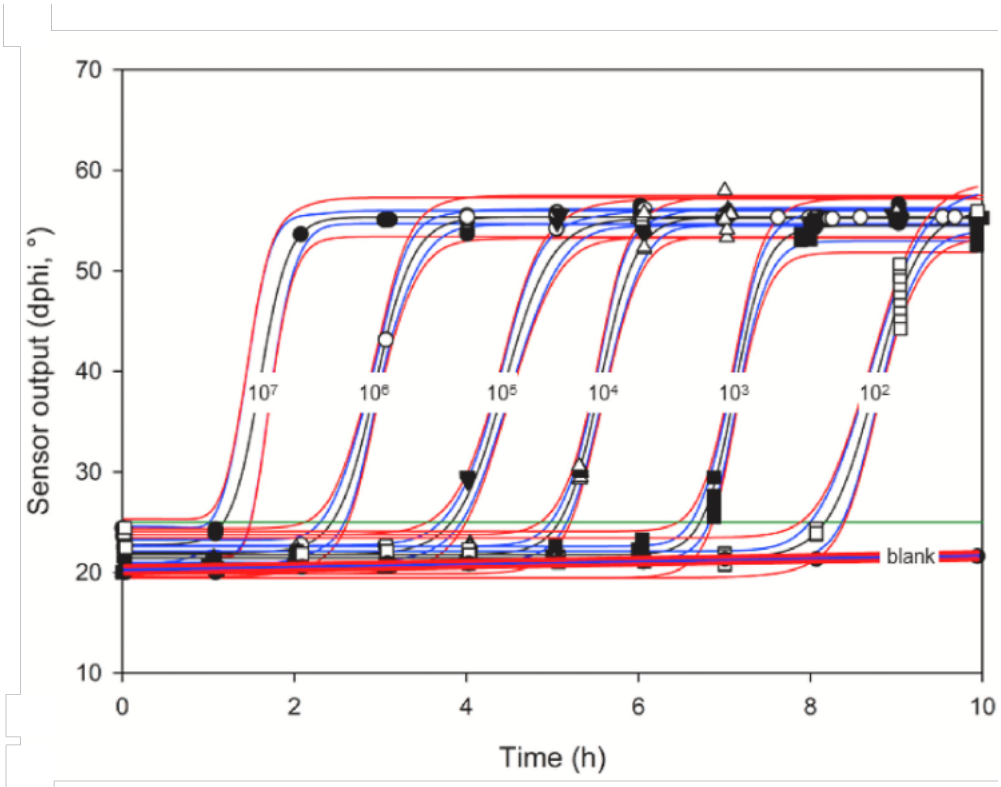

Figure 4.7: Respiration profiles of serial dilutions of *E. coli* cultures ranging 10^7 CFU/cm^2 – 10^2 CFU/cm^2 in NB in 10 mL sensor vials, along with blank (sterile) samples producing flat profiles. Data for three replicates per sample at each time points are shown. Measurements were conducted on three separate occasions. Tubes were incubated at 30 °C and measured hourly with the FirestingGO_2 reader. Green line represents the *dphi* threshold of 25°.

Calibration equations were generated by plotting experimentally determined TT values against known concentrations of *E. coli* (CFU/mL) (Figure 4.8).

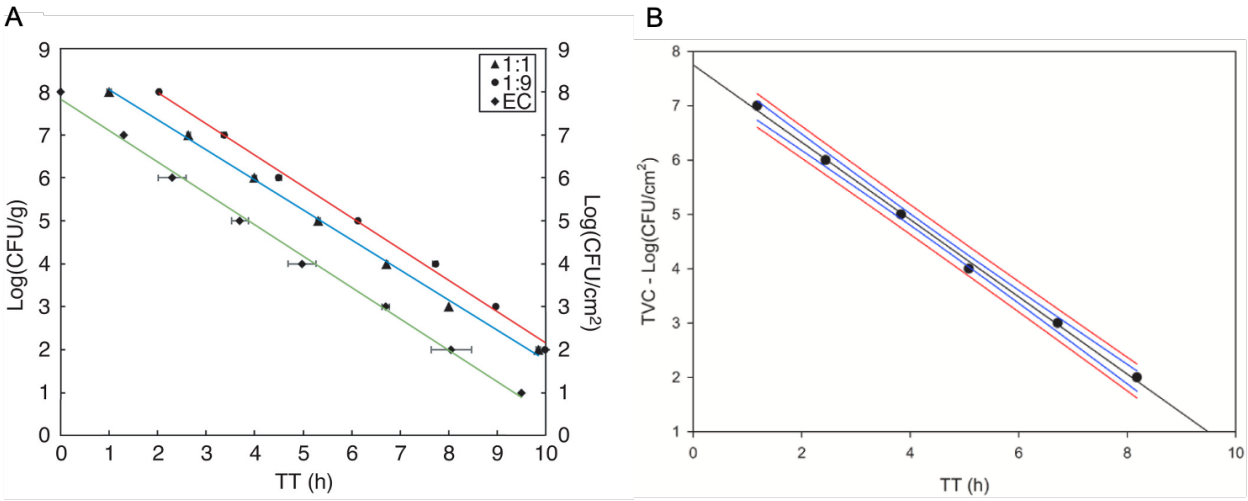

Figure 4.8: Calibration curves derived from respiration profiles of the *E. coli* standards in sensor vials from which equations were derived to calculate microbial load of unknown samples. **(A):** Calibration curves using 30 mL sensor vials with meat matrix in NB (blue and red lines) and swab matrix in NB(green line). **(B):** Calibration curve using 10 mL swab vials with swab matrix in NB. Black line represents linear regression, blue lines represent 95% confidence interval and red lines represent prediction lines.

Using the 0.1X and 1X conversion factors, CFU/mL units can be converted into Log CFU/cm^2 and Log CFU/g, respectively. The following calibration equations for the quantification of microbial load in unknown samples (Log CFU/cm^2 or Log CFU/g) on the basis of measured TT values with the *dphi* threshold of 25° were established:

$$Log\ (CFU\ per\ cm^2) = 7.83\ - 0.73 * (TT) \quad (2)$$

$$Log\ (CFU\ per\ g) = 8.74 - 0.70 * (TT) \quad (3)$$

$$Log\ (CFU\ per\ cm^2) = 7.75 - 0.71 * (TT) \quad (4)$$

Equations 2 and 4 relate to the quantification of total aerobic counts (TVCs) from swab samples with the former being carcass swabs and the latter brush swabs. Equation 3 is for the quantification of TVCs in raw meat samples.

The threshold for the sensor signal used in calibrations was set based on the variability of the phase readings in individual vials (Figure 4.4),the flatness of baseline signals in microbial tests (Figure 4.6), and general system performance. Setting the *dphi* threshold to 25° satisfied the above conditions and allowed for the reliable detection of all positive samples while eliminating the incidence of false-negatives. Occasionally, the first reading (time zero) would exceed the threshold when vials had sub-optimal temperature. This

effect can be easily filtered out at the next measurement point. Furthermore, the signal threshold can be set to different values depending on the samples in question. However, setting the *dphi* threshold too low (23°, Figure 4.9) will produce false positives while setting the threshold too high (27 or 30 °, Figure 4.9) will increase the time to result.

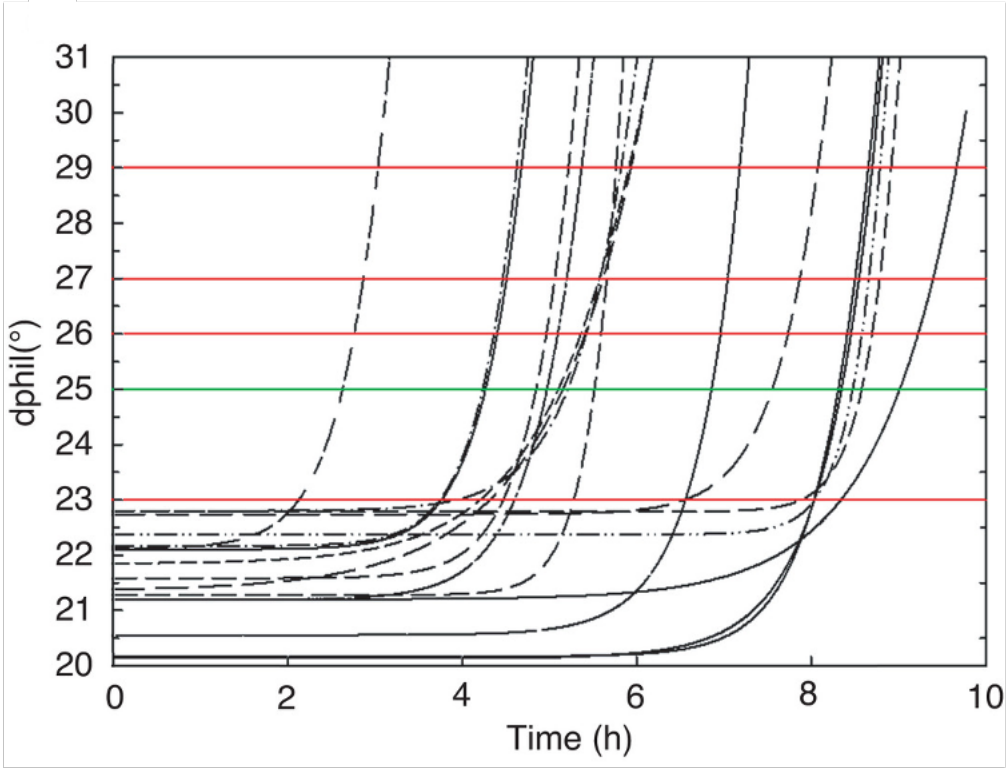

Figure 4.9: Graphical analysis of *dphi* threshold set to 23°, 27°, 30° (red lines) and 25° (green line).

4.2.4. System applications

The application of the sensor based system was validated by a variety of samples. For the 30 mL sensor vials, different types of raw meat cuts and carcass swabs from a local meat processing plant (n = 58 and 24, respectively) were used. The homogenates were added to 10 mL NB (1:1) in vials and analysed for 10 hours at 30°C with measurements taken hourly. Microbial counts were calculated using Equation 3 and also obtained by the conventional agar plating method. The two methods showed a strong positive correlation (Pearson's correlation, $P < 0.05$) with correlation coefficients of 0.85 for meat samples and 0.83 for carcass swab samples (Figure 4.10). It should be noted that the analysis of carcass swab samples showed narrower prediction intervals due to more homogenous distribution of samples in comparison to the meat samples.

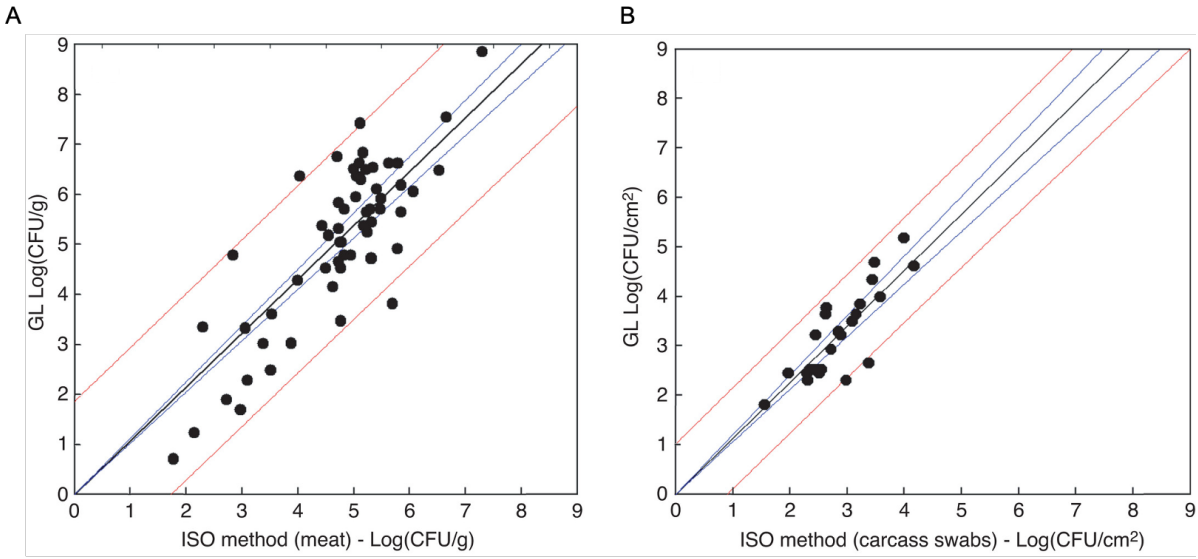

Figure 4.10: Correlation comparison of the enumeration of aerobic bacteria using oxygen respirometry and reference method (ISO 4833-1: 2013). **(A):** using meat samples (n = 58) and **(B):** using carcass swabs (n = 24) obtained from a local meat processing plant. Black line represents linear regression obtained with Pearson test. Blue lines represent 95% confidence intervals and red lines represent prediction interval.

Although the determination of quantitative TVC values is useful for laboratory analysis, industrial applications often require semi-quantitative results. Threshold grading, which is defined as above or below an established safety threshold, is typically applied to meat products (10^5 or 10^6 CFU/g) and used for quality control (QC) within production plants for batch release as well as for making Go/No Go decisions. This can easily be applied to the sensor system as simple end point measurements. Using equations 2 and 3, the time for end-point measurements was calculated based on given TVC thresholds, with the addition of corresponding standard measurement error (SME): 0.17 for carcass swabs and 0.10 for meat samples (Table 4.2). From Table 4.2, based on a TVC threshold of 10^5 CFU/g, which is common for retail meat products, sample vials should be measured at 5.3 hours from the start of incubation. If samples give phase signal readings higher than the *dphi* threshold of 25°, then they can be classified as positive for levels of contamination higher than the safety threshold. On the other hand, if the samples give *dphi* readings below 25° , the samples can be considered negative with TVC levels within the acceptable threshold limit. Similarly, measurements can be taken at 3.9 hours for carcass swabs at the same TVC threshold limit of 10^5 CFU/cm^2. Therefore, the sensor based system can be applied as a traffic light pass/fail system to monitor microbial safety and quality in different samples and at various stages of production.

Table 4.2: Calculated end point measurement times for testing of meat samples and carcass swabs for particular TVC thresholds: positive – above the TVC threshold, negative – below the TVC threshold.

TVC threshold	**Measurement Time (hrs)**	
Log (CFU/g) or Log (CFU/cm^2)	**Raw meat**	**Carcass swab**
≤ 2 ±SME	≥9.63	≥7.99
3	8.20	6.62
4	6.77	5.25
5	5.34	3.88
6	3.91	2.51
7	2.49	1.14
8	1.06	< 1.14
≥9	< 1.06	---

For the 10 mL swab vials, the system was first validated by swabbing 100 cm^2 plastic tray surfaces that were artificially contaminated (AI) with varying *E. coli* dilutions (10^8 to 10^4 CFU/cm^2) using mini-spray bottles. Pre-wetted swabs were then used to swab the top tray area for the sensor system analysis and the bottom tray for the parallel reference method. Although pure cultures are useful in mimicking microbial contamination, they are not reflective of the complex microbiota that can inhabit real surfaces. Thus, the second type of artificial contamination (M) was done with meat microbiota, which can be found on meat processing plant surfaces and on meat samples (Stellato et al., 2017). Different meat cuts were purchased from a local butcher at an open-air market, placed onto 100 cm^2 plastic trays and incubated at 4°C ± 1°C. The initial analysis was done after 24 hrs while for increased microbial contamination, samples were spoiled for 48 and 72 hrs. Following incubation, an imprint of the meat sample on the top tray was done to transfer the meat microbiota onto the surface. Subsequently, pre-wetted swabs were used to sample the footprints of both the top (aerobic) and bottom sides of the meat sample while ensuring that the top and bottom of the plastic trays were swabbed separately. The swab homogenate was then analysed by both the sensor and reference method. Finally, the third group of samples (S) were obtained by swabbing (according to ISO 18593:2018) laboratory surfaces such as benchtops, sinks, wastebins etc., to generate a collection of environmental swab samples. Initial microbial load

of the samples was calculated using equation 4 and compared to the microbial load retrieved from the reference method.

The one-way ANOVA test ($P < 0.05$) showed that there was no statistically significant difference between the two methods ($n = 51$, $P = 0.78$) which can be seen in Figure 4.11. In addition, a strong positive correlation (Pearson correlation) was found between the two methods with a correlation coefficient of 0.99 ($P < 0.05$).

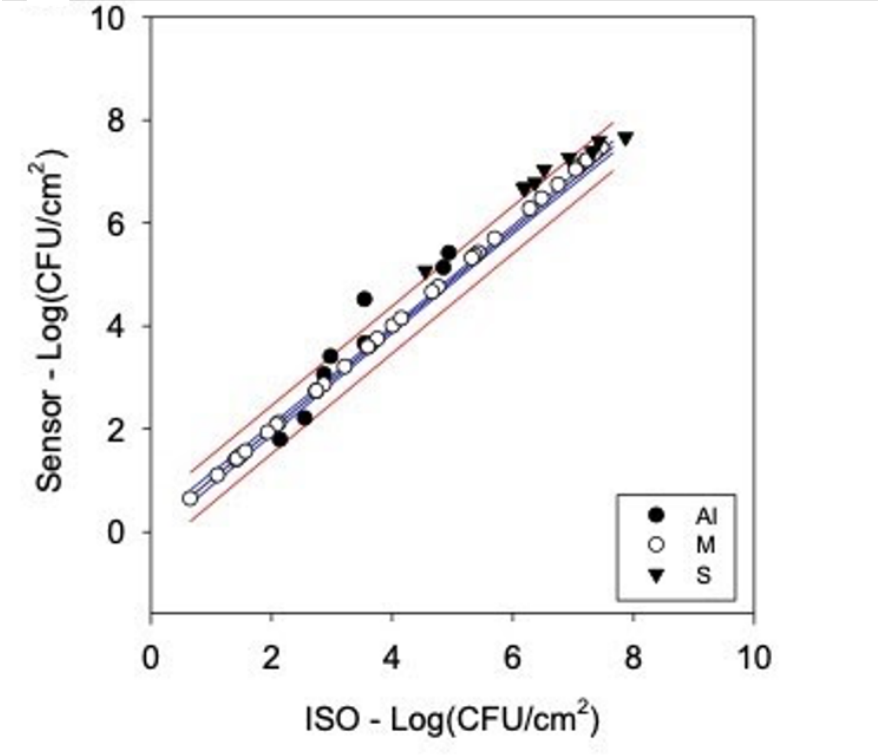

Figure 4.11: Regression plot showing the correlation between the sensor method and the reference ISO method (ISO 18593:2018) using Pearson correlation. Swab samples were obtained from artificially contaminated (*E. coli,* group AI) and natural meat microbiota (group M) from naturally contaminated laboratory surfaces (group S). Black lines represent the regression curve, the blue lines represent the 95% confidence, and the red lines represent the prediction interval.

Overall, the sensor based system was able to handle not only model contamination with pure culture *E. coli*, but also complex meat homogenates and microbiota. Moreover, the proposed method outperformed the conventional TVC test in speed (time to result 2-10 hrs vs 48-72 hrs), simplicity, and user-friendliness (no dilutions, real-time readout).

4.3. Conclusions

A new sensor based testing platform for rapid and simple quantification of TVCs in meat samples, carcass swabs, and environmental swabs was described using oxygen respirometry. The system implemented disposable vials (30 mL for meat/carcass samples and 10 mL for brush swabs) with phosphorescent oxygen sensors integrated in the bottom part, a small block heater/incubator, and a handheld sensor reader. In the testing, groups of 1–20 samples were prepared using the standard method (ISO 4833-1: 2013; ISO 18593:2018) in sensor vials, which were then incubated at 30 °C and measured hourly in a contactless, non-invasive manner. The measurements revealed time profiles of dissolved O_2 in each sample vial, from which Threshold Time of sensor signal was determined and then TVC values (Log CFU/ g or CFU/cm^2) were calculated using the calibration equations. The method covers the range of 0.65 – 8 Log (CFU/cm^2) for carcass and swab samples and 2 – 7 Log (CFU/g) for meat samples. Results are produced in 1– 8 hrs. The test was validated with meat samples and carcass swabs from a local meat processing facility as well as swab samples from surfaces contaminated with *E. coli,* with whole meat microbiota, and with real environmental swabs. The results showed no statistically significant difference with the reference method which takes 48–72 h. The sensor testing platform is fast, accurate, simple (sample-and-measure), portable, low cost (<$5k), requires no serial dilutions and is suitable for on-site deployment and use.

Chapter 5: The analysis of meat microbiota from various mincemeat products using oxygen respirometry and 16S rRNA amplicon sequencing

5.1. Introduction

Meat is a complex ecological niche with various chemical and physical properties that allows for the colonisation of different bacterial species, creating a unique microbiome (Stellato et al., 2016). The colonisation and subsequent development of the microbiome is influenced by both biotic and abiotic factors. Initial colonisation can occur from biotic factors such as water, air, soil, processing equipment, and personnel (Stellato et al., 2016; Odeyemi et al., 2019). The predominance of certain bacterial species over others is influenced by abiotic factors such as temperature, gaseous atmosphere, pH, NaCl content, and water activity of fresh meat (Jayasena & Jo., 2013; Stellato et al., 2016). An overabundance of bacteria can lead to spoilage which is defined as the deterioration of food leading to a reduction in quality and becoming unsuitable for consumption (Stellato et al., 2016; Odeyemi et al., 2019). Spoilage is characterised by changes in organoleptic properties such as changes in texture and colour, and the presence of an off-odour (Stellato et al, 2016). Although there are a variety of meat types, there are commonalities in the bacterial species associated with spoilage. The main culprits are *Enterobacteriaceae*, *Pseudomonas* spp., *Brochothrix thermosphacta*, and *Lactobacillus* spp. (Jayasena & Jo, 2013; Stellato et al., 2016), which are predominantly aerobic or facultative anaerobic species.

The type of packaging used for meat also plays a critical role in the shelf-life and quality of the product. Modified atmosphere packaging (MAP) allows for the alteration of gaseous components, usually a combination of carbon dioxide, oxygen, and nitrogen at different levels within packaging to extend shelf-life (Weinroth et al., 2019). MAP not only minimises microbial growth and lipid oxidation, but also aids in the maintenance of colour (Weinroth et al., 2019). The most common MAP composition for fresh meat products is 70% O_2/ 30% CO_2 (Kolbeck et al., 2020). However, this original gas composition inside MAP packs changes over shelf life, due to absorption of gases by the meat product and their respiration. Depending on the type of meat product and composition of gases in MAP, the initial microbiota can be influenced towards a predominantly aerobic, facultative anaerobic or anaerobic population.

The effects of packaging and storage on meat microbiota have been studied extensively, mainly using traditional culture based methods on solid agar. Oxygen respirometry offers a user-friendly, automated, and quick alternative to conventional TVC testing (O'Mahony et al.,2005; Zitova et al., 2009). However, these methods are limited to the culturable component of the microbiome (Weinroth et al., 2019). With next generation sequencing, whole microbial communities can be examined in greater detail for their functional diversities (Jagadeesan et al., 2019). Sequencing of the 16S rRNA gene can be employed to quantify the relative abundance of bacterial taxa present (Weinroth et al., 2019), and can follow the succession of microbial populations over time and upon different treatments (Jagadeesan et al., 2019). Implementation of next generation sequencing can provide a greater understanding of the complex processes associated with food spoilage, the effects of food processing and agricultural practices on the microbiome (Li et al., 2020).

In this study, we aim to combine respirometric analysis and 16S rRNA amplicon sequencing for a more holistic view of the composition of microbiota in mincemeat products and its dynamics over product shelf-life. Effects of sample preparation and testing methods are also examined.

5.2. Results & Discussion

5.2.1. Analysis of headspace gas composition in MAP mince samples

As previously mentioned, different product types and MAP gas compositions can influence the initial bacterial population to be predominantly aerobic, facultative anaerobic, or anaerobic (Kolbeck et al., 2019). The MAP composition for the different products is summarised in Figure 5.1. With initial packaging conditions being 70% O_2/30% CO_2, O_2 levels decreased to 69.5%-64.1% on Day 3 (Figure 5.1A). There were further decreases on Day 13, with the lowest level of 55.9% for beef mince and the highest level of 63.1% for lamb mince. Overall, O_2 levels remain abundant and rather close to the original level of 70%, which should support the growth of aerobes and facultative anaerobes. CO_2 levels are far from the initial 30% with all packages having values below 21% on Day 3. Unlike O_2 levels, CO_2 levels increased on Day 13 (Figure 5.1B), with the highest value of 30.7% for beef mince. The increase in CO_2 levels is likely from the proliferation of bacteria, as gas production is a common meat spoilage phenotype (Shao et al., 2021).

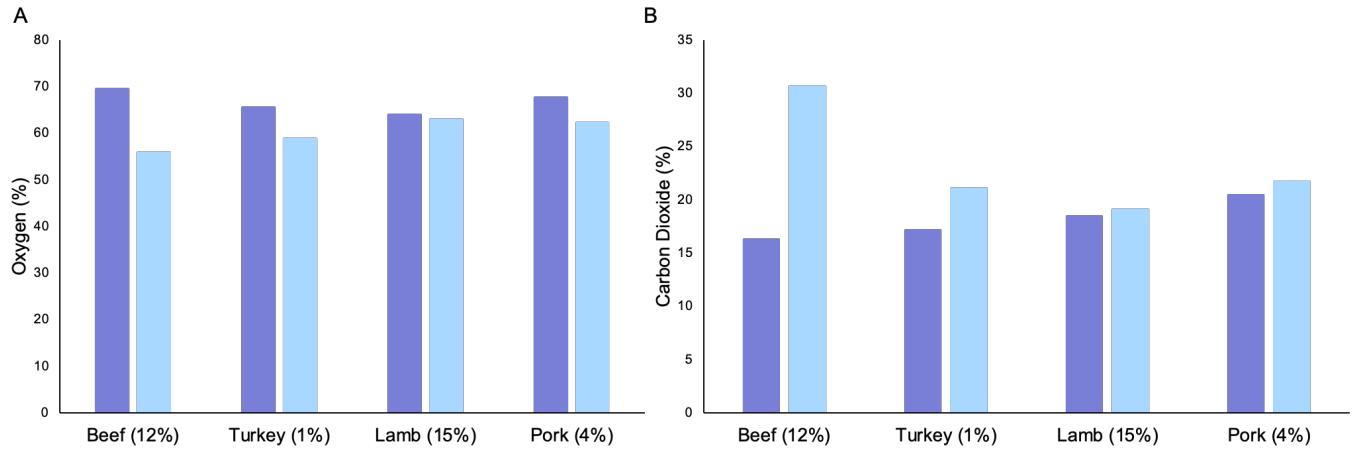

Figure 5.1: Modified Atmosphere Packaging (MAP) compositions of mincemeat samples destructively measured using Dansensor™ at day of purchase (Day 3) (purple) and 3 days past printed Best Before date (Day 13) (blue). Samples were measured once. **A:** Oxygen levels and **B:** Carbon Dioxide levels.

5.2.2. Microbiological assessment of mince samples by culture based methods

A total of 32 mincemeat packs were analysed, including 8 beef mince packs, 8 turkey mince packs, 8 lamb mince packs, and 8 pork mince packs, in two batches of 4 packs for each product. Two sampling points: top and bottom sides of the mince itself and two time points: 0 hours (immediately after stomaching) and 2-5 hours (after respirometry) were used. These points also covered four shelf-life points: three within Best Before date (Days 2 – 10) and one after (Day 13). Each meat homogenate produced by stomaching from a MAP pack was subjected to the following analysis: i) O_2 respirometry; ii) traditional agar plating method for TVC specifically for mesophilic bacteria; and iii) 16S rRNA sequencing (if passed internal and external QC). The list of tested samples, their codes and main characteristics are given below in Tables 5.1-5.4.

Table 5.1. The list of beef mince samples, their codes and characteristics. Red indicates failed external QC and excluded from sequencing analysis. Grey denotes end of shelf-life.

Sample ID	Shelf-life (Days)	Before/after respirometry	DNA concentration (ng/µL)	A260/A280
Batch 1				
BM13TB	3	Before	39.3	1.85
BM13TA	3	After	34	1.85
BM13BB	3	Before	29.4	1.85
BM13BA	3	After	27.6	1.92
BM16TB	6	Before	43.5	1.88
BM16TA	6	After	33.3	1.28
BM16BB	6	Before	69.1	1.87
BM16BA	6	After	33.7	1.9
BM110TB	10	Before	45.1	1.92
BM110TA	10	After	30.8	1.9
BM110BB	10	Before	54.4	1.85
BM110BA	10	After	30	2.03
BM113TB	13	Before	56.9	1.76
BM113TA	13	After	39.2	1.74
BM113BB	13	Before	43.6	1.78
BM113BA	13	After	25.3	1.77
Batch 2				
BM25TB	5	Before	23.4	1.82
BM25TA	5	After	25.2	1.81
BM25BB	5	Before	60.5	1.87
BM25BA	5	After	27	1.86
BM28TB	8	Before	48.4	1.83
BM28TA	8	After	50.4	1.83
BM28BB	8	Before	29.5	1.83
BM28BA	8	After	23.8	1.8
BM210TB	10	Before	46.3	1.85
BM210TA	10	After	37.7	1.82
BM210BB	10	Before	55.2	1.85
BM210BA	10	After	33.4	1.85
BM213TB	13	Before	45.4	1.9
BM213TA	13	After	37.4	1.87
BM213BB	13	Before	47.9	1.86
BM213BA	13	After	44.2	1.84

Table 5.2: The list of turkey mince samples, their codes and characteristics. Red indicates failed external QC and excluded from sequencing analysis. Grey denotes end of shelf-life

Sample ID	Shelf-life (Days)	Before/after respirometry	DNA concentration (ng/µL)	A260/A280
Batch 1				
TM14TB	4	Before	7.5	1.57
TM14TA	4	After	18.3	1.72
TM14BB	4	Before	9.2	1.79
TM14BA	4	After	6	1.6
TM17TB	7	Before	13.3	1.82
TM17TA	7	After	8.1	1.88
TM17BB	7	Before	10	1.81
TM17BA	7	After	7	1.71
TM110TB	10	Before	19.7	1.83
TM110TA	10	After	5.4	1.54
TM110BB	10	Before	15.8	1.75
TM110BA	10	After	13.8	1.78
TM113TB	13	Before	58.3	1.97
TM113TA	13	After	19.9	1.86
TM113BB	13	Before	44.4	1.85
TM113BA	13	After	18.9	1.8
Batch 2				
TM22TB	2	Before	12.3	1.78
TM22TA	2	After	15.7	1.92
TM22BB	2	Before	24	1.87
TM22BA	2	After	4.8	1.82
TM25TB	5	Before	23	1.83
TM25TA	5	After	11.9	1.82
TM25BB	5	Before	21.6	1.72
TM25BA	5	After	21.9	1.79
TM210TB	10	Before	36.1	1.86
TM210TA	10	After	29.8	1.85
TM210BB	10	Before	34.3	1.81
TM210BA	10	After	22.5	1.84
TM213TB	13	Before	61.7	1.88
TM213TA	13	After	36	1.91
TM213BB	13	Before	82.6	1.86
TM213BA	13	After	43.7	1.84

Table 5.3: The list of lamb mince samples, their codes and characteristics. Red indicates failed external QC and excluded from sequencing analysis. Grey denotes end of shelf-life.

Sample ID	Shelf-life (Days)	Before/after respirometry	DNA concentration (ng/µL)	A260/A280
Batch 1				
LM13TB	3	Before	43.1	1.87
LM13TA	3	After	29.5	1.79
LM13BB	3	Before	29	1.82
LM13BA	3	After	16.7	1.8
LM16TB	6	Before	56.9	1.81
LM16TA	6	After	18.3	1.78
LM16BB	6	Before	55.8	1.85
LM16BA	6	After	27.8	1.9
LM110TB	10	Before	139	1.86
LM110TA	10	After	43.5	1.81
LM110BB	10	Before	97.4	1.85
LM110BA	10	After	41	1.83
LM113TB	13	Before	137.9	1.86
LM113TA	13	After	83.8	1.86
LM113BB	13	Before	36.3	1.8
LM113BA	13	After	39.2	1.82
Batch 2				
LM23TB	3	Before	92.3	1.86
LM23TA	3	After	30.8	1.82
LM23BB	3	Before	41.3	1.84
LM23BA	3	After	25.4	1.83
LM26TB	6	Before	59	1.86
LM26TA	6	After	101.9	1.85
LM26BB	6	Before	102.9	1.87
LM26BA	6	After	43.1	1.84
LM210TB	10	Before	125.9	1.87
LM210TA	10	After	46.5	1.86
LM210BB	10	Before	133	1.87
LM210BA	10	After	47.9	1.89
LM213TB	13	Before	93.9	1.87
LM213TA	13	After	67.8	1.85
LM213BB	13	Before	75.6	1.85
LM213BA	13	After	26.7	1.83

Table 5.4: The list of pork mince samples, their codes and characteristics. Red indicates failed external QC and excluded from sequencing analysis. Grey denotes end of shelf-life

Sample ID	Shelf-life (Days)	Before/after respirometry	DNA concentration (ng/µL)	A260/A280
Batch 1				
PM15TB	5	Before	21.9	1.78
PM15TA	5	After	8.7	1.7
PM15BB	5	Before	45.3	1.83
PM15BA	5	After	13.3	2.14
PM18TB	8	Before	29.6	1.79
PM18TA	8	After	18.1	1.78
PM18BB	8	Before	34.9	1.84
PM18BA	8	After	16.3	1.8
PM110TB	10	Before	32.3	1.81
PM110TA	10	After	28.1	1.8
PM110BB	10	Before	25	1.85
PM110BA	10	After	16.6	1.82
PM113TB	13	Before	46.3	1.86
PM113TA	13	After	30.4	1.86
PM113BB	13	Before	40.3	1.89
PM113BA	13	After	28.1	1.89
Batch 2				
PM24TB	4	Before	28.2	1.82
PM24TA	4	After	8.3	1.85
PM24BB	4	Before	34.4	1.7
PM24BA	4	After	8.9	1.81
PM28TB	8	Before	35.1	1.87
PM28TA	8	After	25.4	1.86
PM28BB	8	Before	41	1.83
PM28BA	8	After	21.6	1.82
PM210TB	10	Before	32.6	1.86
PM210TA	10	After	14.2	1.85
PM210BB	10	Before	30.2	1.96
PM210BA	10	After	11.2	2
PM213TB	13	Before	42.3	1.87
PM213TA	13	After	30.8	1.88
PM213BB	13	Before	38.1	1.86
PM213BA	13	After	18.5	1.89

Respiration profiles and corresponding TVC values for each mincemeat type can be seen in Figures 5.2-5.5. There was little to no difference observed in the respirometric profiles between the top and bottom samples (Figures 5.2-5.5). This was further confirmed by plate counts for each mincemeat type (Figures 5.2-5.5), which showed small variation when combined. We attribute this to the nature of the product itself and stable high O_2 levels in the mince packs (Figure 5.1), which is not dense and thus allows for aeration throughout. In addition, we had to increase the *dphi* threshold to 30°, as the baseline for the majority of samples was already at 25°. However, TVC values were still calculated using the equation developed in Chapter 4.

All beef mince samples produced characteristic sigmoidal profiles (Figure 5.2A &B), with a steep transition from oxygenated to deoxygenated condition, due to the exponential growth of oxygen consuming bacteria. A decrease in TT over shelf-life was observed, which reflects an increase in initial microbial load. This was confirmed with plate counts, which showed a linear increase over shelf-life (Figure 5.2C&D). Although similar profiles were seen between batches, there were some small differences. Batch 2 samples (Figure 5.2B) reached the signal threshold faster than Batch 1 (Figure 5.2A). Samples tested on Best Before date BM2T10 and BM2B10 reached the signal threshold faster than 13 Day old samples BM2T13 & BM2B13. This data, together with plate count data, suggests that samples in Batch 2 had higher initial microbial loads than Batch 1. Such variation can be attributed to the inherent variability of retail purchased samples as minute changes in handling, storage, and display can affect the microbial load (Stellato et al., 2016). Calculated TVCs showed similarities to plate count results with the exception of Batch 1 Day 3 sample (Figure 5.2C), which was an overestimation of microbial load due to initial signal already being at the *dphi* threshold of 25°.

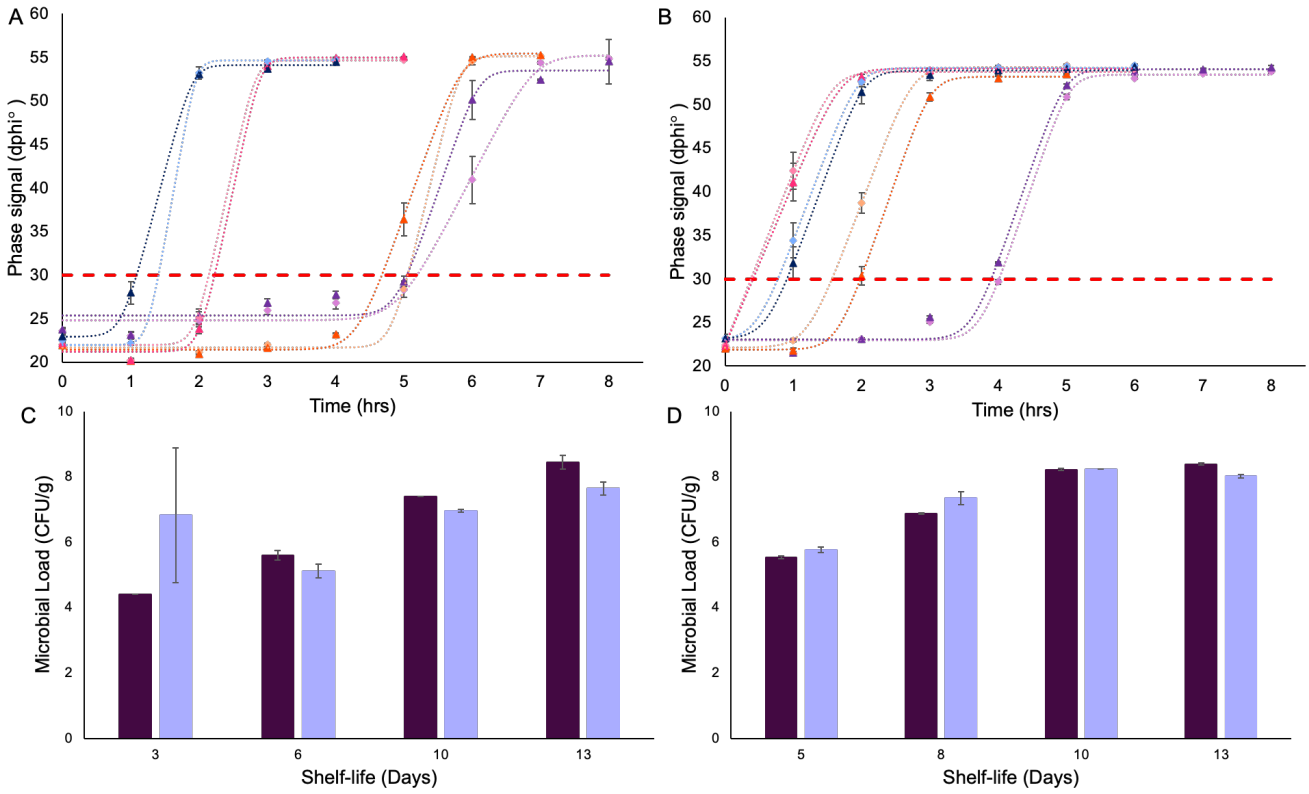

Figure 5.2: Results of microbiological tests for the MAP beef mince samples over shelf-life. Respiration profiles for Batch 1 samples **(A)** BM1T3 (◆); BM1B3(▲); BM1T6 (◆); BM1B6(▲); BM1T10 (◆); BM1B10(▲); BM1T13(◆); BM1B13(▲) and Batch 2 samples **(B)** (BM2T5 (◆); BM2B5(▲); BM2T8 (◆); BM2B8(▲); BM2T10 (◆); BM2B10(▲); BM2T13(◆); BM2B13(▲), signal threshold level is shown as (– –). Data for three replicates per sample at each time points are shown. Total viable counts (TVCs) calculated from respiration profile (light purple) and plate counts (dark purple) for Batch 1 **(C)** and Batch 2 **(D)**. Error bars denote standard deviation of replicates.

Turkey mince exhibited similar profiles to beef mince (Figure 5.3A&B), in which microbial growth was characterised by sigmoidal profiles. The exception was the 13 Day old samples pertaining to 3 days past Best Before (TM2T13 & TM2B13) in Batch 2 (Figure 5.3B), which showed a linear progression of deoxygenation and a delayed time to result. This is the first reported case of a linear profile from oxygen respirometry and could be possibly attributed to an unknown initial microbial population. Plate counts showed an increase in microbial load over time (Figure 5.3 C&D), however the increase was not as clearly linear as seen in beef mince (Figure 5.2 C&D). In addition, there were differences seen between the two batches with Batch 2 (Figure 5.3D) showing an initial increase in microbial load followed by a decrease. This corresponds to the delayed time to result seen in the respiration

profiles described previously. Calculated TVCs (Figure 5.3 C&D) did not show a linear progression over time, instead remained relatively constant throughout shelf-life.

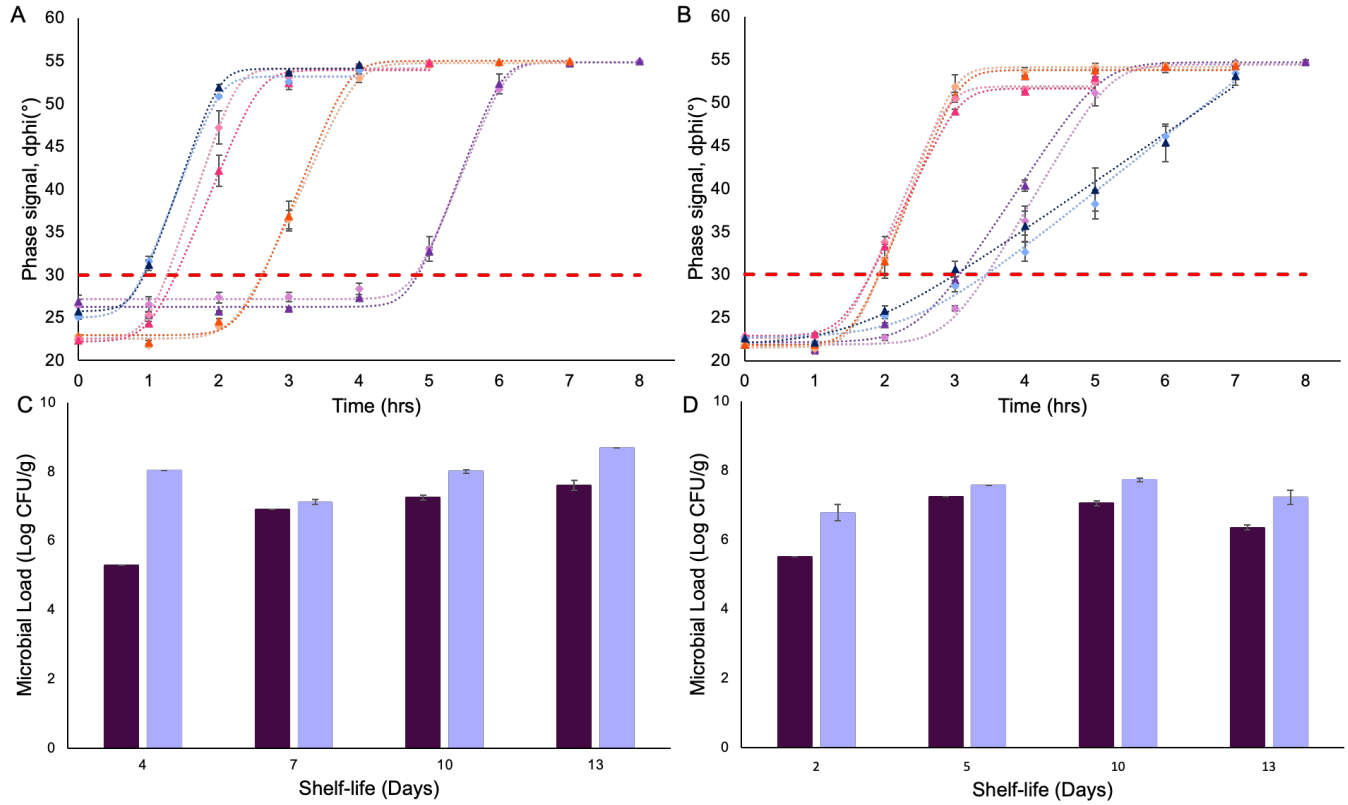

Figure 5.3: Results of microbiological tests for the MAP turkey mince samples over shelf-life. Respiration profiles for Batch 1 samples **(A)** TM1T4 (◆); TM1B4(▲); TM1T7 (◆); TM1B7(▲); TM1T10 (◆); TM1B10(▲); TM1T13(◆); TM1B13(▲) and Batch 2 samples **(B)** TM2T2 (◆); TM2B2(▲); TM2T5 (◆); TM2B5(▲); TM2T10 (◆); TM2B10(▲); TM2T13(◆); TM2B13(▲), signal threshold level is shown as (– –). Data for three replicates per sample at each time points are shown. Total viable counts (TVCs) calculated from respiration profile (light purple) and plate counts (dark purple) for Batch 1 **(C)** and Batch 2 **(D)**. Error bars denote standard deviation of replicates.

Lamb mince exhibited a variety of respiration profiles (Figure 5.3 A&B) ranging from sigmoidal to linear to a combination of both to which curve fitting could not be applied to (solid lines). For Batch 1(Figure 5.4A), the respiration profile for Day of purchase sample LM1B3 showed an initial linear increase followed by a plateau after 3 hours. Similarly, for Batch 2 LM2B13 and LM2T13 (Figure 5.4B) both showed linear respiration profiles. However, both batches exhibited similarities in plate counts, with a linear increase in microbial load over shelf-life (Figure 5.4 C&D). Calculated TVCs, on the other hand, showed an overestimation of microbial load with no consistent pattern. This is due to the respiration profiles already having reached the *dphi* threshold of 25° at the beginning of the assay.

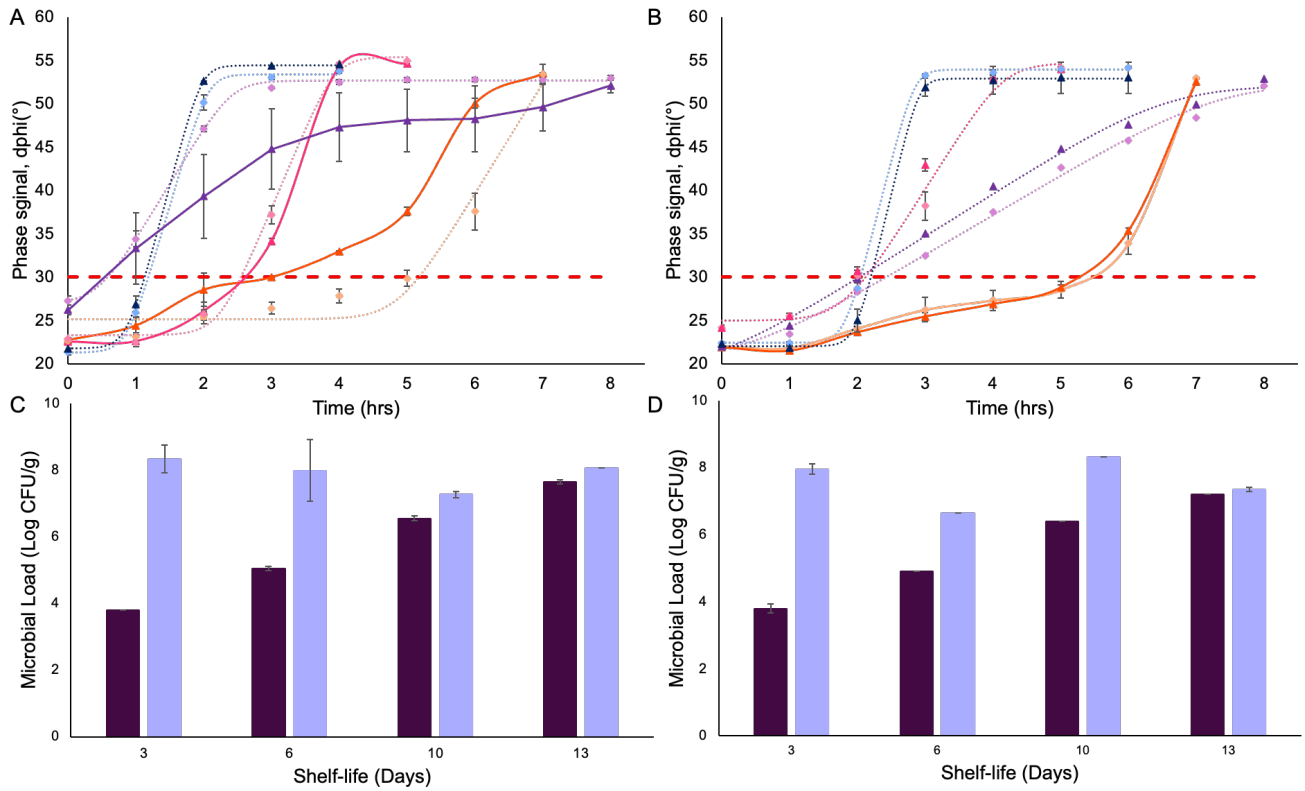

Figure 5.4: Results of microbiological tests for the MAP lamb mince samples over shelf-life. Respiration profiles for Batch 1 samples **(A)** LM1T3 (◆); LM1B3(▲); LM1T6 (◆); LM1B6(▲); LM1T10 (◆); LM1B10(▲); LM1T13(◆); LM1B13(▲) and Batch 2 samples **(B)** LM2T3 (◆); LM2B3(▲); LM2T6 (◆); LM2B6(▲); LM2T10 (◆); LM2B10(▲); LM2T13(◆); LM2B13(▲), signal threshold level is shown as (– –). Data for three replicates per sample at each time points are shown .Total viable counts (TVCs) calculated from respiration profile (light purple) and plate counts (dark purple) for Batch 1 **(C)** and Batch 2 **(D)**. Error bars denote standard deviation of replicates.

The respirometric profiles for pork mince were the most unusual since no sigmoidal profiles were observed (Figure 5.5 A&B). Most of the profiles were linear with some exhibiting a similar plateau effect as first seen in lamb mince (Figure 5.4A). In addition, some of the pork mince profiles could not be curve fitted (solid lines). Plate counts (Figure 5.5 C&D) remained consistent throughout shelf-life at approximately 4 Log CFU/g while calculated TVCs were almost double. This once again was due to initial readings from respirometric profiles already being at the *dphi* threshold of 25°.

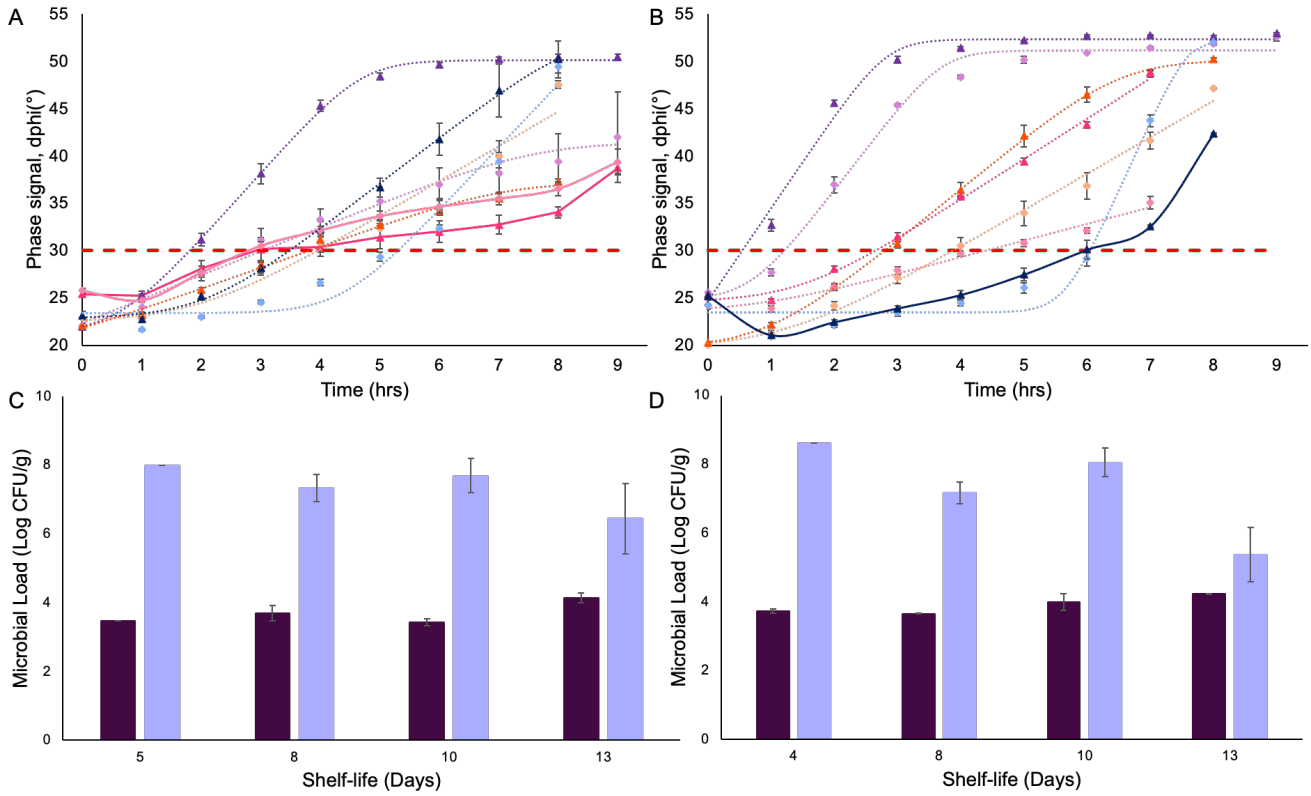

Figure 5.5: Results of microbiological tests for the MAP pork mince samples over shelf-life. Respiration profiles for Batch 1 samples **(A)** PM1T5 (◆); PM1B5(▲); PM1T8 (◆); PM1B8(▲); PM1T10 (◆); PM1B10(▲); PM1T13(◆); PM1B13(▲) and Batch 2 samples **(B)** PM2T4 (◆); PM2B4 (▲); PM2T8 (◆); PM2B8(▲); PM2T10 (◆); PM2B10(▲); PM2T13(◆); PM2B13(▲), signal threshold level is shown as (– –). Data for three replicates per sample at each time points are shown. Total viable counts (TVCs) calculated from respiration profile (light purple) and plate counts (dark purple) for Batch 1 **(C)** and Batch 2 **(D)**. Error bars denote standard deviation of replicates.

5.2.3. 16S rRNA amplicon sequencing and comparison to respirometry

The isolation, quantification and initial quality assessment of DNA from mince sample homogenates (Table 5.1-5.4) were done in-house, using manufacture's protocol. After that DNA samples were sent to an external sequencing services company Macrogen (Korea) for sequencing of the 16S rRNA amplicon. At Macrogen, the DNA samples were subjected to additional QC. The samples which failed this external QC (marked in red) were excluded from sequencing. The majority of failed samples were from lamb mince (Table 5.3) and pork mince (Table 5.4). We also observed a decrease in DNA concentration in samples that were taken after respirometry compared to those taken before. This is likely due to debris precipitating at the bottom of the sensor vials as well as the dilution introduced by the addition of homogenate to NB.

Sequencing data for the mince samples were then analysed using R software (Bates et al., 2015). Alpha diversity, which is the degree of variation within a sample, was measured for each meat type using the following standard indices (Figure 5.6):

i) Chao1 or richness: how many different features a sample has.

ii) Shannon entropy or evenness: how equally the features in a sample are represented.

iii) Simpson's index: the probability that two features picked at random do not have the same name (Bastiaanssen, Quinn, & Loughman, 2022).

Beef mince showed a significant (ANOVA, $P < 0.05$) linear decrease in all indices over shelf-life, while lamb mince showed a significant decrease in Shannon entropy and Simpson's index. These results are indicative of a decrease in microbial diversity over shelf-life for the aforementioned mincemeat types, which is also consistent with the findings of previous studies (Filippis et al., 2013; Palman et al., 2020). These studies found that as time progressed, meat microbiota became less diverse with a handful of taxa dominating in abundance.

Pork mince did not exhibit any significant changes in all three indices, suggesting that microbial diversity remained consistent over shelf-life. However, it should be noted that pork mince had the lowest number of samples for analysis due to the majority of them failing QC (Table 5.4) and/or producing the uncommon respirations profiles (see Figure 5.5).

A significant decrease in Chao1 was observed for turkey mince, while no significant changes were seen in the other two indices. This suggests that although the richness of the turkey microbiota decreased over shelf-life, the evenness and Simpson's index remained consistent. It should be noted that Chao1 is the most sensitive of the indices examined and therefore minute changes in microbial composition will be detected (Bastiaanssen, Quinn, & Loughman, 2022).

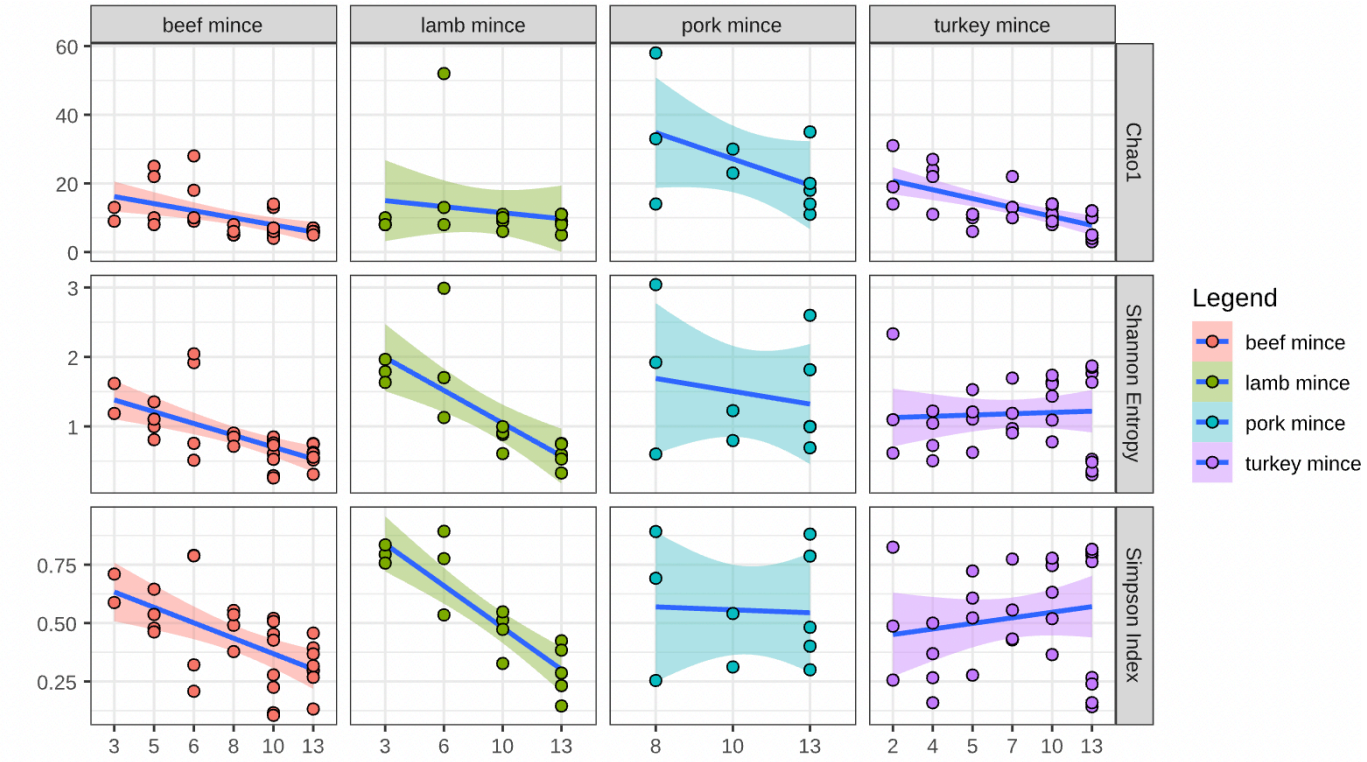

Figure 5.6: Comparison of bacterial alpha diversities for all mincemeat types over shelf-life. Indices include Chao1 (richness), Shannon Entropy (evenness), and Simpson index. Circles represent individual samples while trendlines represent slopes.

To further investigate the compositional differences of the microbiota from different mincemeat types, relative microbial 16S rRNA amplicon read abundance analysis was performed (Figure 5.7). At the beginning of shelf-life, beef mince exhibited compositional diversity, including taxa such as *Escherichia*, S*erratia, Pseudomonas, Carnobacterium, Lactococcus,* and *Stenotrophomonas*. In addition, a small proportion of the beef microbiota included rare taxa, which have yet to be described. However, as shelf-life progressed, two taxa, *Carnobacterium* and *Lactococcus*, became dominating. This result confirms the decrease in alpha diversity observed in Figure 5.6. *Carnobacterium* is a Gram-positive, facultative anaerobic lactic acid bacteria which has been found in the microbiome of chilled MAP meats (Laursen et al., 2005). *Lactococcus* is another lactic acid bacteria which is Gram-positive, microaerophilic, and homofermentative (primarily lactic acid), also known as a key component of the meat spoilage microbiome (Hilgarth, Werum & Vogel, 2020).

Similarly, lamb mince showed greater microbial diversity at the beginning of shelf-life, which included the aforementioned taxa as well as *Fusobacterium* and *Bacteroides.* Interestingly, lamb mince had a greater proportion of rare taxa than beef mince. At the

end of shelf-life, the same two taxa, *Carnobacterium* and *Lactococcus,* were dominating, thus further supporting the observed decrease in alpha diversity (Figure 5.6). Some of the respiration profiles of lamb mince (Figure 5.3) were unusual at the beginning of shelf-life and could potentially be attributed to the presence of rare taxa, but further investigation is required to prove this conclusion.

Although many pork mince samples are missing from the beginning of shelf-life, microbial diversity seems to be maintained, which supports the trends seen in the alpha diversity indices (Figure 5.6). Taxa seen are similar to those described for beef and lamb mince, however the rare taxa remain prevalent and coincide with the unusual respirometric profiles observed in Figure 5.4.

It should also be noted that an inherent limitation of 16S rRNA sequencing is the inability to calculate absolute abundance, or in other words, the total bacterial load of a sample (McLaren, Willis , & Callahan, 2019). Thus, the observed rare taxa could reflect low microbial numbers rather than the true composition of the microbiome since they have a greater chance of being sequenced and inflate the calculated diversity (Bastiaanssen, Quinn, & Loughman, 2022).

Compositional differences in microbial diversity were seen in turkey mince with the presence of *Photobacterium*, a Gram-negative facultative anaerobe. Mostly associated with marine environments, *Photobacterium* has recently been found in the spoilage microbiome of beef mince and poultry (Hilgrath et al., 2018). As shelf-life progressed, a decrease in microbial diversity can be seen, however to a lesser extent than for beef and lamb mince, with 3 to 4 taxa dominating. This supports the decrease in richness observed in Figure 5.6.

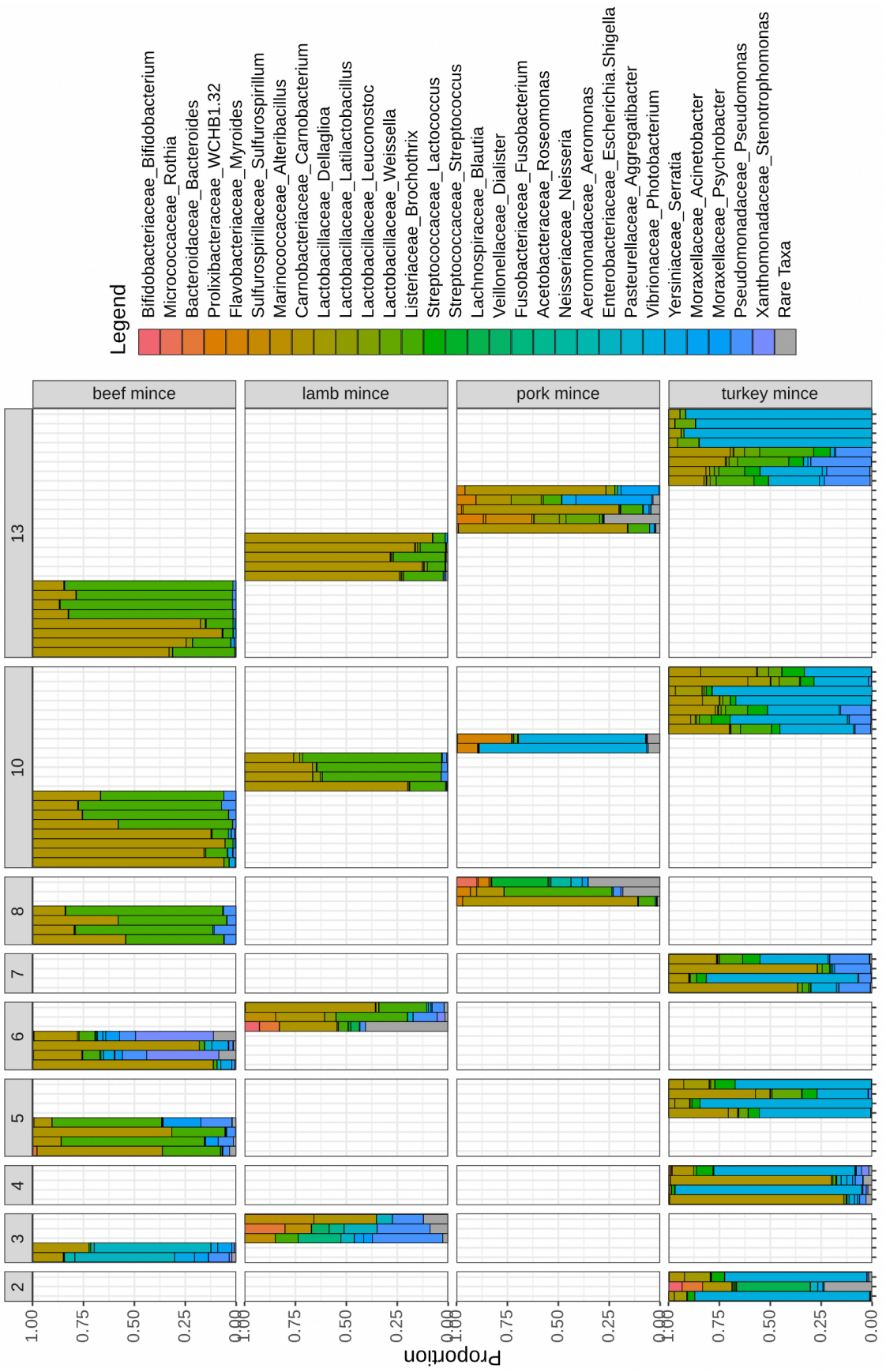

Figure 5.7: Relative microbial 16S rRNA amplicon read abundance analysis over shelf-life for all mincemeat types showing compositional differences between samples and throughout shelf-life.

In the next step, beta diversity, or the degree of difference between two microbiomes, was investigated for the four different mincemeat types using one of the common measures, Aitchison Distance. Aitchison Distance is a related measure of Euclidean Distance, in which the application of the Pythagorean theorem is used to derive the geometric distance between every microbe as a separate dimension (Bastiaanssen, Quinn, & Loughman, 2022). The effects of respirometry on microbiota were also investigated. This was further visualised using principal component analysis (PCA), which revealed four separate clusters (Figure 5.8). Two mincemeat types, beef (red) and turkey (purple), showed distinct, non-overlapping clusters suggesting that the meat type defines the sample. Although turkey mince displayed larger variance than beef mince, samples retained greater similarity to each other than to the other mincemeat types. Pork mince (blue) showed greater variance than lamb mince (green) with both clusters overlapping with beef and turkey. Moreover, respirometry (after respirometry, squares) did not affect the overall microbiota of each mincemeat type as samples remained within their respective clusters. Permutational multivariate ANOVA based on time (shelf-life), type of mincemeat, and effects of respirometry showed that a significant ($P < 0.05$) difference in overall microbiota composition was attributed to mincemeat type.

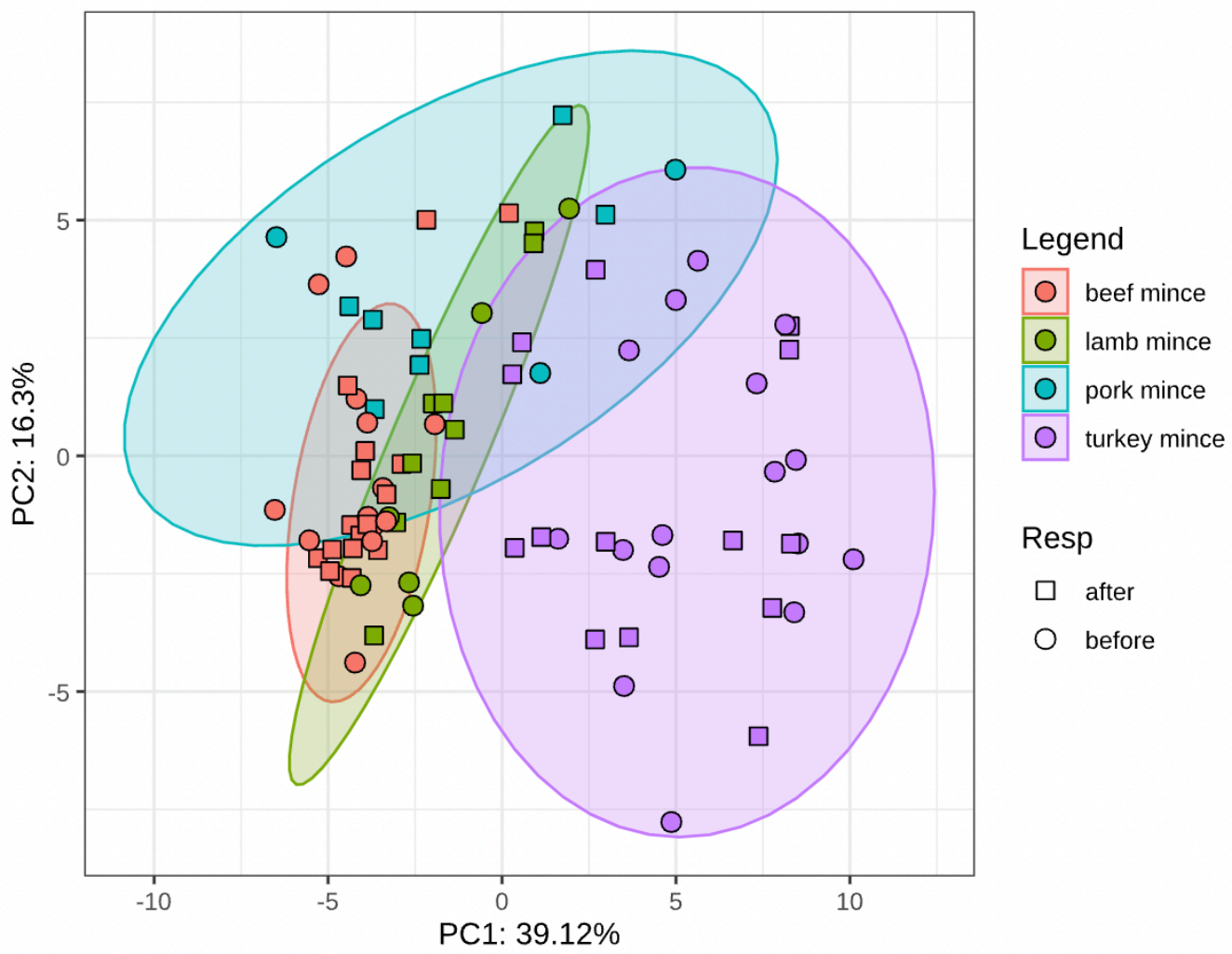

Figure 5.8: Principal components analysis (PCAs) of mincemeat microbiomes. Four major clusters were identified relating to the four types of mincemeat. Circles represent samples taken at 0 hours (before respirometry) and squares represent samples taken after 2-5 hours of culturing (after respirometry).

To estimate the role of time (shelf-life) and respirometry (involves 2-5h incubation in nutrient-rich growth media NB at 30°C) on individual genus abundance, generalised linear mixed effects models were created for two out of the four mincemeat types (Figures 5.9 & 5.10) (Bates et al., 2015). Pork and lamb mince were excluded due to low sample numbers and no observed significant differences at the genus level, respectively.

Within beef mince, 6 taxa showed a significant interaction (ANOVA, Benjamini-Hochberg adjusted q-values of < 0.1) between shelf-life and respirometry status (Figure 5.9). *Carnobacterium* showed a steep linear increase in abundance over shelf-life as well as an increase after respirometry (growth and acute depletion of oxygen). *Alteribacillus*, a Gram-positive, aerobic, endospore forming bacteria decreased in abundance over shelf-

life, but showed a slight increase after respirometry. A steep decrease over shelf-life was observed for the genus *Psychrobacter*, which includes Gram-negative aerobic psychrotrophs that are commonly found in processed meats and poultry (Juni & Heym, 1986). However, after respirometry, levels of *Psychrobacter* remained relatively consistent. *Pseudomonas,* a Gram-negative aerobic bacteria associated with meat spoilage (Jayasena & Jo, 2013; Stellato et al., 2016), decreased over shelf-life and after respirometry. The taxa *Sphingomonas*, which includes Gram-negative aerobic bacteria also decreased over shelf-life but remained consistent after respirometry. Finally *Lactococcus* showed a steep increase over shelf-life but only a slight decrease after respirometry. The general trend over shelf-life was a decrease in aerobic taxa and an increase in lactic acid bacteria. This could potentially be linked to the increase in CO_2 levels observed in Figure 5.1 as lactic acid bacteria are known producers of CO_2 (Shao et al., 2021). Interestingly, beef mince exhibited less overall variance in the PCAs (Figure 5.8), but displayed significant differences in the aforementioned taxa, indicating changes in microbial abundance. This is in agreement with the finding that the alpha diversity of beef mince does change over time and with acute exposure to respirometry, but in terms of abundance rather than introduction or depletion of certain taxa.

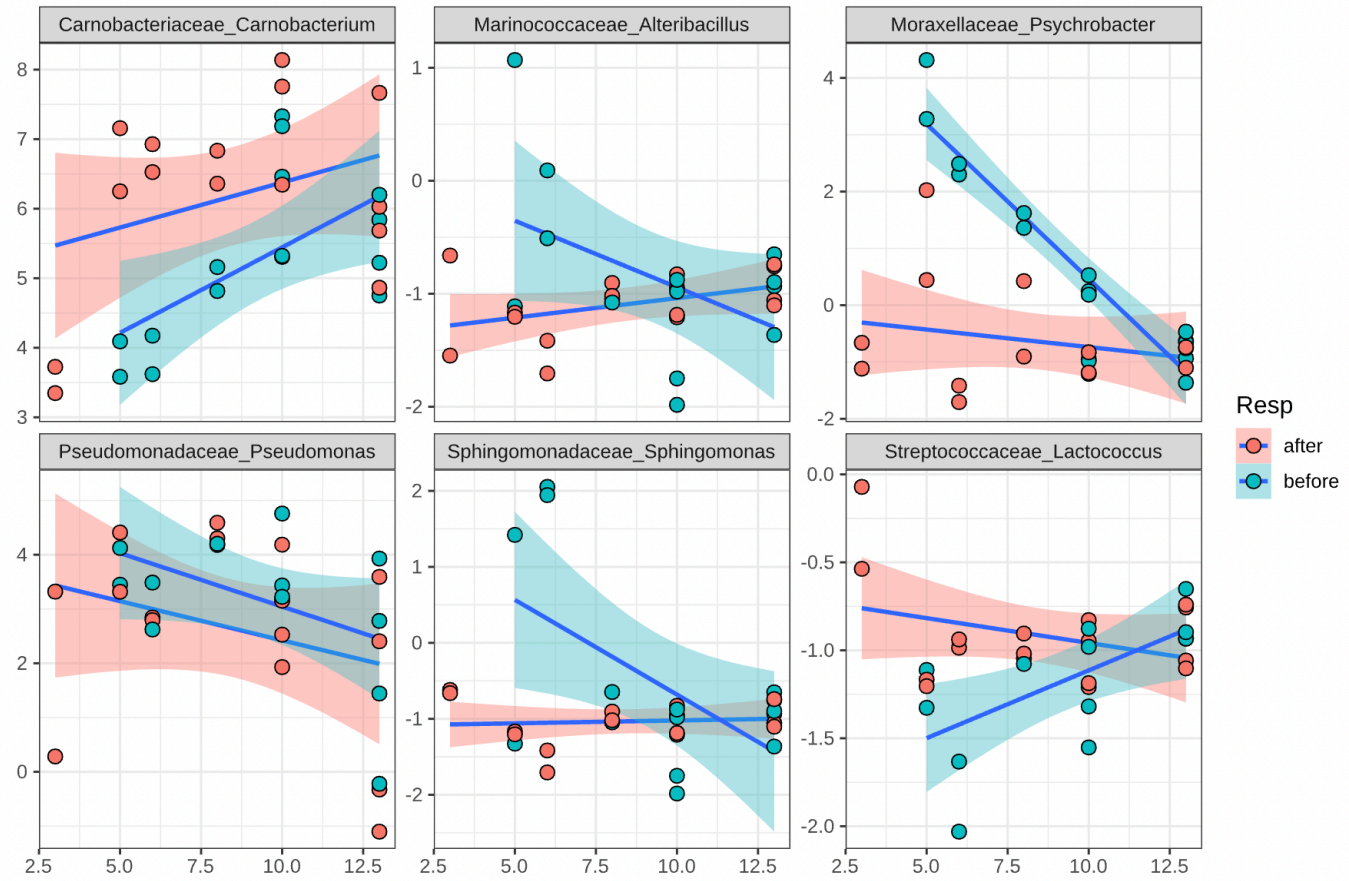

Figure 5.9: Generalised linear models showing differential slopes based on respirometry for beef mince. The y-axis depicts CLR (centred log-ratio) transformed relative bacterial abundance while the x-axis depicts shelf-life (Days). Changes in 6 distinct taxa were observed. Blue circles represent samples taken at 0 hours (before respirometry) and red circles represent samples taken 2-5 hours later (after respirometry).

Turkey mince also showed a significant interaction with 4 distinct taxa between shelf-life and respirometry status (Figure 5.10). Interestingly, two of the taxa, *Carnobacterium* and *Lactococcus,* were the same as in the beef mince generalised linear mixed effects model, however, the trends observed were different. These two taxa were also seen to be shared between beef and turkey mince in the relative microbial 16S rRNA amplicon read abundance (Figure 5.7). *Carnobacterium* stayed relatively consistent over shelf-life, but decreased after respirometry while *Lactococcus* decreased over shelf-life and remained consistent after respirometry. *Photobacterium* showed a decrease over shelf-life, but a steep increase after respirometry. A Gram negative, facultative anaerobe, *Yersinia* remained consistent throughout shelf-life, but decreased after respirometry. *Yersinia* has been found in farm animals, however many members of this taxon are pathogenic, including *Yersinia pestis*, the species responsible for the Bubonic plague (Lorenzo et al.,

2018). Similarly to beef mince, turkey mince also displayed changes in abundance of taxa due to shelf-life and acute exposure to respirometry.

Overall, there was a significant difference for certain taxa seen before and after the effects of respirometry, implying changes based on the promoted growth of aerobes and facultative anaerobes and decreased availability of residual oxygen. For beef mince there was a clear general trend in which aerobic bacteria decreased in abundance and certain facultative anaerobic bacteria increased. Although the mechanism behind the changes in abundance of these bacteria remains to be investigated, it is likely that the facultative anaerobic capacity is a determinant factor. Turkey mince, on the other hand, did not exhibit as a clear a trend as beef mince. Interestingly, only facultative anaerobes displayed significant changes before and after respirometry with no significant changes detected for aerobes. Thus, further investigation into species level differences as well as possible metabolic changes is needed.

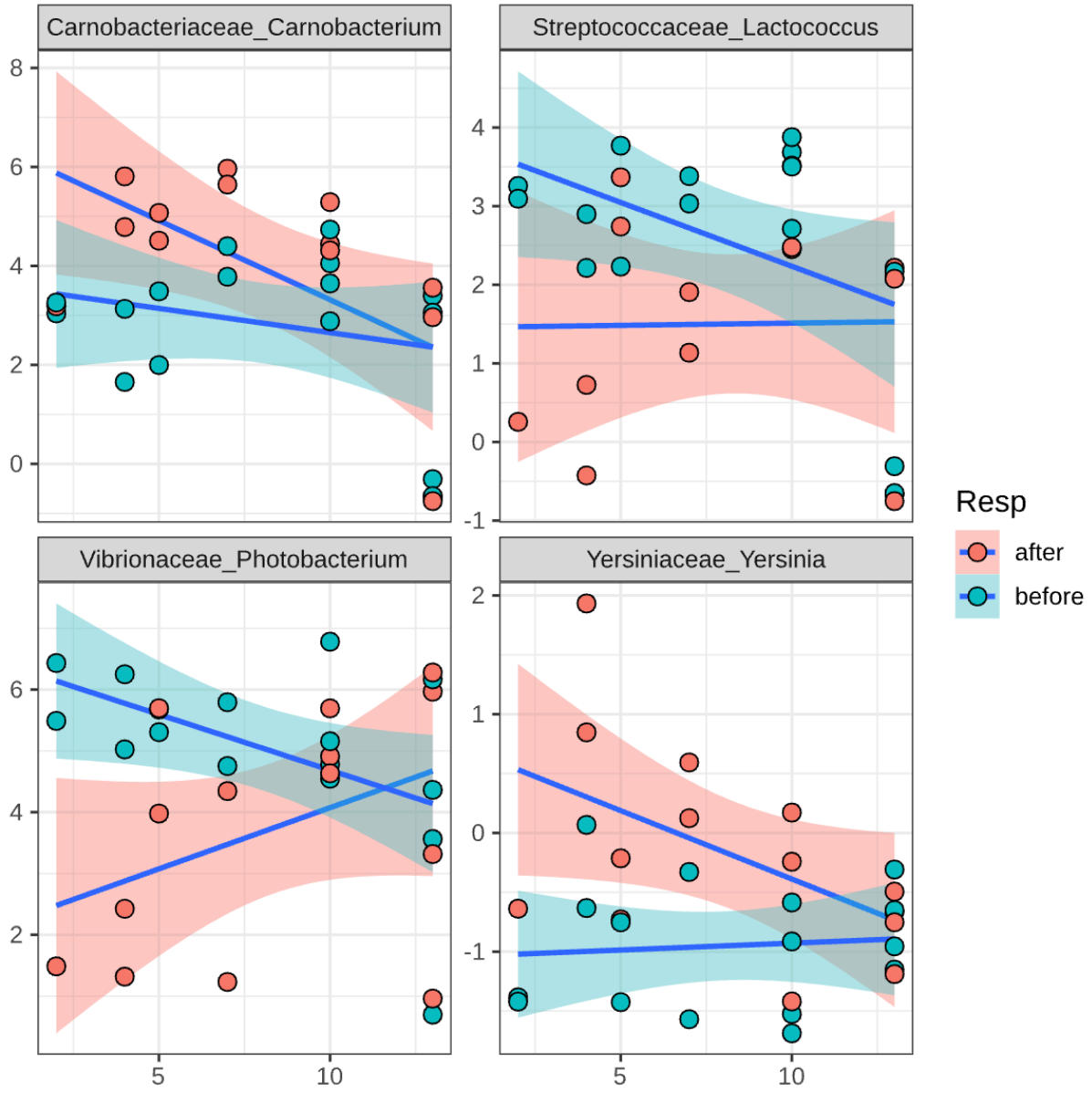

Figure 5.10: Generalised linear models showing differential slopes based on respirometry for turkey mince. The y-axis depicts CLR (centred log-ratio) transformed relative bacterial abundance while the x-axis depicts shelf-life (Days). Changes in 4 distinct taxa were observed. Blue circles represent samples taken at 0 hours (before respirometry) and red circles represent samples taken 2-5 hours later (after respirometry).

5.3. Conclusions

The O_2 sensor based respirometric system developed for rapid microbial testing of food samples was used for a shelf-life study with four different types of mincemeat: beef, turkey, lamb and pork. Occasionally, mince samples produced unusual linear respiration profiles, the origin and underlying mechanism of which remains largely unknown. However, the incidence of such cases related to mincemeat type, being high for lamb and pork mince and low for beef and turkey. Furthermore, calculated TVCs, based on the previously developed

calibration equation (Chapter 4), displayed discrepancies with conventional plate counts (ISO 4833-1: 2013). It is worth noting that such unusual effects were not encountered in all previous studies with various food samples including raw meat, fish, and salads (Hempel et al., 2011; Hempel et al., 2013, Fernandes et al., 2013).

In parallel with the respirometric microbiological assessment, the whole microbiome of each mincemeat type was also analysed using 16S rRNA amplicon sequencing. This method showed an overall decrease in alpha diversity over shelf-life. In addition, both lamb and pork mince maintained a proportion of rare taxa throughout, shelf-life. Also some taxa exhibited significant changes (ANOVA, Benjamini-Hochberg adjusted q-values of < 0.1) in abundance over shelf-life and upon exposure to respirometric analysis, with beef mince exhibiting a decrease in aerobic bacteria and an increase in facultative anaerobes. Finally, beta diversity was seen to be dictated by mincemeat type. All these factors, plus possible treatment of mince samples with antimicrobials (Palman et al., 2020), could potentially explain the observed unusual respiration profiles, which resemble those of slow growing, slow respiring, stressed or injured bacterial cells. However, further investigation into this is warranted. Ultimately, respirometry revealed varying profiles based on mincemeat type while sequencing showed changes in alpha and beta diversity over shelf-life and upon exposure to respirometry. Combining these two techniques gives powerful research tool for food scientists and microbiologists. Future investigations could examine species level changes and metabolic processes associated with respirometry.

General Discussion

Several new analytical methodologies for food safety were developed based on oxygen respirometry and phosphorescent liquid O2 probes and solid-state O2 sensors. Thus, using the commercial MitoXpress-Xtra probe, a standard fluorescent plate reader and LAE (Lauroyl Arignate Ethyl Ester) model, a high-throughput screening assay with multiple functional readouts for testing the antimicrobial efficacy of (bio)chemicals on pure bacterial cultures and whole meat microbiota was designed (Chapter 3). The assay allowed for the automated and parallel analysis of different samples using a range of conditions: antimicrobial concentrations, exposure time, temperature, bacterial concentrations, and growth media (Figure 3.1). Respiration profiles for each pure culture (Figures 3.2 -3.5) visualised the toxicological effects of LAE with higher concentrations (166.7 μg/mL to 18.5 μg/mL) inhibiting growth. The EC50 determined by the new method, which was calculated using reciprocal TT values and concentration of LAE, was similar for *E. coli*, *S. aureus*, and *B. cereus* with values of 6.81 ± 0.64 μg/mL, 6.47 ± 0.27 μg/mL and 6.93 ± 0.10 μg/mL, respectively. *P. fluorescens*, on the other hand, showed an increased resistance to LAE, with an EC50 value of 11.51 ± 1.04 μg/mL. Interestingly, there was little to no difference observed in EC50 values for Gram-positive and Gram-negative species with the exception of *P. fluorescens*. Previous studies have shown that Gram-positive bacteria tend to be more sensitive to antimicrobials than their Gram-negative counterparts as the latter possess an additional outer lipid membrane which restricts the diffusion of exogenous molecules (Russel, 1995; Higueras et al., 2013). However, this effect was not observed. The higher resistance of *P. fluorescens* to LAE was most likely attributed to the extracellular polysaccharide in the cell wall (used for biofilm formation), which has shown to confer stronger resistance to antimicrobials (Baum et al., 2009; Arslan et al., 2011; Becerril et al., 2013). In addition, there were differences in EC50 values based on temperature (*E. coli*) and seeding concentration (*P. fluorescens*) (Figure 3.7). Temperature dependence was seen to increase the efficacy of LAE in a study investigating the synergy between LAE and mild heat (Yang et al., 2019). The effects of seeding concentration observed for *P. fluorescens* in conjugation with incubation time could have led to the formation of a biofilm, incurring further resistance to LAE (Becerril et al., 2013). Overall, the respiration profiles and EC50 values determined by the assay gave valuable insights into the toxicological effects of LAE on pure cultures.

The assay was compared to the established densitometry method, which involved OD600 measurement and MIC determination (Weigand et al., 2008). The determined MIC value for representative Gram-positive (*S. aureus*) and Gram-negative (*E. coli*) bacteria was 18.5 μg/mL, which was consistent with the literature values for *E. coli* but not for *S. aureus* (Rodriguez et al., 2004; Higueras et al., 2013). This could be possibly due to the fact that a higher seeding concentration was used (10^5 CFU/mL versus 10^4 CFU/mL) in the reference method compared to the study done by Rodriguez et al. (2004). A higher seeding concentration in turn, could confer higher resistance to LAE. However, when compared to the EC50 values (Table 3.1), the MIC values obtained were significantly higher. Thus, respirometric assays provide more sensitive detection of antimicrobial action, as they can detect subtle and sublethal changes in cell metabolism. Further limitations of the reference method include lengthy incubation times (18 hours to complete), the inability to determine whether antimicrobials are bacteriostatic or bactericidal, and incapability of handling crude homogenates.

To demonstrate the robustness of the respirometric assay, the efficacy of LAE was further tested on spoiled meat microbiota, in which the EC50 value increased significantly to 39.99 μg/mL and the appearance of bi-phasic respiration profiles was observed (Figure 3.8A). These profiles and significantly higher resistance could be attributed to the increased microbial diversity of the sample (Ray & Bhunia, 2013, Stellato et al., 2016). The bi-phasic respiration profile is indicative of two bacterial populations, with the first population being more abundant or fast growing, producing the first step in the respiration profile. However, being either more sensitive to low O_2 levels or LAE, it ceases to grow and consume oxygen. The second population has a slower growth rate or is more resistant to LAE (Ray & Bhunia, 2013) and can respire at lower oxygen levels than the first population, thus producing the second respiration step. Furthermore, the presence of certain bacterial species such as *Pseudomonas* spp., *Streptococcus* spp., *Brochonthrix* spp. (Stellato et al., 2016), could confer higher resistance to LAE in the spoiled meat homogenate.

Therefore, the assay is applicable to complex food homogenates with little interference to the phosphorescence lifetime of the probe and measured signal onset time. Real-time, robust and sensitive readout was achieved with consistent and reproducible results

(Table 3.1) in as little as 3 to 10 hours. Overall, the utilisation of the assay is not limited to LAE and can be applied to various antimicrobials, food samples, and microbiological samples in a fast and straightforward manner.

Another new O_2 sensor based respirometric platform for testing of meat and environmental samples was developed, which is simple, portable, flexible and modular, and includes the following main components: i) in-house made disposable sterile testing vials each containing a solid-state O_2 sensor coating with modifications depending on the application (meat sample vs swab sample); ii) an autonomous commercial handheld reader, FirestingGO_2, which can read sensor signals from the vials in a non-invasive manner; iii) a benchtop heater/incubator, in which vials are maintained at the assay temperature (normally 30°C) (Figure 4.2). For the 30 Sterilin™ mL vials used for meat samples and carcass swab samples, the sensor coating was applied directly to the bottom of the vial, whereas for the 10 mL brush swab vials the sensor coatings were applied on the side of the vial. Both types of vials underwent quality assessment to ensure that signal readout was consistent within batches. To establish the relationship between the measured parameters (TT values, in hours) and initial TVC load of samples (Log CFU/g or Log CFU/cm^2), the two systems were calibrated using *E. coli* cultures and also different matrices pertaining to different sample types (Figure 4.8). From the calibrations, corresponding analytical equations were derived for meat samples, carcass swab samples, and brush swab samples. Despite previous studies having established calibrations, they were conducted under different experimental settings including the type of sensor/probe, temperature, assay substrate (microplate or tube) as well as sample (food homogenate) used (O'Mahony et al., 2005; O'Mahony & Papkovsky, 2006; Jasionek et al., 2013). Therefore, the established calibrations were not valid for the new platform and new calibrations were necessary.

The systems were then validated with panels of real samples. For the 30 mL vials, different types of raw meat cuts and carcass swabs from a local meat processing plant were used. Similarly, the 10 mL swab vials were validated using three different surface sample types: i) artificially contaminated with *E. coli*, ii) environmental swabs, and iii) contaminated with meat microbiota. Both systems were compared to the conventional plating method (ISO 4833-1: 2013; ISO 18593:2018) and showed a strong positive correlation (Pearson's correlation, $P < 0.05$) (Figures 4.10 & 4.11). Albeit the system was designed primarily for the

meat industry, it could also be readily applied in laboratories conducting food research as the TVC test is common practice (Hauge et al., 2017; Biasino et al., 2018). In addition, the system could be applied to various crude homogenates as the solid state O_2 sensor remains protected from the aqueous environment due to its immobilisation within the polymer. Moreover, oxygen respirometry has a wide range of applications including the analysis of isolated mitochondria, mammalian cells and small animal metabolism, and enumeration of bacteria in food samples (Hynes et al. 2006, Will et al., 2007, Hempel et al., 2011). However, the application of oxygen respirometry to a completely portable system is novel and has the potential to become a stable in both processing plants and laboratories.

Ultimately, the sensor based system demonstrated its capabilities of handling both model contamination with *E. coli* and complex meat homogenates. Moreover, the proposed method outperformed the conventional TVC test in speed (time to result 2-10 hrs vs 48-72 hrs), simplicity, and user-friendliness (no dilutions, real-time readout). The cost of the system is less than $5K: $1.5 – $4.5k for the reader, $300 for the block heater, and $1- $3 for disposable sensor vials. Although the materials for the TVC method are normally considered inexpensive, they are required in large amounts and additional costs are incurred through labour associated with the lengthy procedure. Most of the components listed for the sensor vial system are a one-time expense and the cost of the vials can be further reduced. The entire system can be deployed in production facilities such as meat processing plants or environmental labs, i.e. directly where initial samples are taken with minimal training. Furthermore, since the sample preparation method remains unchanged and complaint with the standard ISO method, the two methods are directly comparable and thus interchangeable with the possibility of sensor based system replacing the standard method.

The newly developed O_2 sensor based respirometric system was further implemented in a shelf-life study regarding different types of MAP mincemeat samples: beef, turkey, lamb, and pork. Beef and turkey mince produced traditional sigmoidal profiles (Figures 5.2 & 5.3) with no differences between top and bottom samples as well as showing a linear progression of onset times relating to shelf-life. Lamb mince exhibited a variety of profiles with some being sigmoidal, others linear, and some a combination of both to which curve fitting could not be applied (Figure 5.4). Finally, pork mince had the most unusual profiles, as all were linear and none were sigmoidal (Figure 5.5). Interestingly, these profiles were not previously encountered in various food samples including raw meat, salads, and fish (Hempel et al.,

2011; Hempel et al., 2013, Fernandes et al., 2013). The mechanisms involved in these unusual respiration profiles warrant further investigation. Alongside respirometric analysis, the whole microbiome of each mincemeat type was analysed using 16S rRNA amplicon sequencing. There was an overall decrease in alpha diversity over shelf-life (Figure 5.6 & 5.7) which was consistent with the findings of previous studies (Filippis et al., 2013; Palman et al., 2020). These studies found that as time progressed, meat microbiota became less diverse, with a handful of taxa dominating in abundance (Filippis et al., 2013; Palman et al., 2020). Beta diversity was seen to be related to mincemeat type (Figure 5.8), in which samples pertaining to a given mincemeat type were more closely related in diversity than to samples from other mincemeat types. Although other studies have examined the microbial diversity of meat products, there has been little investigation into the diversity between products from different animals (Filippis et al., 2013; Stellato et al., 2016; Weinworth et al., 2019; Palman et al., 2020; Esteves et al., 2021). In addition, there were significant changes (ANOVA, Benjamini-Hochberg adjusted q-values of < 0.1) in abundance over shelf-life and upon acute exposure to respirometric analysis, with beef mince exhibiting a decrease in aerobic bacteria and an increase in facultative anaerobes (Figure 5.9). The effects of respirometry on bacterial composition have not been formerly investigated and further investigation into species level changes and metabolic processes is warranted.

The newly developed optical O_2 respirometry systems offer the food industry an improvement on pre-existing methods by providing faster time to result, on site deployment, increased accuracy and a reduction in cost. Moreover, the portable sensor based system can be easily combined with cutting edge techniques such as next generation sequencing, giving food scientists and microbiologists a powerful research tool.

References

Aitchison J, Barceló-Vidal C, Martín-Fernández JA, Pawlowsky-Glahn V. Logratio analysis and compositional distance. Mathematical geology. 2000 Apr;32(3):271-5.

Afari GK, Hung YC. Detection and verification of the viable but nonculturable (VBNC) state of Escherichia coli O157: H7 and Listeria monocytogenes using flow cytometry and standard plating. Journal of food science. 2018 Jul;83(7):1913-20.

Alamer S, Eissa S, Chinnappan R, Zourob M. A rapid colorimetric immunoassay for the detection of pathogenic bacteria on poultry processing plants using cotton swabs and nanobeads. Microchimica Acta. 2018 Mar;185(3):1-0.

Andrzejewski D, Klimant I, Podbielska H. Method for lifetime-based chemical sensing using the demodulation of the luminescence signal. Sensors and Actuators B: Chemical. 2002 May 15;84(2-3):160-6.

Ast C, Schmälzlin E, Löhmannsröben HG, Van Dongen JT. Optical oxygen micro-and nanosensors for plant applications. Sensors. 2012 May 25;12(6):7015-32.

Banerjee S, Kelly C, Kerry JP, Papkovsky DB. High throughput non-destructive assessment of quality and safety of packaged food products using phosphorescent oxygen sensors. Trends in Food Science & Technology. 2016 Apr 1;50:85-102.

Banerjee S, Kuznetsova RT, Papkovsky DB. Solid-state oxygen sensors based on phosphorescent diiodo-borondipyrromethene dye. Sensors and Actuators B: Chemical. 2015 Jun 1;212:229-34.

Bastiaanssen TF, Quinn TP, Loughman A. Treating Bugs as Features: A compositional guide to the statistical analysis of the microbiome-gut-brain axis. arXiv preprint arXiv:2207.12475. 2022 Jul 25.

Bates, D., Mächler, M., Bolker, B., & Walker, S.. Fitting Linear Mixed-Effects Models Using lme4. Journal of Statistical Software, 2015 Oct 7; 67(1): 1–48.

Biasino W, De Zutter L, Mattheus W, Bertrand S, Uyttendaele M, Van Damme I. Correlation between slaughter practices and the distribution of Salmonella and hygiene indicator bacteria on pig carcasses during slaughter. Food microbiology. 2018 Apr 1;70:192-9.

Bondi M, Messi P, Halami PM, Papadopoulou C, De Niederhausern S. Emerging microbial concerns in food safety and new control measures. BioMed Research International. 2014 Jul 6;2014.

Bonnet M, Lagier JC, Raoult D, Khelaifia S. Bacterial culture through selective and non-selective conditions: the evolution of culture media in clinical microbiology. New microbes and new infections. 2020 Mar 1;34:100622.

Borchert N, Hempel A, Walsh H, Kerry JP, Papkovsky DB. High throughput quality and safety assessment of packaged green produce using two optical oxygen sensor based systems. Food Control. 2012 Nov 1;28(1):87-93.

Borisov SM, CHAPTER 1:Fundamentals of Quenched Phosphorescence O_2 Sensing and Rational Design of Sensor Materials , in *Quenched-phosphorescence Detection of Molecular Oxygen: Applications in Life Sciences*, 2018, pp. 1-18

Borisov SM, Fischer R, Saf R, Klimant I. Exceptional Oxygen Sensing Properties of New Blue Light-Excitable Highly Luminescent Europium (III) and Gadolinium (III) Complexes. Advanced functional materials. 2014 Nov;24(41):6548-60.

Bottari B, Santarelli M, Neviani E. Determination of microbial load for different beverages and foodstuff by assessment of intracellular ATP. Trends in Food Science & Technology. 2015 Jul 1;44(1):36-48.

Bunge F, van den Driesche S, Waespy M, Radtke A, Belge G, Kelm S, Waite AM, Mirastschijski U, Vellekoop MJ. Microfluidic oxygen sensor system as a tool to monitor the metabolism of mammalian cells. Sensors and Actuators B: Chemical. 2019 Jun 15;289:24-31.

Capita R, Prieto M, Alonso-Calleja C. Sampling methods for microbiological analysis of red meat and poultry carcasses. Journal of Food Protection. 2004 Jun;67(6):1303-8.

De Filippis F, La Storia A, Villani F, Ercolini D. Exploring the sources of bacterial spoilers in beefsteaks by culture-independent high-throughput sequencing. PLoS One. 2013 Jul 25;8(7):e70222.

Demas JN, DeGraff BA, Xu W. Modeling of luminescence quenching-based sensors: comparison of multisite and nonlinear gas solubility models. Analytical Chemistry. 1995 Apr 1;67(8):1377-80.

Domínguez I, Frenich AG, Romero-González R. Mass spectrometry approaches to ensure food safety. Analytical Methods. 2020;12(9):1148-62.

Doster E, Thomas KM, Weinroth MD, Parker JK, Crone KK, Arthur TM, Schmidt JW, Wheeler TL, Belk KE, Morley PS. Metagenomic Characterization of the Microbiome and Resistome of Retail Ground Beef Products. Frontiers in Microbiology. 2020;11:2826.

Fercher A, Borisov SM, Zhdanov AV, Klimant I, Papkovsky DB. Intracellular O2 sensing probe based on cell-penetrating phosphorescent nanoparticles. ACS nano. 2011 Jul 26;5(7):5499-508.

Fernandes R, Carey C, Hynes J, Papkovsky D. GreenLight™ model 960. Journal of AOAC International. 2013 Mar 1;96(2):369-85.

Fricke C, Harms H, Maskow T. How to speed up the detection of aerobic microbial contaminations by using isothermal microcalorimetry. Journal of Thermal Analysis and Calorimetry. 2020 Dec;142(5):1933-49.

Genovese M, Poulain E, Doppler F, Toussaint R, Boyer M. Bacillus spore enumeration using flow cytometry: A proof of concept for probiotic application. Journal of Microbiological Methods. 2021 Nov 1;190:106336.

A) Hadjilouka A, Loizou K, Apostolou T, Dougiakis L, Inglezakis A, Tsaltas D. Newly developed system for the robust detection of Listeria monocytogenes based on a bioelectric cell biosensor. Biosensors. 2020 Nov 17;10(11):178.

B) Hadjilouka A, Loizou K, Apostolou T, Dougiakis L, Inglezakis A, Tsaltas D. A cell-based biosensor system for Listeria monocytogenes detection in food. Multidisciplinary Digital Publishing Institute Proceedings. 2020;60(1):49.

Hameed S, Xie L, Ying Y. Conventional and emerging detection techniques for pathogenic bacteria in food science: A review. Trends in Food Science & Technology. 2018 Nov 1;81:61-73.

Hauge SJ, Østensvik Ø, Monshaugen M, Røtterud OJ, Nesbakken T, Alvseike O. Enumeration of Escherichia coli in swab samples from pre-and post-chilled pork and lamb carcasses using 3M™ Petrifilm™ Select E. coli and Simplate® Coliforms/E. coli. Meat science. 2017 Aug 1;130:26-9.

Hempel A, Borchert N, Walsh H, Choudhury KR, Kerry JP, Papkovsky DB. Analysis of total aerobic viable counts in raw fish by high-throughput optical oxygen respirometry. Journal of food protection. 2011 May;74(5):776-82.

Hempel AW, O'Sullivan MG, Papkovsky DB, Kerry JP. Assessment and use of optical oxygen sensors as tools to assist in optimal product component selection for the development of packs of ready-to-eat mixed salads and for the non-destructive monitoring of in-pack oxygen levels using chilled storage. Foods. 2013 May 22;2(2):213-24.

Hilgarth M, Fuertes S, Ehrmann M, Vogel RF. Photobacterium carnosum sp. nov., isolated from spoiled modified atmosphere packaged poultry meat. Systematic and applied microbiology. 2018 Jan 1;41(1):44-50.

Hilgarth M, Werum V, Vogel RF. Lactococcus carnosus sp. nov. and Lactococcus paracarnosus sp. nov., two novel species isolated from modified-atmosphere packaged beef steaks. International Journal of Systematic and Evolutionary Microbiology. 2020 Nov 1;70(11):5832-40.

Hsieh TC, Ma KH, Chao A. iNEXT: an R package for rarefaction and extrapolation of species diversity (H ill numbers). Methods in Ecology and Evolution. 2016 Dec;7(12):1451-6.

Hynes J, Floyd S, Soini AE, O'Connor R, Papkovsky DB. Fluorescence-based cell viability screening assays using water-soluble oxygen probes. SLAS Discovery. 2003 Jun 1;8(3):264-72.

Hynes J, Marroquin LD, Ogurtsov VI, Christiansen KN, Stevens GJ, Papkovsky DB, Will Y. Investigation of drug-induced mitochondrial toxicity using fluorescence-based oxygen-sensitive probes. Toxicological Sciences. 2006 Jul 1;92(1):186-200.

ISO 4833-1:2013. Microbiology of the food chain — Horizontal method for the enumeration of microorganisms — Part 1: Colony count at 30 °C by the pour plate technique. International Organization for Standardization. Switzerland

ISO 18593, 2018. Microbiology of the food chain — Horizontal methods for surface sampling, International Organization for Standardization. Switzerland

Jadhav S, Sevior D, Bhave M, Palombo EA. Detection of Listeria monocytogenes from selective enrichment broth using MALDI–TOF Mass Spectrometry. Journal of proteomics. 2014 Jan 31;97:100-6.

Jadhav SR, Shah RM, Karpe AV, Morrison PD, Kouremenos K, Beale DJ, Palombo EA. Detection of foodborne pathogens using proteomics and metabolomics-based approaches. Frontiers in microbiology. 2018 Dec 18;9:3132

Jagadeesan B, Gerner-Smidt P, Allard MW, Leuillet S, Winkler A, Xiao Y, Chaffron S, Van Der Vossen J, Tang S, Katase M, McClure P. The use of next generation sequencing for improving food safety: Translation into practice. Food microbiology. 2019 Jun 1;79:96-115

Jasionek G, Ogurtsov V, Papkovsky D. Rapid detection and respirometric profiling of aerobic bacteria on panels of selective media. Journal of applied microbiology. 2013 Feb;114(2):423-32.

Jasson V, Jacxsens L, Luning P, Rajkovic A, Uyttendaele M. Alternative microbial methods: An overview and selection criteria. Food microbiology. 2010 Sep 1;27(6):710-30.

Jayasena DD, Jo C. Essential oils as potential antimicrobial agents in meat and meat products: A review. Trends in Food Science & Technology. 2013 Dec 1;34(2):96-108.

Jiang Y, Chen S, Zhao Y, Yang X, Fu S, McKillip JL, Fox EM, Man C. Multiplex loop-mediated isothermal amplification-based lateral flow dipstick for simultaneous detection of 3 food-borne pathogens in powdered infant formula. Journal of dairy science. 2020 May 1;103(5):4002-12.

Jones SL, Ricke SC, Keith Roper D, Gibson KE. Swabbing the surface: Critical factors in environmental monitoring and a path towards standardization and improvement. Critical reviews in food science and nutrition. 2020 Jan 19;60(2):225-43.

Juni E, Heym GA. Psychrobacter immobilis gen. nov., sp. nov.: genospecies composed of gram-negative, aerobic, oxidase-positive coccobacilli. International Journal of Systematic and Evolutionary Microbiology. 1986 Jul 1;36(3):388-91.

Kasturi KN, Drgon T. Real-time PCR method for detection of Salmonella spp. in environmental samples. Applied and environmental microbiology. 2017 Jul 15;83(14):e00644-17.

Kelly CA, Santovito E, Cruz-Romero M, Kerry JP, Papkovsky DP. Application of O2 sensor technology to monitor performance of industrial beef samples packaged on three different vacuum packaging machines. Sensors and Actuators B: Chemical. 2020 Feb 1;304:127338.

Khalef N, Campanella O, Bakri A. Isothermal calorimetry: methods and applications in food and pharmaceutical fields. Current Opinion in Food Science. 2016 Jun 1;9:70-6.

Li S, Mann DA, Zhang S, Qi Y, Meinersmann RJ, Deng X. Microbiome-Informed Food Safety and Quality: Longitudinal Consistency and Cross-Sectional Distinctiveness of Retail Chicken Breast Microbiomes. Msystems. 2020 Oct 27;5(5).

Kolbeck S, Reetz L, Hilgarth M, Vogel RF. Quantitative oxygen consumption and respiratory activity of meat spoiling bacteria upon high oxygen modified atmosphere. Frontiers in microbiology. 2019 Nov 8;10:2398.

Lakowicz, J.R., *Principles of Fluorescence Spectroscopy*. Third Edition ed.; Springer, USA: 2006.

Laursen BG, Bay L, Cleenwerck I, Vancanneyt M, Swings J, Dalgaard P, Leisner JJ. Carnobacterium divergens and Carnobacterium maltaromaticum as spoilers or protective cultures in meat and seafood: phenotypic and genotypic characterization. Systematic and applied microbiology. 2005 Mar 16;28(2):151-64.

Lebedev AY, Cheprakov AV, Sakadzic S, Boas DA, Wilson DF, Vinogradov SA. Dendritic phosphorescent probes for oxygen imaging in biological systems. ACS applied materials & interfaces. 2009 Jun 24;1(6):1292-304.

Li S, Mann DA, Zhang S, Qi Y, Meinersmann RJ, Deng X. Microbiome-Informed Food Safety and Quality: Longitudinal Consistency and Cross-Sectional Distinctiveness of Retail Chicken Breast Microbiomes. Msystems. 2020 Oct 27;5(5)

Liu S, Wang B, Sui Z, Wang Z, Li L, Zhen X, Zhao W, Zhou G. Faster Detection of Staphylococcus aureus in milk and milk powder by flow cytometry. Foodborne Pathogens and Disease. 2021 May 1;18(5):346-53.

Liu N, Zou D, Dong D, Yang Z, Ao D, Liu W, Huang L. Development of a multiplex loop-mediated isothermal amplification method for the simultaneous detection of Salmonella spp. and Vibrio parahaemolyticus. Scientific reports. 2017 Mar 28;7(1):1-7.

Liu Y, Lehnert T, Mayr T, Gijs MA. Antimicrobial susceptibility testing by measuring bacterial oxygen consumption on an integrated platform. Lab on a Chip. 2021;21(18):3520-31.

Lladó Maldonado S, Panjan P, Sun S, Rasch D, Sesay AM, Mayr T, Krull R. A fully online sensor-equipped, disposable multiphase microbioreactor as a screening platform for biotechnological applications. Biotechnology and bioengineering. 2019 Jan;116(1):65-75.

Lorenzo JM, Munekata PE, Dominguez R, Pateiro M, Saraiva JA, Franco D. Main groups of microorganisms of relevance for food safety and stability: general aspects and overall description. InInnovative technologies for food preservation 2018 Jan 1 (pp. 53-107). Academic Press.

Lubbe S, Filzmoser P, Templ M. Comparison of zero replacement strategies for compositional data with large numbers of zeros. Chemometrics and Intelligent Laboratory Systems. 2021 Mar 15;210:104248.

Mandli J, Fatimi IE, Seddaoui N, Amine A. Enzyme immunoassay (ELISA/immunosensor) for a sensitive detection of pork adulteration in meat. Food chemistry. 2018 Jul 30;255:380-9.

McLaren MR, Willis AD, Callahan BJ. Consistent and correctable bias in metagenomic sequencing experiments. Elife. 2019 Sep 10;8:e46923.

Meisel S, Stöckel S, Rösch P, Popp J. Identification of meat-associated pathogens via Raman microspectroscopy. Food microbiology. 2014 Apr 1;38:36-43.

Monica S, Bancalari E, Castellone V, Rijkx J, Wirth S, Jahns A, Bottari B. ATP Bioluminescence for Rapid and Selective Detection of Bacteria and Yeasts in Wine. Applied Sciences. 2021 Jan;11(11):4953.

Møretrø T, Normann MA, Sæbø HR, Langsrud S. Evaluation of ATP bioluminescence-based methods for hygienic assessment in fish industry. Journal of applied microbiology. 2019 Jul;127(1):186-95.

Morozova K, Armani M, Scampicchio M. Isothermal calorimetry for monitoring of grape juice fermentation with yeasts immobilized on nylon-6 nanofibrous membranes. Journal of Thermal Analysis and Calorimetry. 2020 Jan;139(1):375-82.

Müller B, Sulzer P, Walch M, Zirath H, Buryška T, Rothbauer M, Ertl P, Mayr T. Measurement of respiration and acidification rates of mammalian cells in thermoplastic microfluidic devices. Sensors and Actuators B: Chemical. 2021 May 1;334:129664.

Nagaraj S, Ramlal S, Kingston J, Batra HV. Development of IgY based sandwich ELISA for the detection of staphylococcal enterotoxin G (SEG), an egc toxin. International Journal of Food Microbiology. 2016 Nov 21;237:136-41.

Notomi T, Okayama H, Masubuchi H, Yonekawa T, Watanabe K, Amino N, Hase T. Loop-mediated isothermal amplification of DNA. Nucleic acids research. 2000 Jun 15;28(12):e63-.
Pahlow S, Meisel S, Cialla-May D, Weber K, Rösch P, Popp J. Isolation and identification of bacteria by means of Raman spectroscopy. Advanced drug delivery reviews. 2015 Jul 15;89:105-20.

O'Donovan C, Hynes J, Yashunski D, Papkovsky DB. Phosphorescent oxygen-sensitive materials for biological applications. Journal of Materials Chemistry. 2005;15(27-28):2946-51.

O'Donovan C, Twomey E, Alderman J, Moore T, Papkovsky D. Development of a respirometric biochip for embryo assessment. Lab on a Chip. 2006;6(11):1438-44.

O'Mahony F, Green RA, Baylis C, Fernandes R, Papkovsky DB. Analysis of total aerobic viable counts in samples of raw meat using fluorescence-based probe and oxygen consumption assay. Food Control. 2009 Feb 1;20(2):129-35.

O'Mahony FC, O'Donovan C, Hynes J, Moore T, Davenport J, Papkovsky DB. Optical oxygen microrespirometry as a platform for environmental toxicology and animal model studies. Environmental science & technology. 2005 Jul 1;39(13):5010-4.

O'Mahony FC, O'Riordan TC, Papkovskaia N, Kerry JP, Papkovsky DB. Non-destructive assessment of oxygen levels in industrial modified atmosphere packaged cheddar cheese. Food Control. 2006 Apr 1;17(4):286-92.

O'Mahony FC, Papkovsky DB. Rapid high-throughput assessment of aerobic bacteria in complex samples by fluorescence-based oxygen respirometry. Applied and environmental microbiology. 2006 Feb;72(2):1279-87.

O'Riordan TC, Buckley D, Ogurtsov V, O'Connor R, Papkovsky DB. A cell viability assay based on monitoring respiration by optical oxygen sensing. Analytical Biochemistry. 2000 Feb 15;278(2):221-7.

Palman Y, De Leo R, Pulvirenti A, Green SJ, Hayouka Z. Antimicrobial peptide cocktail activity in minced turkey meat. Food Microbiology. 2020 Dec 1;92:103580.

Pang B, Zhao C, Li L, Song X, Xu K, Wang J, Liu Y, Fu K, Bao H, Song D, Meng X. Development of a low-cost paper-based ELISA method for rapid Escherichia coli O157: H7 detection. Analytical Biochemistry. 2018 Feb 1;542:58-62.

Papkovsky DB. New oxygen sensors and their application to biosensing. Sensors and Actuators B: Chemical. 1995 Oct 1;29(1-3):213-8.

Papkovsky DB, Smiddy MA, Papkovskaia NY, Kerry JP. Nondestructive measurement of oxygen in modified atmosphere packaged hams using a phase-fluorimetric sensor system. Journal of Food Science. 2002 Oct;67(8):3164-9.

Papkovsky DB, Zhdanov AV. Cell energy budget platform for multiparametric assessment of cell and tissue metabolism. InMitochondrial Medicine 2021 (pp. 305-324). Springer, New York, NY.

Papkovsky DB, Zhdanov AV, Fercher A, Dmitriev RI, Hynes J. *Phosphorescent oxygen-sensitive probes*. Springer Science & Business Media; 2012.

Peruzy MF, Murru N, Yu Z, Kerkhof PJ, Neola B, Joossens M, Proroga YT, Houf K. Assessment of microbial communities on freshly killed wild boar meat by MALDI-TOF MS and 16S rRNA amplicon sequencing. International journal of food microbiology. 2019 Jul 16;301:51-60.

Plitzko B, Loesgen S. Measurement of oxygen consumption rate (OCR) and extracellular acidification rate (ECAR) in culture cells for assessment of the energy metabolism. Bio-protocol. 2018 May 20;8(10):e2850-.

Quaranta M, Borisov SM, Klimant I. Indicators for optical oxygen sensors. Bioanalytical reviews. 2012 Dec;4(2):115-57.

Rodríguez A, Gordillo R, Andrade MJ, Córdoba JJ, Rodríguez M. Development of an efficient real-time PCR assay to quantify enterotoxin-producing staphylococci in meat products. Food Control. 2016 Feb 1;60:302-8.

Ríos-Castillo AG, Ripolles-Avila C, Rodríguez-Jerez JJ. Evaluation of bacterial population using multiple sampling methods and the identification of bacteria detected on supermarket food contact surfaces. Food Control. 2021 Jan 1;119:107471.

Santovito E, Greco D, Marquis V, Raspoet R, D'Ascanio V, Logrieco AF, Avantaggiato G. Antimicrobial activity of yeast Cell Wall products against Clostridium perfringens. Foodborne Pathogens and Disease. 2019 Sep 1;16(9):638-47.

Seddaoui N, Amine A. Smartphone-based competitive immunoassay for quantitative on-site detection of meat adulteration. Talanta. 2021 Aug 1;230:122346.

Shao L, Chen S, Wang H, Zhang J, Xu X, Wang H. Advances in understanding the predominance, phenotypes, and mechanisms of bacteria related to meat spoilage. Trends in Food Science & Technology. 2021 Dec 1;118:822-32.

Singhal N, Kumar M, Kanaujia PK, Virdi JS. MALDI-TOF mass spectrometry: an emerging technology for microbial identification and diagnosis. Frontiers in microbiology. 2015 Aug 5;6:791.

Stellato G, La Storia A, De Filippis F, Borriello G, Villani F, Ercolini D. Overlap of spoilage-associated microbiota between meat and the meat processing environment in small-scale and large-scale retail distributions. Applied and environmental microbiology. 2016 Jul 1;82(13):4045-54.

Suaifan GA, Alhogail S, Zourob M. Rapid and low-cost biosensor for the detection of Staphylococcus aureus. Biosensors and Bioelectronics. 2017 Apr 15;90:230-7.

Sukigara C, Mino Y, Yasuda A, Morimoto A, Buranaprattheprat A, Ishizaka J. Measurement of oxygen concentrations and oxygen consumption rates using an optical oxygen sensor, and its application in hypoxia-related research in highly eutrophic coastal regions. Continental Shelf Research. 2021 Nov 1;229:104551.

Vizzini P, Manzano M, Farre C, Meylheuc T, Chaix C, Ramarao N, Vidic J. Highly sensitive detection of Campylobacter spp. In chicken meat using a silica nanoparticle enhanced dot blot DNA biosensor. Biosensors and Bioelectronics. 2021 Jan 1;171:112689.

von Ah U, Shani N, Chollet M, Solokhina A, Braissant O. Measuring antibiotic resistance in mixed cultures: Isothermal microcalorimetry as a novel analytical tool. International dairy journal. 2018 Feb 1;77:73-9.

Wang Y, Salazar JK. Culture-independent rapid detection methods for bacterial pathogens and toxins in food matrices. Comprehensive Reviews in Food Science and Food Safety. 2016 Jan;15(1):183-205.

Wang XD, Wolfbeis OS. Optical methods for sensing and imaging oxygen: materials, spectroscopies and applications. Chemical Society Reviews. 2014;43(10):3666-761.

Will Y, Hynes J, Ogurtsov VI, Papkovsky DB. Analysis of mitochondrial function using phosphorescent oxygen-sensitive probes. Nature protocols. 2006 Dec;1(6):2563-72.

Xiao X, Hu S, Lai X, Peng J, Lai W. Developmental trend of immunoassays for monitoring hazards in food samples: A review. Trends in Food Science & Technology. 2021 May 1;111:68-88.

Yamamoto T, Taylor JN, Koseki S, Koyama K. Classification of food spoilage bacterial species and their sodium chloride, sodium acetate and glycine tolerance using chemometrics analysis and Raman spectroscopy. Journal of Microbiological Methods. 2021 Nov 1;190:106326.

Yan S, Wang S, Qiu J, Li M, Li D, Xu D, Li D, Liu Q. Raman spectroscopy combined with machine learning for rapid detection of food-borne pathogens at the single-cell level. Talanta. 2021 May 1;226:122195.

Zitova A, O'Mahony FC, Cross M, Davenport J, Papkovsky DB. Toxicological profiling of chemical and environmental samples using panels of test organisms and optical oxygen respirometry. Environmental Toxicology: An International Journal. 2009 Apr;24(2):116-27.